Production of functionalized nanocelluloses from different sources using deep eutectic solvents and their applications

Ricardo O. Almeida [a], Thaddeus C. Maloney [b], José A.F. Gamelas [a,*]

[a] *University of Coimbra, CIEPQPF, Department of Chemical Engineering, Pólo II, R. Sílvio Lima, PT - 3030-790 Coimbra, Portugal*
[b] *Department of Bioproducts and Biosystems, Aalto University, P.O. Box 16300, Aalto, Finland*

ARTICLE INFO

ABSTRACT

Nanocelluloses have gained increasing attention over the years due to their attractive intrinsic properties, such as high strength and stiffness, high biocompatibility, good film-forming ability, easy surface functionalization, tunable optical properties, etc. With these unique features, nanocelluloses have the potential to be applied in a wide range of applications. However, the economic and environmental problems associated to the conventional methods of producing nanocelluloses make it difficult to produce them on a large scale. Therefore, the scientific community has been studying new alternatives. One alternative that has recently emerged is the use of deep eutectic solvents (DESs) for the production of nanocelluloses. The biodegradable and biocompatible character of the DESs combined with their low toxicity, easy preparation, tunability and recyclability turn them promising alternatives for the nanocellulose isolation. In this sense, this article provides a comprehensive overview of the production of (ligno)cellulose nanofibrils ((L)CNFs) and (ligno)cellulose nanocrystals ((L)CNCs) from woody resources and non-woody/agricultural residues using DESs. Additionally, the applications of the produced DES-(L)CNFs and DES-(L)CNCs are also discussed. From this review, it was possible to conclude that by using different DES components, different types of surface chemical functionalization on the (L)CNFs are obtained, which confer to the final material distinct properties. Additionally, films produced from the DES-(L)CNFs showed very good mechanical properties. On the other hand, the DES-(L)CNCs can be produced with higher yields and showing better thermal stability compared to the conventional methods of CNC production. Despite the promising results, an in-depth economic analysis on the use of DES for nanocellulose production is still lacking. Notwithstanding, favorable DES recyclability and reuse results indicate that they are good candidates for the nanocellulose (and nanocellulose-based films) production in a large scale.

1. Introduction

Nowadays, bio-based materials are being intensively studied by the scientific community, aiming to be applied in different fields to replace materials obtained from non-renewable resources and/or with harmful effects to the environment. In this context, nanocelluloses could play a prominent role. The high strength and stiffness, high biocompatibility, and easy surface functionalization are just some of the intrinsic properties that make nanocelluloses attractive to a wide range of applications (Fang et al., 2019). This can be of tremendous interest to pulp industries and agricultural sectors in the scope of circular bioeconomy and waste valorization.

Despite the huge potential of nanocelluloses, the conventional processes normally used to produce them are still quite expensive and,

depending on the pretreatment applied, hazardous chemicals that are difficult to recycle and reuse may be involved (Mokhena and John, 2020). Greener alternatives for the production of nanocelluloses have been studied, including the use of enzymes, subcritical water, liquid plasma, ionic liquids and deep eutectic solvents (Ai et al., 2022; Pradhan et al., 2022). Among these options, the use of deep eutectic solvents (DESs) for the nanocellulose production has received special attention by the scientific community since they are easily prepared with relatively low-cost components, highly tunable, capable of performing different types of surface chemical functionalization on cellulose (esterification, succinylation, cationization and sulfation), and, can also be recycled by relatively simple methods and reused.

This review will then be focused on the role of DESs for the production of cellulose nanofibrils and cellulose nanocrystals not only from

woody biomass, but also from non-woody/agricultural residues (e.g., wheat straw, rice straw, corn stalk, sugarcane bagasse, rapeseed stem, grape pomace, elephant grass, etc.). The properties and applications of the DES-nanocelluloses will also be discussed.

1.1. Cellulose

Cellulose is considered an infinite source of raw materials due to its enormous abundance on Earth, with an estimated annual production of ~1.5×10^{12} tons. Since it is a renewable, biodegradable, and non-toxic material, it is seen as an option with a lot of potential to address the current environmental concerns. The versatility that cellulose possesses to be modified by physicochemical methods allows it to be used in several applications, such as, filler, packaging films, textiles, paper products, building materials and so many others. This biopolymer occurs in nature in wood, plants, animals, algae, fungi, and bacteria, being wood and cotton the two major sources of cellulose (Heinze, 2015; Klemm et al., 2005). Cotton is almost pure cellulose while the cellulose present in wood is attached to hemicelluloses and both linked to lignin, by hydrogen and covalent bonds, which implies the use of pretreatment methods to isolate cellulose (e.g., Kraft process).

On molecular level, cellulose is defined as a linear homopolymer composed of D-anhydroglucopyranose units (AGU) connected through β (1→4) glycosidic bonds. The structural repeating unit is cellobiose, a dimer of glucose, with a length of 1.03 nm. The general formula of cellulose is $(C_6H_{10}O_5)_n$, where *n* represents the degree of polymerization (DP), which ranges in nature from approximately 10,000 AGU units in wood cellulose to 15,000 in native cotton cellulose (Sjöström, 1993). Each AGU unit possesses three reactive hydroxyl groups, a primary OH-group at C6 position and two secondary OH-groups at C2 and C3 positions, which confers to cellulose a highly functional character (Fig. 1) (Noremylia et al., 2022). These groups are responsible for the formation of intramolecular and intermolecular hydrogen bonding. In native cellulose (or Cellulose I), Infrared and C-Nuclear Magnetic Resonance analyses revealed that the intramolecular H-bonds are established between OH-group at C3 position and adjacent ether oxygen (O5) of the AGU and between the OH-group at C6 and adjacent OH-group of C2. On the other hand, the intermolecular bonds are formed mainly between the OH-group at C6 and oxygen atom in C3 of the neighboring cellulose chains (Dufresne, 2012; Gopi et al., 2019). The chain ends of cellulose are chemically distinct: one end has a free OH-group at C4 (nonreducing end) while the other end shows reducing properties possessing a free hemiacetal or aldehyde group at C1 (Nechyporchuk et al., 2016; Thomas et al., 2018).

Given the numerous cellulose sources, extraction and treatment methods, the hydrogen bonding network and molecular arrangement in cellulose can be highly variable resulting in different cellulose polymorphs (or allomorphs), which have been broadly identified as cellulose I, II, III and IV (Mateo et al., 2021).

Cellulose type I, also known as native cellulose, is the most common polymorph found in nature, and can be subdivided into I_α and I_β. These two subpolymorphs of cellulose I coexist in different ratios depending on the cellulose source. The I_α polymorph has a triclinic unit cell containing only one cellulose chain per unit cell, while I_β possesses a monoclinic unit cell with two cellulose chains per unit cell. I_α is a metastable polymorph that can be partially converted to I_β by hydrothermal treatments in an alkaline solution. Both I_α and I_β have the "parallel up" configuration, in which the cellulose chains have a parallel arrangement with the β (1→4) glycosidic bonds oriented in the same direction, i.e., in the positive c-axis direction of their respective unit cells (Moon et al., 2011). More detailed information about the crystalline structure of cellulose can be found elsewhere (Habibi, and Moon et al., 2010, 2011).

In nature, cellulose is present in the form of elementary fibrils that are further assembled in larger units, called micro/nanofibrils, which are then aggregated into cellulosic fibers (Fig. 1). The diameter of the elementary fibrils is estimated to be comprised between 3.5 and 5 nm while for nanofibrils the diameter ranges from 10 to 50 nm. The nanofibril lengths can reach to hundreds of nanometers or even a few microns (Lavoine et al., 2012). The fibril aggregates can be laterally disintegrated by mechanical processes to produce cellulose nanofibrils or can be cleaved transversally at the less ordered regions to form cellulose nanocrystals (Habibi, 2014).

1.2. Nanocellulose

Extracted from cellulose, nanocellulose is a fibrous material with at least one dimension on the nanometric scale (1–100 nm), possessing interesting properties such as large specific surface area (100–200 g/m^2), excellent mechanical behavior of the films (e.g., stiffness up to 30 GPa and tensile strength up to 300 MPa), tunable aspect ratios and easy surface functionalization (Fang et al., 2019; Phanthong et al., 2018). These unique properties allow them to have a broad spectrum of applications, for instance, energy devices, packaging, nanocomposite materials, bio-medicine, etc (Pradhan et al., 2022). Nanocelluloses are typically divided into three groups: (1) cellulose nanofibrils (CNFs) also called nanofibrillated cellulose, microfibrillated cellulose or cellulose nanofibers, (2) cellulose nanocrystals (CNCs) also known as nanocrystalline cellulose or cellulose whiskers, and (3) bacterial nanocellulose (BNC). Contrary to CNF and CNC, the latter is produced by a bottom-up process, where the BNC is obtained from the fermentation of low molecular weight sugars through microorganisms (mainly by *Gluconacetobacter xylinum*) (Abitbol et al., 2016; Pradhan et al., 2022).
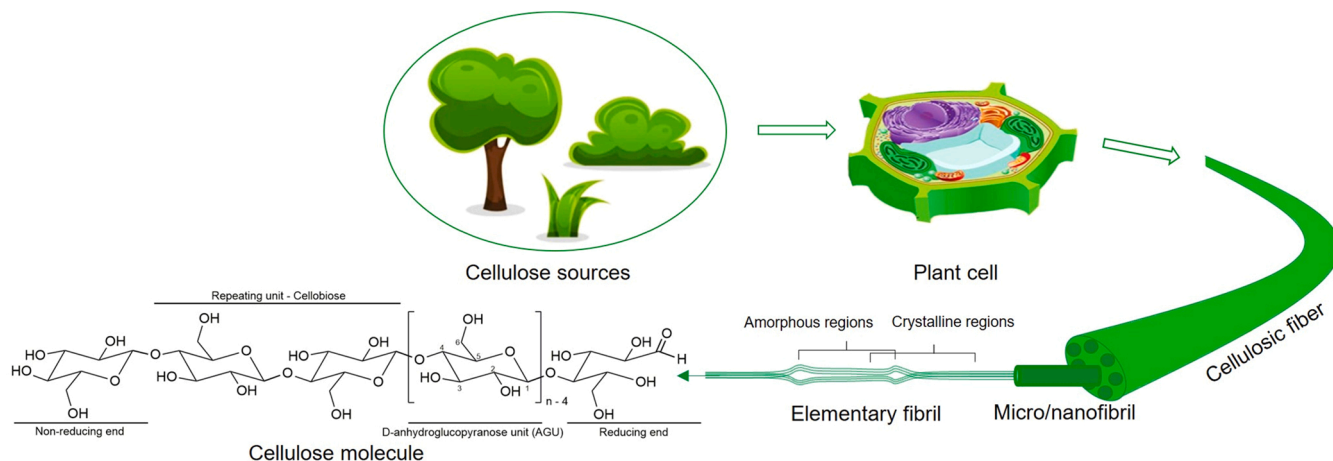

Fig. 1. Illustration of the hierarchical structure of cellulose fibers. Adapted from Lavoine et al. (2012).

BNCs will not be further explored in this review; the focus will be on CNFs and CNCs.

2. Cellulose nanofibrils production

CNFs are composed of fibril strands with crystalline and disordered domains forming a web-like structure with long, flexible and entangled nanofibers. The diameters of CNFs are typically in the range of 10–50 nm and the lengths of a few micrometers; however, these dimensions are strongly influenced by the cellulose feedstock and the extraction methods and conditions (Dhali et al., 2021).

2.1. Mechanical treatments

CNFs are mostly produced from aqueous suspensions of wood pulps by applying high shear forces using mechanical processes to cause the delamination/fibrillation of cellulosic fibers, isolating the nanofibers. The most common mechanical techniques used to produce CNFs include high-pressure homogenization (Amiralian et al., 2015; Turbak et al., 1983), microfluidization (Lee et al., 2009; Taheri and Samyn, 2016), grinding (Rambabu et al., 2016; Supian et al., 2020), high-intensity ultrasonication (Amiralian et al., 2015; Frone et al., 2011), twin screw extrusion (Espinosa et al., 2019; Ho et al., 2015) and ball milling (Yu et al., 2019; L. Zhang et al., 2015).

In high-pressure homogenization (HPH), cellulose pulp at low consistency is pumped at high pressure and passed through a set of valves, which opens and closes in a fast succession, subjecting the fibers to a large pressure drop and to impact and shear forces. The degree of cellulose fibrillation will be dependent on the number of passes through the homogenizer and the applied pressure (Kargarzadeh et al., 2018). The main limitations of this process are associated to the high energy consumption and the potential clogging problems that may arise during the operation of homogenizers (Petroudy et al., 2021).

Microfluidization has been used as an alternative to HPH. In this technique, the cellulose suspension is pumped under high pressure using an intensifier pump into thin Z- or Y-shaped chambers and passed through them. The strong shear and impact forces that are generated in these chambers will break the hydrogen bonds leading to the cellulose fibrillation. Similar to HPH, the degree of fibrillation will depend on the number of passes through the microfluidizer and, in this case, of chamber sizes also (Missoum et al., 2013).

In the grinding process, the cellulose pulp is passed between a static stone and a rotating stone revolving at ca. 1500 rpm. The shearing forces generated by the stones will break the cell wall structure, thus individualizing the CNFs (Siro and Plackett, 2010). The distance between stones, the morphology of the stone channels and the number of passes are important parameters that will define the extent of fibrillation (Kargarzadeh et al., 2018).

High-intensity ultrasonication (HIUS) is another strategy sometimes used to isolate CNFs, in which high-intensity ultrasonic waves (>20 kHz) absorbed by liquid molecules produce a mechanical oscillating motion resulting in the formation, growth, and implosion of gas bubbles. The strong hydrodynamic forces generated in this process are responsible to liberate cellulose nanofibers (Kumar et al., 2021). The morphology of the CNFs obtained by HIUS will be dependent of sonication time and ultrasonic power (Mokhena and John, 2020). Typically, higher power and time of ultrasonication lead to higher yields of nanofibers with smaller size.

Twin screw extrusion (TSE) is considered very promising for the CNF production. In this method, cellulose pulp is fibrillated by two co-rotating screws assembled in a closed barrel. As it passes through the extruder, the cellulose suspension is submitted to heat, compression, and shear forces leading to the delamination of the fibers (Kargarzadeh et al., 2018; Nechyporchuk et al., 2016). The morpho-structural properties of the CNFs produced by TSE will depend on the screw speed, configuration and length/diameter ratio, as well as, on temperature, feed rate and die shape/size (Mokhena and John, 2020). TSE allows the use of cellulose suspensions with high solid content (25–40 wt%) through the extruder and the resultant CNFs are obtained as moist powders (Ho et al., 2015).

Ball milling has also been used for the production of CNFs. Here, the raw material suspension is introduced in a hollow container partially filled with balls (e.g. balls of metal, zirconia or ceramic) and the high-energy collision between the balls and fibers caused by the rotation of the containers around their axes promotes the defibrillation (Nechyporchuk et al., 2016). The morphology and physical characteristics of the CNFs are dependent of the number and size of the balls, mass ratio (ball/cellulosic material), milling time, rotation speed and the state of the milling (dry or wet) (Phanthong et al., 2018). Despite some advantages of ball milling, this process has a poor energy efficiency (Teo and Wahab, 2020).

Fig. 2 shows the equipment often used for each of the aforementioned mechanical processes.

2.2. Pretreatments

To decrease the energy demand during mechanical processing and achieve higher fibrillation degrees, several solvent-assisted pretreatments have been developed, such as enzymatic hydrolysis (Pääkkö et al., 2007; Pere et al., 2020), TEMPO mediated oxidation (Saito et al., 2007, 2009), carboxymethylation (Im et al., 2019; Wågberg et al., 2008), cationization (Olszewska et al., 2011; Pedrosa et al., 2022), periodate oxidation (Liimatainen et al., 2012, 2013), phosphorylation (Ghanadpour et al., 2015; S. Zhang et al., 2021), and ionic liquid pretreatments (Berglund et al., 2017; Phanthong et al., 2017). Basically, the enzymatic hydrolysis "cuts" the cellulose chains into smaller fragments, while the chemical pretreatments introduce charged functional groups on the cellulose surface, thus improving the cellulose fibrillation. The charged (positive or negative) groups introduced by the chemical methods generate repulsive forces which in turn weaken the hydrogen bonding network between the cellulose chains. Additionally, to reduce the osmotic pressure between the charged fibers and dispersing medium, water penetrates the fibers causing them to swell. As result, the intermolecular bonds of cellulose fibers are also weakened, and the disruption of cell walls is facilitated (Rol et al., 2019; Yi et al., 2020).

2.2.1. Enzymatic hydrolysis

In this pretreatment, enzymes (mostly cellulases) are used as biocatalysts to cleave the glycosidic bonds in cellulose chains, improving its fibrillation. These enzymes are commonly categorized into three distinct groups: (i) endoglucanases, which attack the disordered regions of cellulose by randomly breaking the glycosidic bonds resulting in new nonreducing ends of cello-oligosaccharides, (ii) exoglucanases, that hydrolyze these ends of the chain producing tetrasaccharides and disaccharides (cellobiose), (iii) β-glucosidases, which hydrolyze the products generated by the exoglucanases into glucose molecules. Fig. 3 presents a simplified scheme of these actions on cellulose.

Endoglucanases are the most important cellulases for nanocellulose production, due to their ability to selectively hydrolyze the amorphous regions of cellulose and keep the crystalline parts intact (Ribeiro et al., 2019). The use of these specific enzymes usually leads to a decrease in the cellulose DP and promotes fiber peeling, thus facilitating cellulose fibrillation in the subsequent mechanical processes (Xie et al., 2018).

The enzymatic hydrolysis of cellulose is typically carried out at a pH ranging from 5 to 7, using an incubation temperature between 45 and 50 ºC. These mild conditions combined with the non-toxic nature of the enzymes and the non-production of hazardous byproducts make this process a more environmentally friendly approach compared to chemical pretreatments (Arantes et al., 2020).

In 2019, Liu et al. reported that the enzymatic pretreatment of cellulose fibers could save more than 60% of electrical energy in the posterior mechanical grinding used for the CNF production (X. Liu et al., 2019a). In another study, Pere et al. (2020), reported an
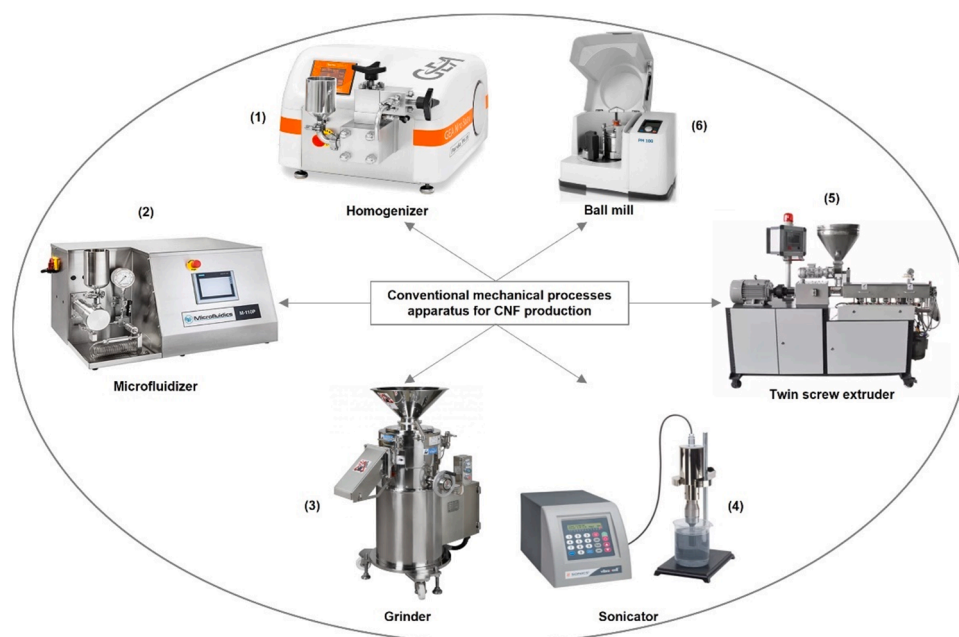
Fig. 2. Apparatus of the most applied mechanical treatments for CNF production. (Adapted from (1) www.gea.com; (2) www.microfluidics-mpt.com; (3) www.mtmarconi.com; (4) www.sonics.com; (5) www.haisiextrusion.com; (6) www.profilab24.com).
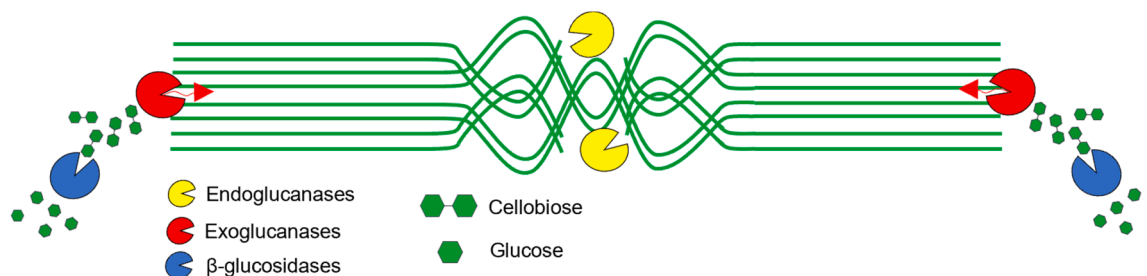

Fig. 3. Simplified schematic representation of different cellulase actions on cellulose. Adapted from Pirich et al. (2020).

enzyme-assisted fibrillation at a significantly high solid loading (25 wt %) for the production of a new type of nanocellulose called HefCel (high-consistency enzymatically fibrillated cellulose) without the requirement of a high shear disintegration. Compared to conventional mechanical processes, the energy consumption associated to the HefCel production (0.6 MWh/t) can actually be 50 times lower.

2.2.2. TEMPO mediated oxidation

Tempo mediated oxidation is one of the most popular methods for cellulose surface modification, in which negatively charged carboxyl groups are introduced into cellulosic fibers promoting an easier delamination of the nanofibrils due to the electrostatic repulsions established between the negatively charged fibers (Almeida et al., 2021; Xie et al., 2018). In this pretreatment, the OH-groups at the C6 of anhydroglucose units are selectively oxidized to carboxylic groups using NaClO as the primary oxidant, in the presence of catalytic amounts of 2,2,6,6-tetramethylpiperidine-1-oxyl radical (TEMPO) and NaBr, typically under alkaline conditions (pH 10–11) at room temperature (Fig. 4a) (Lavoine et al., 2012). However, the TEMPO/NaBr/NaClO system causes a high depolymerization of cellulose chains which may result from β-elimination of glycosidic bonds due to the presence of C6 aldehyde groups under alkaline conditions, and/or from the cleavage of anhydroglucose units caused by hydroxyl radicals formed during TEMPO mediated oxidation (Isogai et al., 2018). Saito et al. (2009) demonstrated that this severe

depolymerization can be avoided using the TEMPO/NaClO/NaClO₂ system under neutral or weakly acidic conditions; however, higher reaction times and temperatures are required. In this system, the NaClO₂ is used as primary oxidant, oxidizing the formed aldehydes into carboxylic groups (Fig. 4b) (Tanaka et al., 2012).

Despite high degree of fibrillation and energy savings in mechanical treatment, the scale up of the TEMPO process is constrained by the high cost of TEMPO reactant and the environmental impact of the resultant reaction media. In this regard, Sanchez-Salvador et al. (2021) studied the possibility of reusing the reaction medium. For the oxidation of cotton cellulose and eucalyptus cellulose, the authors reused 75% of the reaction media for ten cycles, introducing 25% of fresh medium in each cycle. After these ten cycles, they noted that the obtained CNFs showed similar properties to those obtained in the first cycle.

2.2.3. Carboxymethylation

Carboxymethylation is another chemical pretreatment based on the random etherification of the cellulose OH-groups with monochloroacetic acid, under strong alkaline conditions using an alcoholic solution as a solvent medium. From this reaction, carboxymethyl groups are introduced onto the cellulose fibers, which, similar to TEMPO oxidation, generate electrostatic repulsions among the charged fibers promoting the fibrillation of the fibers for CNF production (Habibi, 2014; Thomas et al., 2018).
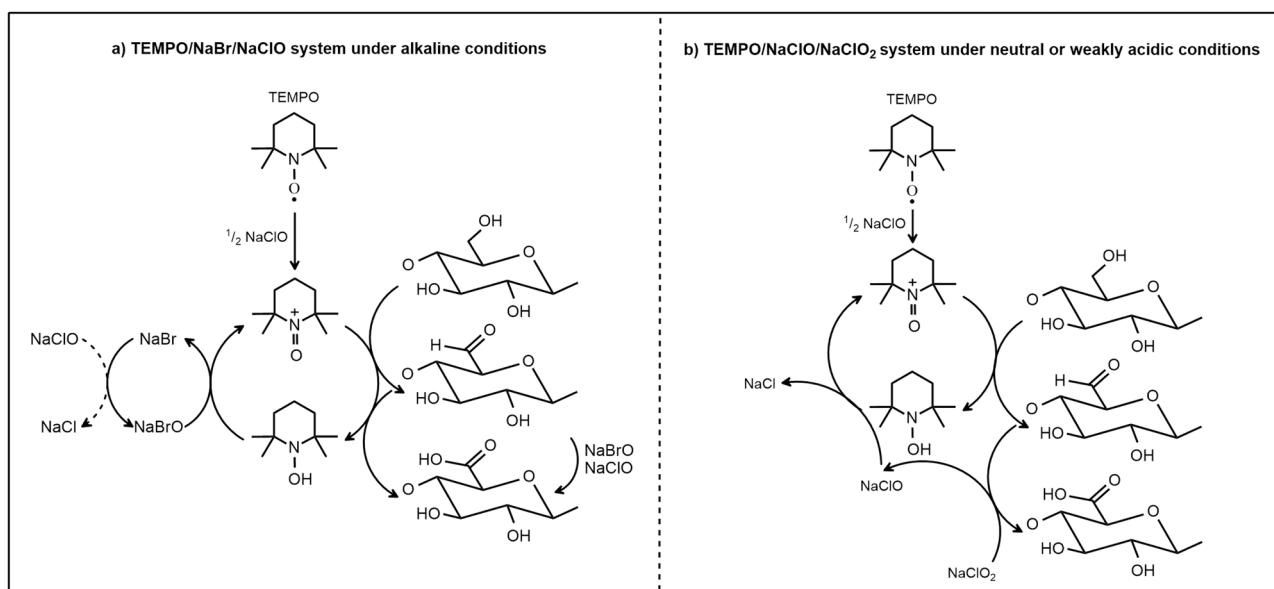
Fig. 4. Oxidation mechanism of cellulose by a) TEMPO/NaBr/NaClO under alkaline conditions and b) TEMPO/NaClO/NaClO$_2$ under neutral or weakly acidic conditions. Adapted from Isogai et al. (2018).

In order to save costs and minimize the environmental impact of this pretreatment, Im et al. (2019) studied the recycling and reutilization of the solvent medium in the carboxymethylation of a bleached eucalyptus kraft pulp (BEKP). For the first carboxymethylation reaction, they used fresh isopropanol (IPA) as the reaction medium, and, after that, the used IPA was recovered, passed through a molecular sieve to dehydrate it, and reused again for the following carboxymethylation reactions. With this strategy, the authors obtained CNFs with nearly constant values of carboxyl groups and intrinsic viscosities in cupriethylenediamine, irrespective of the IPA recycling number.

2.2.4. Cationization

The cationization of cellulose can also be used as a pretreatment to produce CNFs. In this pretreatment, the electrostatic repulsions between the quaternary ammonium groups introduced into the cellulose structure, enhance the nanofibrillation of cellulose. (Xie et al., 2018). Different reactants such as 2,3-epoxypropyl trimethylammonium chloride (EPTMAC) (Aulin et al., 2010; Olszewska et al., 2011), Girard's reagent T ((2-hydrazinyl-2-oxoethyl) trimethylazanium chloride, GT) (Liimatainen et al., 2014) and chlorocholine chloride (Ho et al., 2011) are some of the agents that have been used to perform the cationization modification on the cellulose structure.

Aulin et al. (2010), were the first authors to use this pretreatment for CNF production. They cationized a dissolving pulp using EPTMAC in the presence of water, isopropanol and NaOH followed by homogenization in a high-pressure fluidizer. The obtained CNFs exhibited diameters of ~ 3 nm (individual nanofibrils) and a cationic charge density of 0.35 meq/g (Olszewska et al., 2011). Alternatively, Ho et al. (2011) were able to produce cationic CNFs by introducing quaternary ammonium groups into cellulose (oat straw pulp) with chlorocholine chloride in the presence of dimethylsulfoxide and NaOH, followed by microfluidization. Liimatainen et al. (2014), on the other hand, adopted another cationization pathway, which involved a periodate oxidation followed by a quaternization with Girard' reagent T. After HPH, the obtained CNFs exhibited widths of 10–50 nm, cationic charges ranging from 1.1 to 2.1 meq/g and a transmittance of 80–95% (at 800 nm).

2.2.5. Periodate oxidation

Cellulose oxidation with periodate can be used as the starting point for the production of nanocellulose with different functionalities. First,

periodate selectively oxidizes the vicinal OH-groups at the C2 and C3 positions of cellulose breaking the corresponding C-C bond of the glucopyranose unit to form 2,3-dialdehyde cellulose (DAC) (Yi et al., 2020). The highly reactive aldehyde groups of the DAC can be further converted into carboxyl (Liimatainen et al., 2012), sulfonic (Liimatainen et al., 2013) and quaternary ammonium groups (as mentioned in the previous section).

The sequential periodate-chlorite oxidation reaction, which adds carboxyl groups on the cellulose structure, was firstly investigated by Liimatainen et al. (2012), as a pretreatment to promote the fibrillation of a hardwood cellulose pulp using HPH. After the periodate oxidation followed by the chlorite oxidation, the carboxyl groups varied from 0.38 to 1.75 mmol/g. Highly viscous and transparent gel-like suspensions, containing nanofibrils with an average width of approximately 25±6 nm were obtained after HPH.

Periodate oxidation followed by sulfonation is another alternative for the introduction of negatively charged groups on cellulose fibers. Aiming to obtain sulfonated CNFs, Liimatainen et al. (2013) pretreated a hardwood pulp with periodate and bisulfite that was subsequently mechanically treated using a high-pressure homogenizer. The prepared CNFs displayed widths in the range of 10–60 nm and low anionic charge densities (0.18–0.51 mmol/g).

2.2.6. Phosphorylation

Phosphorylation is another chemical pretreatment to produce CNFs, where phosphate ester groups are incorporated into the cellulose backbone, aiming at improving the nanofibrillation of cellulose fibers (Rol et al., 2019). Although it has only recently been used as a pretreatment for the production of nanocelluloses, phosphorylation of cellulosic materials has been studied for decades. To perform this cellulose functionalization, several phosphorylating agents such as phosphorus oxychloride (POCl$_3$) (Reid and Mazzeno, 1949), phosphorus pentoxide (P$_2$O$_5$) (Granja et al., 2001), phosphoric acid (H$_3$PO$_4$) (Inagaki et al., 1976), diammonium hydrogen phosphate ((NH$_4$)$_2$HPO$_4$) (Nuessle et al., 1956), and organophosphates (Aoki and Nishio, 2010) have been studied. The phosphorylation reaction is usually performed in the presence of *N,N*-dimethylformamide, pyridine or urea to promote the swelling of cellulose fibers (Thomas et al., 2018).

Ghanadpour et al. (2015) were the first to report the production of cellulose nanofibrils from phosphorylated fibers. In this work, a sulfite

softwood pulp was phosphorylated using $(NH_4)_2HPO_4$ in the presence of urea, and then cured at 150 ºC for different periods of time. Then, a suspension of the treated fibers (2 wt%) was passed through a micro-fluidizer resulting in fibrils with widths of about 3 nm and lengths in the range of 500–1000 nm. A high concentration of phosphate groups at the surface of the nanofibrils allowed them to obtain nanopaper sheets with enhanced thermal and flame-retardant properties.

Highly transparent CNFs with a uniform width of 3–4 nm were also obtained by Noguchi et al. (2017). Phosphate groups were attached to the cellulose nanofibrils without significant decrease in the pulp recovery ratio, DP and crystallinity index. They also reported that an insufficient or excessive phosphorylation negatively affects the CNF properties (degree of fibrillation, transparency and viscosity).

This type of pretreatment seems to have a great industrialization potential due to its easy implementation and non-toxic character. However, there are still no studies about the mechanical energy savings that this pretreatment can provide (Petroudy et al., 2021).

2.2.7. Ionic liquid pretreatments

Ionic liquids (ILs) are organic salts containing an organic cation and an organic or inorganic anion possessing melting points typically bellow 100 ºC. Due to their chemical and thermal stability, low vapor pressure/volatility and high tunability, ILs are being used for multiple applications, namely for the dissolution of lignocellulosic materials (Raza and Abu-Jdayil, 2022). In addition to this, they have also been used for the CNF production.

In 2017, Phanthong et al. successfully produced CNFs by planetary ball milling of cellulose powder in the presence of 1-butyl-3-methylimidazolium chloride ([BMIM]Cl) at room temperature. This procedure allowed them to obtain a CNF with a mass yield of 93.1%, diameters of 10–25 nm and lengths of few micrometers. To circumvent the high cost of the IL, the authors were able to recover more than 90% of the [BMIM]Cl and reuse it at least 4 times, achieving CNFs with similar properties to those obtained by using the fresh IL. Alternatively to the conventional

ILs, Berglund et al. (2017) used a switchable ionic liquid (SIL) combined with grinding to obtain CNFs with diameters below 15 nm, which in turn resulted in SIL-CNF films with high tensile strength and elastic modulus (ca. 150 MPa and 12 GPa, respectively).

A schematic representation of the cellulose modifications for the abovementioned chemical pretreatments is presented in Fig. 5.

3. Cellulose nanocrystals production

CNCs are "rod-like" or "needle-like" cellulose crystals with high crystallinity (up to ∼ 90%), having diameters of 5–70 nm and lengths between 100 nm and several micrometers. The size and crystallinity of these nanocrystals are dependent on the cellulose source, isolation methods and their respective experimental conditions (Brinchi et al., 2013; Raza and Abu-Jdayil, 2022). Acid hydrolysis (Bondeson et al., 2006; Brinchi et al., 2013), ionic liquid treatment (Iskak et al., 2017; Man et al., 2011), enzymatic hydrolysis (Cui et al., 2016; Pereira and Arantes, 2020), and oxidation (Cao et al., 2012; H. Zhang et al., 2020) are some of the extraction methods that have been used to prepare CNCs.

3.1. Acid hydrolysis

Acid hydrolysis is the most used isolation method for the CNC production. Here, the glycosidic bonds of the disordered domains of cellulose are easily hydrolyzed by mineral acids (mainly) while the crystalline regions are preserved since the acid cannot easily penetrate these well-ordered regions (Vanderfleet and Cranston, 2021). At the end of the hydrolysis, the resulting suspension is diluted in water to stop the reaction. Dialysis against deionized water is then carried out to remove the residual acid and neutralized salts. Finally, a mechanical treatment is applied, usually sonication, to obtain a homogeneous dispersion of CNCs (Brinchi et al., 2013). Sulfuric acid and hydrochloric acid are the typical mineral acids applied for the hydrolysis of cellulose. When H_2SO_4 is used, the sulphate ester groups introduced on cellulose surface will lead
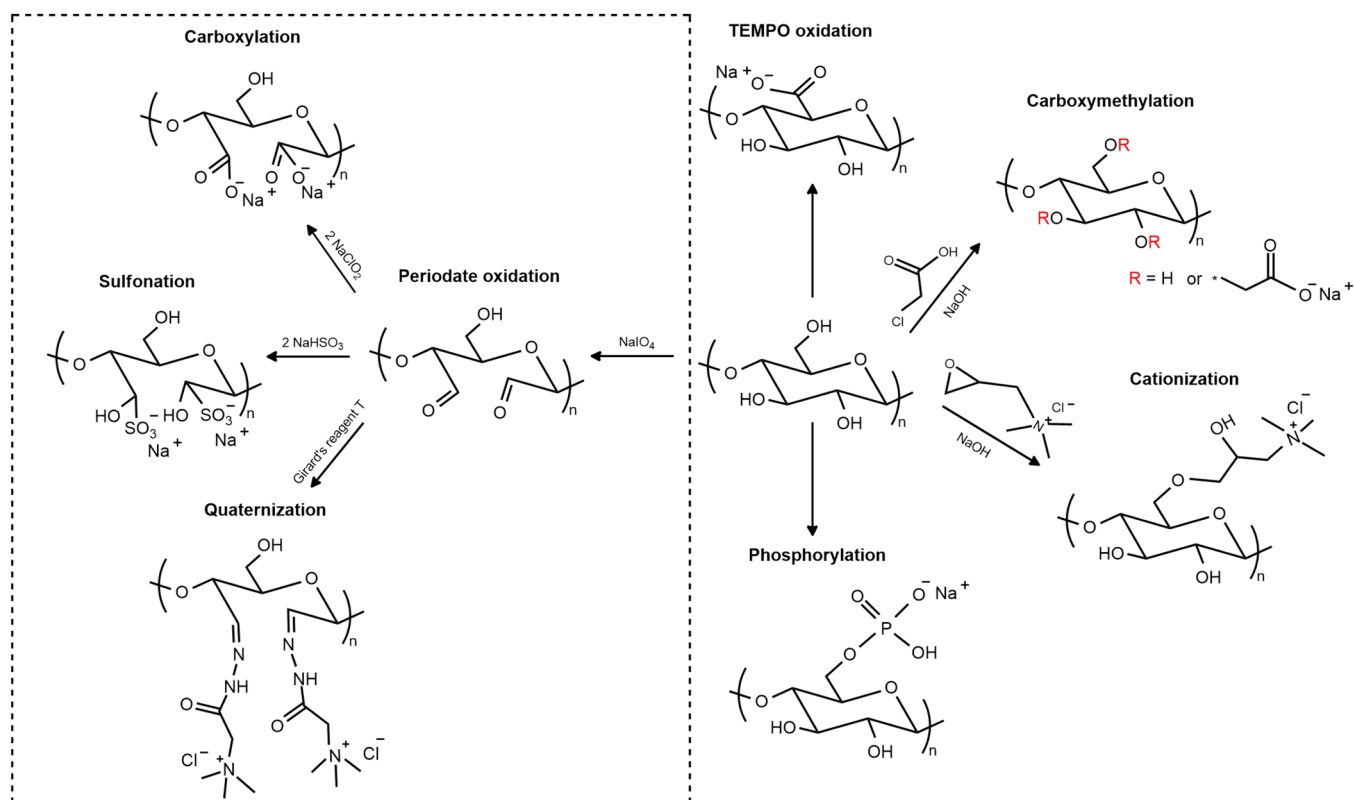

Fig. 5. Schematic representation of the cellulose modifications by chemical pretreatments used to produce nanocellulose.

to CNCs with high colloidal stability, while the CNCs prepared by HCl tend to flocculate due to the absence of charged groups. To overcome the environmental implications associated to the use of these strong acids, organic acids such as formic (C. Liu et al., 2016), oxalic and maleic acids (Chen et al., 2016), as well as solid acids (e.g., $H_3PW_{12}O_{40}$) (Y. Liu et al., 2014), have been investigated for the production of CNCs.

3.2. Ionic liquid treatment

Ionic liquids are considered a promising alternative to conventional acid hydrolysis for the isolation of CNCs. The first attempt to produce CNCs from ILs was carried out by Man et al. (2011) where they used a Brønsted acidic IL (1-Butyl-3-methylimidazolium hydrogen sulfate, [BMIM]HSO$_4$) to obtain CNCs from microcrystalline cellulose (MCC) at different temperatures (70–90 ºC) for 1 h reaction time. Needle-like shape CNCs with high crystallinity indices (82–91%) having dimensions of 14–22 nm in diameter and 50–300 nm in length were obtained. The crystalline structure of MCC was preserved, but a considerable decrease in the thermal stability, compared to MCC, was observed, which was probably caused by the presence of sulfate groups in the CNCs introduced by [BMIM]HSO$_4$. Later, it was reported that the mechanism of hydrolysis of MCC in [BMIM]HSO$_4$ has some similarities with acid hydrolysis (Tan et al., 2015).

Another relevant study in this field was conducted by Abushammala et al. (2015), in which they extracted CNCs directly from wood using [EMIM]OAc. After two cycles of treatment of Angelim-Vermelho wood with this IL, partially acetylated (DS of 0.28) CNCs with a crystallinity index of about 75% having diameters of 2–5 nm and lengths of 75–125 nm were obtained. The [EMIM]OAc was able to dissolve the lignin in situ and catalyze the cellulose hydrolysis at the same time.

On the other hand, other researchers reported that some ILs such as [BMIM]Cl could be applied as a pretreatment step to improve the accessibility of the cellulose fibers, allowing the use of milder conditions and lower amounts of H_2SO_4 in the subsequent acid hydrolysis (Lazko et al., 2014; Pang et al., 2018).

In spite of their advantages, the high costs of the ILs and the questions that have recently arisen about their biodegradability and toxicity, restrict their application on a large scale to produce CNCs.

3.3. Other methods to produce CNCs

Enzymatic hydrolysis and TEMPO-mediated oxidation can also be employed for the CNC extraction. Regarding enzymatic hydrolysis, it is worth highlighting the study conducted by Pereira and Arantes (2020), where they successfully integrated the CNC isolation method, via enzymatic hydrolysis at high solid loading, with the production of sugars from sugarcane bagasse. This strategy allowed them to obtain CNCs with a considerable yield (~ 50%), high crystallinity (96.5%) and diameters around 20 nm. On the other hand, although TEMPO oxidation is mainly used as a pretreatment for the production of CNFs, it has also been tested for the preparation of CNCs. For instance, Cao et al. (2012) were able to extract CNCs with a high yield (> 80%) and super thin diameter (3–10 nm) in the form of a very transparent and stable dispersion from pretreated jute fibers by combination of TEMPO/NaBr/NaClO system oxidation and mechanical homogenization.

Despite the methods listed above for the production of CNFs and CNCs, over the last few years the research community has focused on the development of greener and more sustainable routes to produce nanocellulose. An alternative that has aroused considerable interest is the use of deep eutectic solvents for the pretreatment of cellulose fibers. In this context, this review will be focused on the use of DESs for the production of CNFs and CNCs, as well as on the potential applications for these types of nanocellulose.

4. Deep eutectic solvents

DESs are typically composed by a hydrogen bond acceptor (HBA) and a hydrogen bond donor (HBD) capable of forming eutectic mixtures with a melting point (below 100 ºC) lower than that of the individual constituents. The decrease in the melting point is a consequence of the presence of nonsymmetric ions that confer a low lattice energy and charge delocalization which occurs through the H-bond interaction between HBA and HBD (Chang et al., 2021). As an example, a mixture composed of choline chloride (ChCl) and malonic acid (1:1 molar ratio) was shown to give a DES with a melting point of 10 ºC, a significantly lower value compared to the melting points of ChCl (303 ºC) and malonic acid (135 ºC) (Abbott et al., 2004). However, the definition of DES remains a controversial topic, with some misconceptions being widespread in the literature. A DES is often described as a mixture that presents a eutectic point and as a hydrogen bond complex; however, these two statements are not sufficient to define a deep eutectic solvent, because all mixtures composed of immiscible solid compounds exhibit a eutectic point and numerous compounds are capable of forming hydrogen bonds when mixed together (Coutinho and Pinho, 2017; El Achkar et al., 2021). In order to clearly differentiate a deep eutectic solvent from other eutectic mixtures, Martins et al. (2019) defined deep eutectic solvent as "a mixture of two or more pure compounds for which the eutectic point temperature is below that of an ideal liquid mixture, presenting significant negative deviations from ideality ($\Delta T_2 > 0$)", where ΔT_2 is the temperature depression, i.e., the difference between the ideal ($T_{E, ideal}$) and the real eutectic point (T_E) (Fig. 6). These authors also stated that the temperature depression should be sufficient for the mixture to be in the liquid state at the operating temperature for a given composition range (x_1 to x_2 in Fig. 6).

DESs are generally classified into four types. Type I DES have limited applications due to the small number of unhydrated metal halides with adequate low melting points for their synthesis. However, the hydrated metal halides combined with ChCl in the formation of type II DESs allow them to have a wider range of applications. The relatively low costs and air/moisture insensitivity of the hydrated metal halides make the DESs obtained from it viable to be used in industrial processes. Type IV DESs are formed by metal salts (e.g., $ZnCl_2$) and HBDs such as urea,
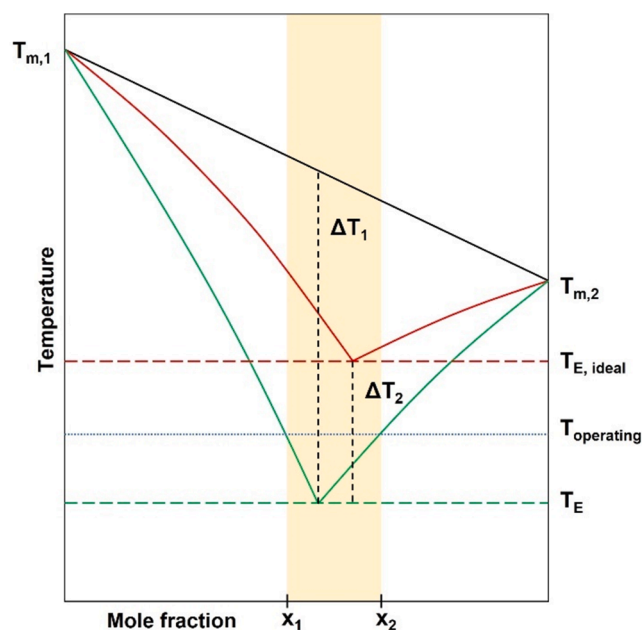

Fig. 6. Representation of the solid-liquid phase diagram of a simple eutectic mixture (red line) and a deep eutectic mixture (green line). Adapted from Martins et al. (2019).

acetamide, and ethylene glycol. Type III DESs are the most studied/used DESs since they are easily prepared, biodegradable and relatively inexpensive (Loow et al., 2017; Smith et al., 2014). Typically, this type of DES contains a quaternary ammonium salt as HBA (namely ChCl) and amides, carboxylic acids and alcohols as HBDs. The interactions established between HBA and HBD are mainly hydrogen bonds, although electrostatic and Van der Waals forces may also be involved (Tomé et al., 2018).

After the first work on DESs (Abbott et al., 2003), several investigations were conducted aiming to find new compounds for DES synthesis. In this sense, Choi et al. (2011) found a new DES class consisting of combinations of ubiquitous natural compounds present in living cells (sugars, amino acids, organic acids, amines) and even water, which they named as "natural deep eutectic solvents" (NADESs). The usual HBAs used to prepare NADES are amines (ChCl, ammonium chloride) or amino acids (alanine, proline, glycine, betaine) while organic acids (e.g., oxalic acid, lactic acid, malic acid) or carbohydrates (e.g., glucose, fructose, maltose) are typically used as HBDs (Cunha and Fernandes, 2018).

As with ILs, DESs are also characterized by their chemical and thermal stability, low vapor pressure/volatility and tunability. However, DESs can overcome the main limitations of ILs since they can be easily prepared from relatively inexpensive components by simply mixing and heating them without the need of purification steps. The biocompatibility, biodegradability and low toxicity of the DESs are also advantageous features over traditional ILs (Francisco et al., 2013; Smith et al., 2014). The non-toxic nature of DESs has been intensively highlighted in literature and, many times, described as an absolute truth; however, this generalization should be avoided due to the lack of DES toxicological studies and also to some contradictory results reported on this topic. This widespread assumption is typically made based on the toxicity profile of the individual constituents of the DESs, ignoring that synergistic effects between them may lead to different toxicological behaviors of the DES systems (Martínez et al., 2022). A few review articles present in the literature have compiled and thoroughly discussed the toxicity of the DESs, in which it is easily perceived that some DESs can be toxic against various organisms/cells (Marchel et al., 2022; Martínez et al., 2022). Therefore, DES utilization at a large scale should be reevaluated, in order to prevent them from becoming potentially harmful to the environment.

In this sense, the recycling and reuse of the DESs are essential to circumvent eventual future environmental problems that can be raised by their widespread use in industrial applications and to reduce costs associated to their utilization. In the field of biomass processing, several methodologies (e.g., anti-solvent addition followed by evaporation, liquid-liquid and solid-liquid extraction, crystallization, membrane processes) have been applied for the recovery and recycling of DESs. Promising recovery rates of DESs were already achieved using these technologies. To choose the most appropriate recycling process, different factors should be considered, such as the physiochemical properties of the DESs, the type of biomass conversion/extraction method, the costs associated to the recycling methodology, among others (Isci and Kaltschmitt, 2022).

Knowledge about the physiochemical properties of DESs is therefore crucial for a better selection of their potential applications, especially in industry. In this regard, some of the DES properties will be presented and briefly discussed below.

4.1. Density

Density is one of the key physical properties for chemical processing that can be measured by using a specific gravity meter. Apart from some hydrophobic DESs, most of the DES densities reported in the literature are higher than water, with values mostly in the range of 1.0–1.35 g/cm^3 at room temperature. However, type IV DESs based on metal salts have shown superior densities than other classes (1.3–1.6 g/cm^3)

(García et al., 2015; Satlewal et al., 2018). The density of the DESs depends on the characteristics of their individual components and respective molar ratios, as well as on the molecular arrangement and packaging of their components. The DES densities are also temperature dependent, i.e., the density decreases as temperature increases due to increased molecular activity and mobility resulting in the increase of the molar volume of DESs (Bhagwat et al., 2021).

4.2. Viscosity

For potential application of DESs as green solvents, lower viscosities are desirable, since most DESs are highly viscous (>100 cP) at room temperature. The high viscosity of DESs can be attributed to the strong network established between their constituents in the liquid state. Generally, the viscosity of DESs is substantially affected by the chemical nature of their components, molar ratio, temperature and water content (Ijardar et al., 2022; Kalhor and Ghandi, 2019). Depending on the DES constituents, they can have a broad range of viscosities. For instance, it has been reported that a DES composed of ChCl and ethylene glycol (1:4) has a viscosity of 19 cP (at 20 ºC), whereas for DESs of ChCl with carbohydrates as HBDs, the viscosities are significantly higher (e.g., 12, 730 cP for ChCl-sorbitol (1:1) at 30 ºC) (Q. Zhang et al., 2012). Similar to the density of DESs, their viscosities are also inversely proportional to temperature, due to decreased internal resistance of the molecules and weakened hydrogen bonds with temperature rise.

4.3. The chemical nature of the DES

Acidic DESs can be easily prepared using organic acids as HBDs. ChCl-citric acid, ChCl-maleic acid and ChCl-oxalic acid are some examples of acidic DESs. Owing to their ability to dissolve different types of materials, they have been widely used in extraction and separation processes, biomass conversion, delignification, acid-catalyzed reactions, etc. On the other hand, basic DESs (e.g., ChCl-urea, ChCl-triethanolamine, potassium carbonate-glycerol) are more appropriate for cellulose dissolution, and have also been used as catalysts in base-catalyzed reactions. Lastly, when sugars and polyols are used as HBDs, neutral DES systems can be obtained (M. Zhang et al., 2021).

4.4. The role of water

The effect of water on DESs is also very important and cannot be neglected since the presence of water may either affect the physiochemical properties of the DESs and also their supramolecular network. The hygroscopic character of most DESs will inevitably cause them to absorb water. Owing to the high polarity, water can act as hydrogen bond acceptor or hydrogen bond donor, and can interact with both HBA and HBD of the DESs. As a result, the water absorption by the DESs or the addition of water in DES mixtures to tune some of their properties must be carefully handled (El Achkar et al., 2019; Omar and Sadeghi, 2022). A relevant study on this issue was conducted by Meng et al. (2016), in which they reported that a 48-hour exposure of a dry ChCl-urea (1:2) DES to the atmosphere led to a water uptake of about 5 wt% which caused the melting temperature of the DES to decrease by half, from 30 ºC (dry DES) to ca. 15 ºC (with 5 wt% of water).

In terms of hydrogen bonding, at low water content, the water molecules are incorporated into the DES network and may reinforce the hydrogen bonding of the DES. However, over a certain limit, the interactions between DES components are weakened and disrupted by water, which basically leads to a solution of the DES free components (Hammond et al., 2017; Zhekenov et al., 2017). Further investigations are needed for better understanding the effect of water on the physiochemical properties and molecular network of the DESs.

4.5. Thermal and chemical stability

The stability is another crucial aspect to consider about DESs, since their stability can influence their physical properties and potential applications. The stability of DESs can be dependent of many factors, e.g., of DES composition, molar ratio, preparation conditions, functional groups, number of hydrogen bonds, etc. (M. Zhang et al., 2021).

The thermal stability of DESs has been investigated in different studies. Rodriguez et al. (2019) reported that the thermal decomposition temperature of different ChCl-carboxylic acid DESs followed the order: ChCl-glutaric acid (235 ºC) > ChCl-glycolic acid (218 ºC) > ChCl-malic acid (211 ºC) > ChCl-lactic acid (173 ºC) > ChCl-levulinic acid (159 ºC) > ChCl-malonic acid (125 ºC). Alternatively, González-Rivera et al. (2020) studied the thermal behavior of DESs composed of choline chloride as HBA and two types of HBDs (carboxylic acids or polyols) and found that a complex decomposition process of the entire DES occurs, instead of a sum of evaporation steps of its individual components.

Rodriguez et al. (2019) observed that ChCl-carboxylic acid DESs are not chemically stable even prepared at room temperature for a long period of time (11 months) due to the esterification reaction that occurs between the OH-group of ChCl and COOH-groups of the HBDs in the DESs. If the individual components of DESs do not have chemical stability, the formed DES cannot be chemically stable either. More information regarding the thermal and chemical stability, as well as the electrochemical, radiolytic and biological stability of DESs can be found in the study of Chen et al. (2022).

A more in-depth discussion about the aforementioned properties of DESs, as well as other properties, such as polarity, surface tension, vapor pressure and refractive index of DES can be found elsewhere (El Achkar et al., 2021; Hansen et al., 2021; Omar and Sadeghi, 2022; M. Zhang et al., 2021).

The large variety of compounds that can act as HBAs and HBDs in the formation of the DESs enables their application in a broad range of areas, including metallurgy and electrodeposition, separations, gas capture, battery technologies, bio-catalysis, organic synthesis, biomass processing, delignification, pharmaceuticals and medical research (Hansen et al., 2021; Smith et al., 2014). One application that has recently emerged is the use of DESs for nanocellulose production. To the best of our knowledge no review article has been published yet dedicated exclusively to the use of DESs to produce nanocelluloses.

5. Deep eutectic solvents for the production of cellulose nanofibrils

5.1. Non-derivatizing DES pretreatments

The first paper on the production of CNFs with DESs was published recently, in 2015, by Sirviö et al., in which a DES of ChCl-urea (1:2) was used to facilitate the nanofibrillation of a bleached birch pulp by microfluidization. The DES pretreatment of cellulose pulp was carried out at 100 ºC for 2 h after which different CNF samples were obtained by varying the chamber size and pressure conditions of the microfluidizer. After mechanical disintegration, a homogeneous, turbid and gel-like material was obtained, displaying a web-like nanofibrous structure composed of nanofibril bundles with widths ranging from 15 to 200 nm and individual nanofibrils of 2–5 nm. The ChCl-urea DES treatment did not cause any change in the DP and crystalline structure of cellulose. This DES system was also used by Suopajärvi et al. (2017) to pretreat several cellulose board pulp grades and a bleached birch pulp (reference), under the same reaction conditions (100 ºC, 2 h), prior to the nanofibrillation with a Masuko grinder or a microfluidizer. Both mechanical treatments were effective, resulting in gel-like CNFs with widths from 2 nm to 80 nm. However, Masuko-ground samples had slightly more bunches of nanofibrils than the microfluidized ones. In 2020, the same research group, used the same DES pretreatment methodology plus mechanical grinding to produce micro/nanofibrils

from recycled boxboard pulp. The produced cellulose fibrils were also further used as reinforcements (2–6 wt%) in board sheets, leading to better mechanical properties (tear index, elongation at break, tensile strength and tensile stiffness) compared to the pulp only treated by grinding (reference). However, after a preliminary cost assessment, the authors reported that the costs associated with DES-micro/nanofibrils as reinforcement agent were around 30% higher when compared to reference material, considering the costs of the chemicals involved (ChCl and urea) as well as their recycling (Laitinen et al., 2020). At the same year, Jonasson et al. (2020) applied two conventional pretreatments (TEMPO-oxidation at near neutral pH, and carboxymethylation) and two non-derivatizing DES pretreatments (ChCl-urea and ChCl-imidazole (IMI)) to aspen wood pulp, and after microfluidization, CNFs of fine grade (height ∼ 2 nm) were obtained from the derivatizing pretreatments, whereas for the CNFs from the non-derivatizing pretreatments, both fine (height ∼ 2 nm) and coarse (2 nm < height < 100 nm) grades were observed. The DES-CNFs possessed higher thermal stability and stiffness than the TEMPO and carboxymethylated CNFs. Sirviö et al. (2020) found that among these two DES systems, the ChCl-IMI showed higher swelling ability of cellulose fibers than ChCl-urea under the same conditions, which was attributed to the higher alkalinity of IMI. Furthermore, the authors observed that the ChCl-IMI pretreatment had a minimal impact on the DP and crystallinity of the treated pulps (hardwood kraft pulp), whereas the ChCl-urea led to a slight decrease in the DP. Despite that, the microfluidization of the DES treated pulps led to CNFs with a heterogeneous diameter distribution ranging from about 5 nm (individual nanofibrils) to tens of nanometers (nanofibril aggregates). According to the authors, the ChCl-urea and ChCl-IMI apparently have a different behavior when used to pretreat cellulose fibers. In an aqueous solution, urea interacts weakly with the carbon ring plane of cellulose by either van der Waals forces or electrostatic interactions. In addition, the two NH_2 groups and the oxygen atom of urea contribute to the H-bond interaction with cellulose. In the case of imidazole, glucose ring and imidazole ring stacking was proposed by molecular studies, which was attributed to van der Walls forces. Due to the low polarity of the NH group (N1) of imidazole, the hydrogen bonding with glucose is established by the nitrogen atom (N3). Two different non-derivatizing DES systems based on ammonium thiocyanate-urea and guanidine hydrochloride-urea (both with molar ratio of 1:2) were also successfully used by Li et al. (2017) for the production of CNFs with widths ranging from 13 to 19 nm. Both DESs were able to swell and loosen the cellulose fiber structure, and then facilitating the mechanical treatment (microfluidization).

5.2. Derivatizing DES pretreatments

In addition to the abovementioned non-derivatizing DES treatments, several authors have reported that acidic DESs composed of ChCl and carboxylic acids can lead to the esterification of cellulose which in turn facilitates the nanofibrillation. In this context, Li et al. (2020) compared the utilization of three different DESs (ChCl-oxalic, ChCl-glycerol and ChCl-urea) for the pretreatment of okara to prepare CNFs by high-pressure homogenization. Under the same homogenization conditions, they found that ChCl-oxalic acid was the only DES that resulted in a CNF with a loose network structure (Fig. 7) with the highest cellulose content and improved thermal stability.

A year earlier, Yu et al. (2019) showed that ChCl-oxalic acid DES could be used as an efficient pretreatment to enhance the nanofibrillation of degummed ramie fibers (RFs), shortening the time required for the subsequent ball milling from 11 to 5 h. Unlike the ChCl-urea DES (used as comparison), ChCl-oxalic acid pretreatment significantly decreased the DP of cellulose from 1733 to 876 and increased the crystallinity index (CrI) of the pretreated RFs (from 78.8% to 82.4%). According to Yu and coworkers, the DP decrease resulted from cellulose chain breakage in the amorphous regions, while the increase of CrI was probably due to the dissolution of amorphous cellulose
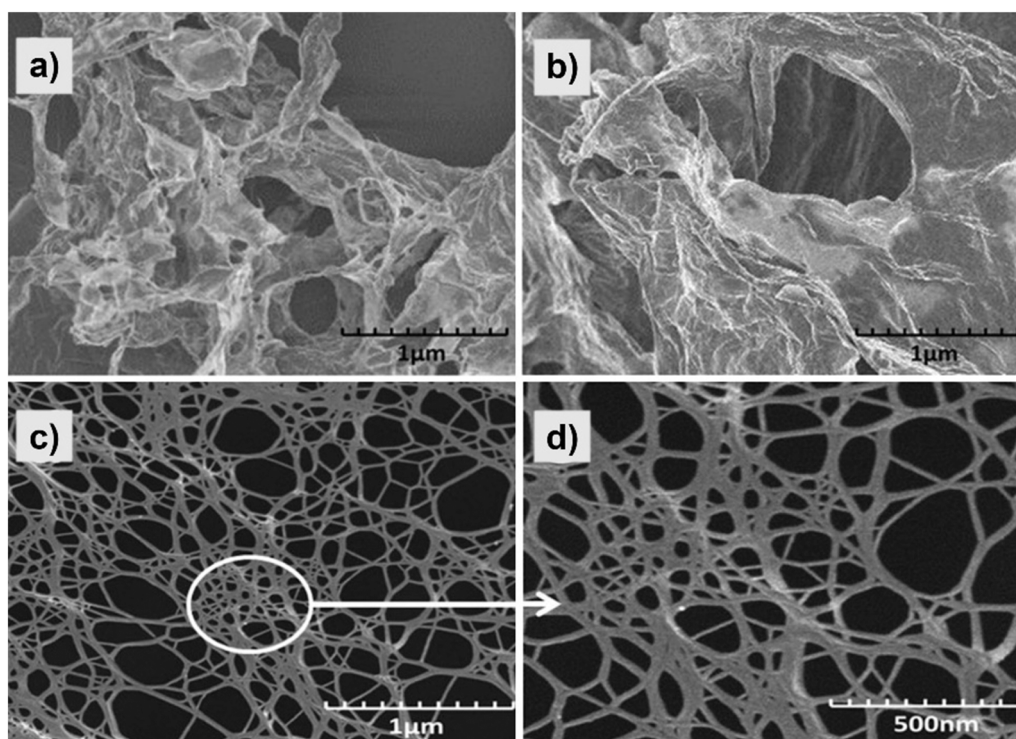
Fig. 7. SEM images of okara after the pre-treatment with DES followed by high-pressure homogenization: ChCl-glycerol (a), ChCl-urea (b), and ChCl-oxalic (c and d). Adapted from Li et al. (2020).

and the removal of some oligosaccharides. After 5 h of ball milling, a CNF with a mass yield of 94%, mean equivalent spherical diameter of 262 nm and lower thermal stability than the original RFs (T_{max} reduction from 365 to 323 ºC) was obtained. In another work conducted by the same research group, they found that the ChCl-oxalic acid pretreatment could be also efficiently applied to nanocellulose extraction from raw ramie fibers without requiring additional pulping/bleaching processes (Yu et al., 2021). After DES pretreatment, glucan content increased from 67.9% to 90.3%, and the removals of xylan and lignin reached 55.3% and 27.4%, respectively. Similar to their previous study Yu et al. (2019), ChCl-oxalic acid pretreatment significantly reduced the time needed for the ball milling and the resulting CNF exhibited an elongated network morphology with an average width of fibrils of 14 nm and length of 523 nm. A different approach to produce nanocellulose was adopted by Ma et al. (2019). Here, three hydrated DESs were synthesized by mixing the ChCl-oxalic acid (1:1 molar ratio) with 10%, 20%, and 30% (v/v) of water and were used to pretreat kraft pulp from poplar wood before an ultrasonic treatment. By molecular dynamics simulation, they proposed that water addition led to the formation of new Cl-H_2O and oxalate-H_2O hydrogen bonds rather than destroying the molecular interactions between the DES components. Furthermore, water did not affect greatly the solvatochromic parameters of the DES, but instead facilitated the ionization of oxalic acid and delocalization of Cl$^-$ ions. After the hydrated DES pretreatments (80 ºC, 1 h) and posterior ultrasonication, the 10% DES-pretreated pulp was nanofibrillated into a CNF and the 20% and 30% DES-pretreated pulps were disintegrated into CNCs. Two morphologically distinct nanocelluloses, both within the nanometer scale, were thus claimed to be obtained.

Recently, Wei et al. (2022) carried out a study aiming to investigate the hydrogen bond evolution in CNFs post-treated with ChCl-oxalic acid using different CNF:DES mass ratios (1:1, 1:2 and 1:3) and reaction times (30, 60, 90, 120 min). After treatment, CNFs exhibited lower H-bond energies and longer bond lengths than the untreated CNF, which indicated that ChCl-oxalic acid was effective in reducing the H-bond extent

in the CNFs. This happened because the ChCl-oxalic acid system formed new H-bonds with the OH-groups of CNFs, causing the partial disruption of the original CNF H-bonds. According to the authors, the DES first diffuses into the amorphous regions and attacks the O(3)H...O(5) intramolecular H-bonds that are present in larger number than the intermolecular H-bonds. Then, the DES is diffused into the crystalline regions and preferentially destroys the O(6)H...O(3′) intermolecular H-bonds.

Besides oxalic acid, other carboxylic acids were already used for the esterification of cellulose. For instance, different DES systems composed of ChCl and carboxylic acids (lactic acid (LA), formic acid (FA) and acetic acid (AA), malonic acid (MA), oxalic acid (OA) and citric acid (CA)), were used as a pretreatment combined with mechanical extrusion and colloid milling to prepare esterified CNFs from a hardwood bleached kraft pulp (S. Liu et al., 2021). All CNFs showed diameters of less than 100 nm and lengths of several microns, which means that all carboxylic acid-based DESs showed some efficiency for the production of CNFs. However, esterification was only confirmed for the CNFs pretreated with ChCl-FA and ChCl-LA, as shown by FTIR spectroscopy (peak at 1720 cm^{-1} associated to the carbonyl vibration in esters). For the remaining CNFs, this peak was not detected, meaning that weak or none cellulose esterification occurred with the other DES systems, under the used conditions (100 ºC, 3 h).

Other studies should be highlighted, such as the work done by Q. Liu et al. (2019), in which they used ChCl-LA to delignify moso bamboo (26.1% of lignin) and at same time, to produce CNFs from the pretreated fibers by microfluidization. Under optimal conditions (120 ºC, 3 h, S:L ratio of 1:25), 94.4% of lignin was removed and more than 91% of cellulose was preserved. The pretreated fibers were further subjected to mechanical disintegration resulting in a network-structured CNF with nanofiber widths of 20–80 nm, high DP value (904) and 0.26 mmol/g of carboxylic acid content. Similar to the findings of S. Liu et al. (2021), the esterification of cellulose was also observed by M. Wu et al. (2021) when they used ChCl-FA to pretreat MCC. However, the introduction of hydrophobic ester groups on the surface of cellulose resulted in

nanocelluloses with a poor dispersion in water. A distinguishing aspect about this work was the research made on the possibility of recycling and reuse of ChCl-FA and ChCl-urea (used as comparison throughout the paper). Both DESs were recycled by rotary evaporation and the corresponding recovery rates obtained for both were over 90% for each cycle. Both recycled DESs were reused to pretreat MCC under the same conditions of the fresh DESs, and after 16 h of ball milling, similar average diameters of nanocelluloses were obtained compared to those of fresh DESs. The recycling of the DESs was successfully achieved and their reuse did not significantly affect their performance to produce nanocelluloses compared to using pure DESs. Two DESs composed of ChCl and anhydrous citric acid (aCA) or citric acid monohydrate (CAm) were used by W. Liu et al. (2021) to pretreat bleached softwood kraft pulp for further production of CNFs by high-pressure homogenization. It was shown that the water of crystallization in the citric acid had a negative effect on the reactivity of the DES, which led to CNFs with larger sizes for ChCl-CAm compared to ChCl-aCA. Under optimized conditions (90 °C, 2 h), the latter DES pretreatment allowed to obtain a CNF with a mass yield of 84.2% and a uniform diameter distribution, averaging 21 ±3 nm, as well as an excellent dispersibility in water. Additionally, different DES pretreatment procedures have also been explored by some authors to prepare CNFs. For instance, an ultrafast method of CNF production was reported by Ji et al. (2021), where they used microwave-assisted (20 min, 2800 W, 80–120 °C) ternary carboxylic acid DESs (ChCl-LA-AlCl$_3$0.6 H$_2$O and ChCl-OA-AlCl$_3$0.6 H$_2$O) to pretreat sugarcane bagasse. After delignification with these two ternary DESs, the cellulose enriched materials were nanofibrillated by high-intensity ultrasonication, yielding CNFs with up to 0.84 mmol/g of carboxylic acid groups and high thermal stability. X.-Q. Wu et al. (2021) also proposed a novel three-step method to produce CNFs from elephant grass, consisting of: (1) ChCl-glycerol pretreatment in combination with a spent coffee-derived solid acid catalyst (SC-SO$_3$H); (2) bleaching step (with NaClO$_2$); and (3) ChCl–oxalic acid pretreatment. The delignified cellulose was then ultrasonicated resulting in CNFs with diameters in the range of 2–6 nm and lengths of about 800–1000 nm. The recovery of the SC-SO$_3$H catalyst and its posterior reutilization was also successfully demonstrated. The authors also found that oxalic acid dihydrate could be easily recovered with high purity by recrystallization from the resulting filtrate. Alternatively, Selkälä et al. (2016) used urea-LiCl DES system (molar ratio 5:1) as reaction medium for the succinylation of softwood dissolving pulp with succinic anhydride, under different temperatures (70–110 °C) and times (2, 6 and 24 h). Carboxyl groups (ranging from 0.34 to 0.95 mmol/g) were successfully introduced into the cellulose chain through the esterification reaction of succinic anhydride with the cellulose OH-groups in the DES. After the pretreatment under optimal conditions (70–80 °C for 2 h) followed by microfluidization, CNFs with an entangled network structure, high transparency and viscosities were claimed to be obtained.

The introduction of cationic groups on the cellulose structure was also attained by different DES systems. A recyclable DES composed of aminoguanidine hydrochloride and glycerol (AhG) was used by Li et al.

(2018) for the cationization (at 70 °C for 10 min) of two dialdehyde celluloses, with different aldehyde contents (2.18 and 3.79 mmol/g), previously obtained by sodium periodate oxidation from bleached kraft birch pulp (reaction scheme in Fig. 8). The obtained cationic dialdehyde celluloses with a charge density of 0.92 and 1.21 mmol/g were then mechanically treated (microfluidization) resulting into nanocelluloses with average individual widths of 5–6 nm. The AhG DES was also recycled using a rotatory evaporator and reused five times with a similar reaction efficiency to that of the original DES. A DES based on glycerol and betaine hydrochloride (Bh) was also tested in order to enhance the nanofibrillation of birch cellulose pulp (Hong et al., 2020a). A mechanism based on the swelling of the cellulose fibers, caused by glycerol, and subsequent esterification (with cationization) by Bh of the exposed OH-groups was proposed. After microfluidization, the authors were able to obtain CNFs with diameters of 17–20 nm, CrI of 67.7–74.4% and thermal stability similar to that of the original birch pulp.

The sulfation of cellulose using DESs was also investigated by some authors to facilitate the cellulose nanofibrillation. In this context, Sirviö et al. (2019) were able to produce sulfated celluloses with a charge density ranging from 1.4 to 3 mmol/g using softwood dissolving pulp pretreatment with sulfamic acid and urea. After passing the DES pretreated sample having 2.4 mmol/g of sulfate groups through the microfluidizer, a CNF with high viscosity and transparency (transmittances over 95%, 390–700 nm), with an average width of 4.4 nm was obtained. The carbamation of cellulose also occurred due to the reaction between cellulose and urea. In order to avoid side reactions, Li et al. (2021) replaced urea by glycerol forming a sulfamic acid-glycerol DES that was used as a pretreatment to synthesize sulfated CNFs by grinding. The prepared CNFs showed diameters of 10–25 nm (which were of 30–35 nm without DES pretreatment) and no side reactions were detected. Compared to the untreated CNF (only treated by grinding), the DES treatment facilitated the mechanical disintegration and reduced the energy consumption up to 35%. The sulfamic acid reaction with cellulose is illustrated in Fig. 9.

A summary illustration of the CNF production with DESs is shown in Fig. 10. The main DES pretreatment conditions and the corresponding CNF properties from several studies are resumed in Table 1.

6. Deep eutectic solvents for the production of lignin-containing cellulose nanofibrils

CNFs are typically produced from bleached cellulose pulps with low lignin contents. However, over the years, the use of lignocellulosic materials for the production of lignin-containing cellulose nanofibrils (LCNFs) has gained considerable interest. The use of lignocellulosic materials is more economically and environmentally advantageous, since it allows not only to save costs associated to lignin removal and bleaching steps, but also to significantly reduce or completely avoid the use of toxic and hazardous chemicals that are commonly employed, for instance, to obtain bleached pulps (Trovagunta et al., 2021). It has also been reported that the presence of lignin can confer to LCNFs a high
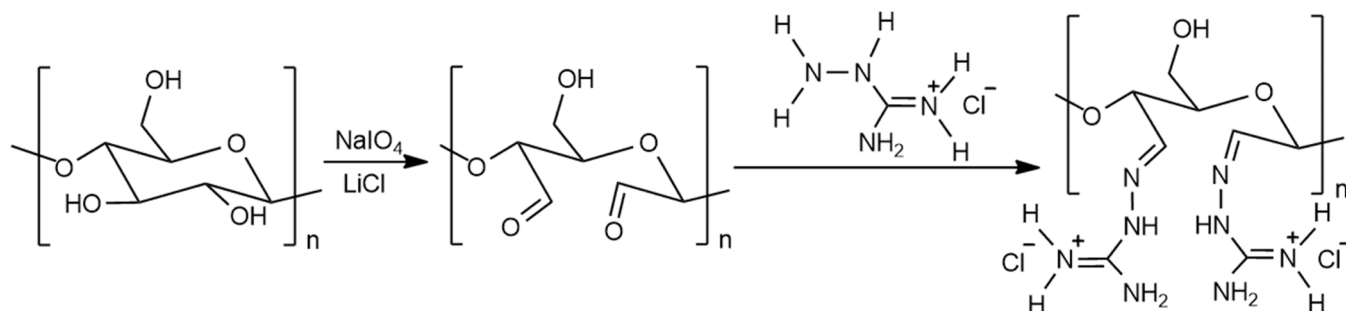

Fig. 8. Sequential periodate oxidation and cationization with aminoguanidine hydrochloride of cellulose (Li et al., 2018).
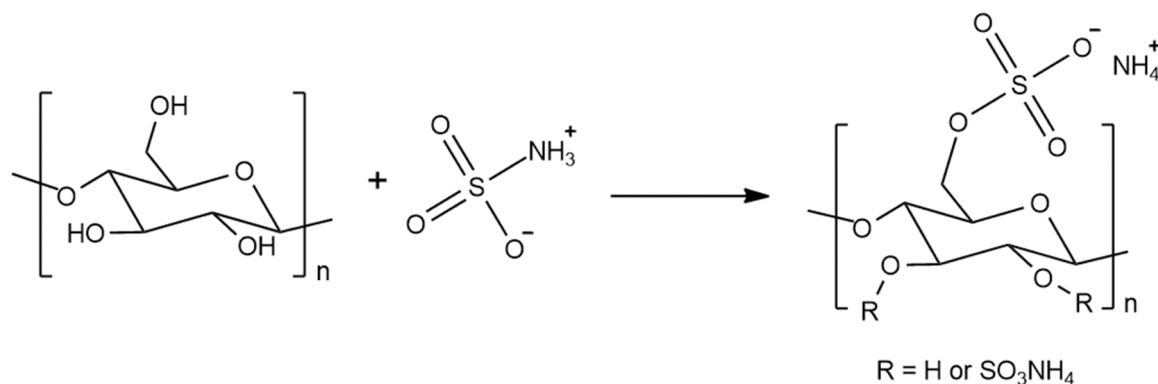
Fig. 9. Reaction between sulfamic acid and cellulose (Sirviö et al., 2019).
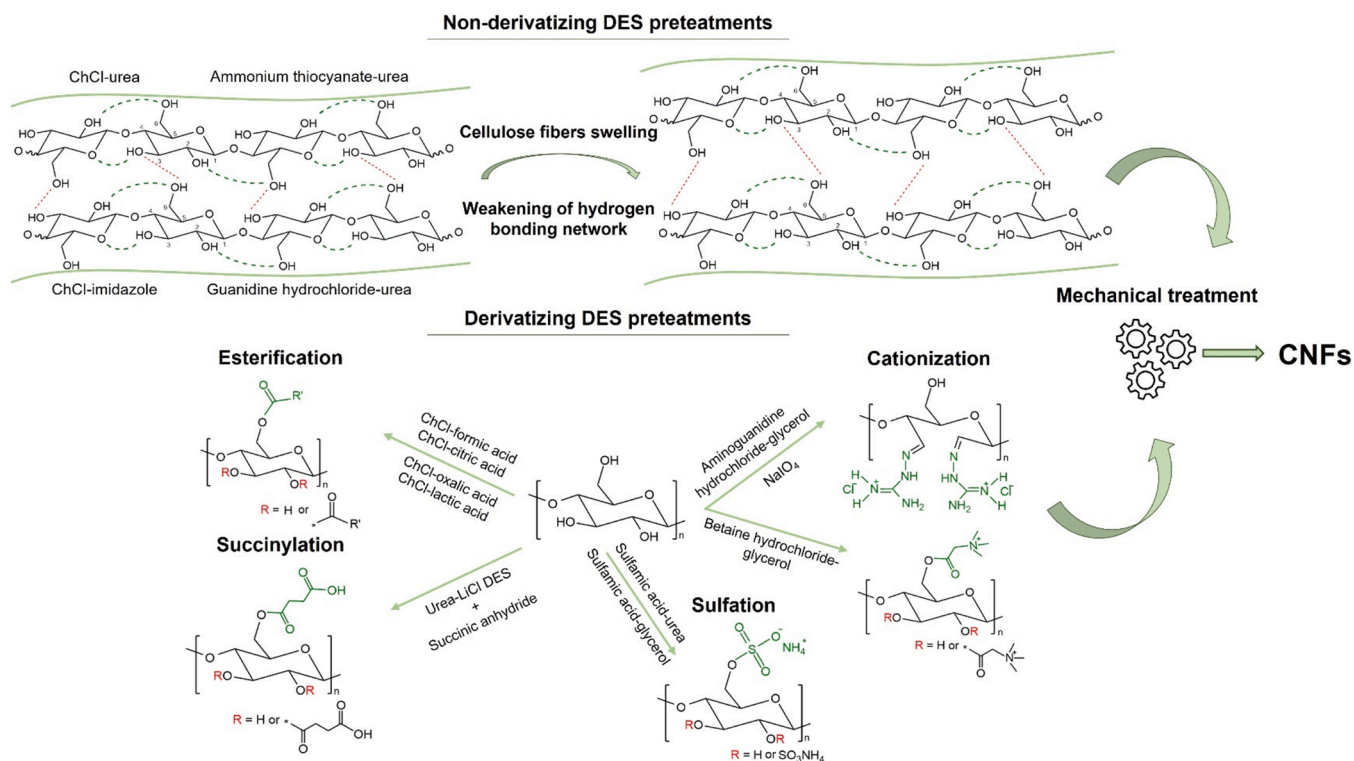

Fig. 10. Schematic illustration of CNF production using DESs.

thermal stability, UV-blocking performance, antioxidant activity and increased hydrophobicity (K. Liu et al., 2021).

Several DES systems have already been applied in this regard, i.e., for the pretreatment of lignocellulosic feedstocks to subsequently obtain LCNFs. For example, Hong et al. (2020b) used an acidic DES (ChCl-OA, 1:1) for the partial delignification of luffa sponge followed by the fibrillation of the obtained cellulose-rich residue into nanocelluloses by a two-step ultrasonication treatment. The DES pretreatment under optimal conditions (90 ℃ and 150 min) resulted in a lignin containing nanocellulose with a high total yield of 59% and an average diameter of 28 nm. The presence of lignin (ca. 11 wt%) on the nanofiber surfaces possibly mitigated the esterification of cellulose. On the other hand, using ChCl-LA DES to pretreat lignocelluloses (at 100 ℃ for 3 h) with different lignin contents (0.8–17.5%) combined with mechanical colloid milling, Q. Zhang et al. (2021) were able to obtain esterified LCNFs with diameters within 20–100 nm and high yields (up to 85%). No significant differences were observed between the diameters of LCNFs prepared from the lignocelluloses with different lignin contents, meaning that the

presence of lignin had a minor influence on the efficiency of the treatments using ChCl-LA. Furthermore, C. Liu et al. (2020) reported that lignin may be able to act as a cross-linking (binder) agent promoting the formation of a strong network structure in LCNFs. In this study, a LCNF was obtained from energy cane bagasse using microwave assisted ChCl-LA pretreatment (at 110 ℃ for 30 min) in combination with ultrasonication. The LCNF obtained from DES pretreatment showed a more entangled structure, higher viscosities, storage modulus and loss modulus than the reference CNF isolated by NaOH/NaClO₂ treatment and ultrasonication. Four acidic DESs (ChCl-LA, ChCl-levulinic acid, ChCl-malic acid and ChCl-glutaric acid) and one alkaline DES (K₂CO₃-glycerol) were tested and compared for the sequential delignification and nanofibrillation of wheat straw, corn stalk and rapeseed stem (Suopajärvi et al., 2020). Both ChCl-LA and K₂CO₃-glycerol DESs exhibited a good delignification performance and led to the pretreated samples with the highest cellulose contents. The microfluidization of these samples resulted in LCNFs with individual nanofibers with diameters of 4–6 nm and CrIs of 38–54%. Meanwhile, Taheri et al. (2021)

Table 1

Pretreatment conditions and CNF properties obtained by different DES systems.

Raw material	DES pretreatment			Mechanical treatment	CNF properties				Ref.
	DES system (Molar ratio)	Functionalization	Conditions		Dimensions	Crystallinity (%)	DP	Additional outcomes	
Bleached birch pulp (*Betula pendula*)	ChCl-urea (1:2)	-	100 °C; 2 h	Microfluidization (Mf)	Nanofibril bundles: W: 15–200 nm Individual nanofibrils: W: 2–5 nm	Before Mf: No change After Mf: ↓ from 66 to 41–63	Before Mf: No change After Mf: ↓ from ~3500 to ~1750–~2850	0.1% CNF suspensions transmittance up to 71% (700 nm); DES-treated pulp with 90% of mass yield	(Sirviö et al., 2015)
-Waste board -Waste milk container board -Fluting	ChCl-urea (1:2)	-	100 °C; 2 h	Grinding or Microfluidization	W: 2–80 nm	47–61	-	CNFs in form of viscous gels with shear thinning behavior	(Suopajärvi et al., 2017)
Aspen wood pulp	ChCl-urea (1:2); ChCl-imidazole (3:7)	-	100 °C; 2 h 100 °C; 4 h	Microfluidization	Fine grade: H ~2 nm Coarse grade: 2 < H < 100 nm	-	-	Mass yields of 52% and 43% for ChCl-urea and ChCl-imidazole CNFs, respectively	(Jonasson et al., 2020)
Hardwood kraft pulp	ChCl-imidazole (3:7)	-	60–100 °C; 15–180 min	Microfluidization	Individual nanofibrils: D ~ 5 nm Nanofibril aggregates: D of tens of nanometers	Before Mf: ↓ from 69 to 64–67	Before Mf: Maximum ↓ from 3960 to 3740	DES-CNFs showed an onset temperature (T$_{on}$) slightly lower than that of the original cellulose pulp (273–278 °C vs. 288 °C, respectively)	(Sirviö et al., 2020)
Bleached birch Kraft pulp (*Betula pendula*)	Ammonium thiocyanate-urea (1:2); Guanidine hydrochloride-urea (1:2)	-	100 °C; 2 h	Microfluidization	W: 13–19 nm	-	Before Mf: ↓ from 3500 to 3315–3337	Both DES-pretreated birch fibers exhibited a slight increase in fiber width (from 17.8 to 18.0–18.4 μm) indicating the fiber swelling; The mass yields after DES pretreatments were around 90%	(Li et al., 2017)
Okara	ChCl-oxalic acid; ChCl-glycerol; ChCl-urea	-	100 °C; 30–120 min	High-pressure homogenization (HPH)	ChCl-oxalic acid CNF: Aver. D: 27 nm; D distribution between 11–65 nm	-	After HPH: ↓ from 346 to 307–329	The ChCl-oxalic acid CNF was the only one with a loose network structure; The thermal stability was improved	(Li et al., 2020)
Degummed ramie fibers	ChCl-oxalic acid (1:1)	Esterification	~25 °C; 7 h	Ball milling (BM)	Mean equivalent spherical diameter of 262 nm (determined by DLS)	Before BM: ↑ from 78.8 to 82.4 After BM: ↓ to 66.5	Before BM: ↓ from 1733 to 876 After BM: ↓ to 305	The mass yield of CNF after DES pretreatment was 94%; Decrease in thermal stability: T$_{max}$ decreased from 365 to 323 °C; DES pretreatment shortened the ball milling time from 11 to 5 h	(Yu et al., 2019)
Raw ramie fibers	ChCl-oxalic acid (1:1)	Esterification	100 °C; 4 h	Ball milling	Aver. W: 14 nm Aver. L: 523 nm	79	-	Thermal stability: T$_{on}$ = 308 °C T$_{max}$ = 340 °C	(Yu et al., 2021)
Poplar wood kraft pulp	ChCl-oxalic acid (1:1) + 10% (v/v) of H$_2$O	Esterification	80 °C; 1 h	Ultrasonication (Us)	D: 11–20 nm; L: 300–2000 nm	Before Us: ↑ from 66 to 69	Before Us: ↓ from 1452 to 791	Water facilitated the ionization of oxalic acid and delocalization of Cl⁻ ions; CNF with good thermal stability (T$_{on}$ ~ 280 °C)	(Ma et al., 2019)
Hardwood bleached kraft pulp	1-ChCl-formic acid (1:2) 2-ChCl-lactic acid (1:9) 3-ChCl-acetic acid (1:2) 4-ChCl-malonic acid (1:1) 5-ChCl-oxalic acid (1:1) 6-ChCl-citric acid (1:1)	Esterification	50–100 °C; 3 h	Extrusion + Colloid milling	CNFs from DES 1–3: D: 15–30 nm CNFs from DES 4–5: D: 20–50 nm CNFs from DES 6: D: 10–25 nm Lengths of several microns	1- 79 2- 80 3- 74 4- 73 5- 74 6- 75	↓ from 680 to 300–500	DES3-DES6 were inefficient for the esterification of cellulose, according to FTIR; The yields of all CNFs remained at 72–88%	(S. Liu et al., 2021)

Table 1 (*continued*)

Raw material	DES pretreatment			Mechanical treatment	CNF properties				Ref.
	DES system (Molar ratio)	Functionalization	Conditions		Dimensions	Crystallinity (%)	DP	Additional outcomes	
Moso bamboo	ChCl-lactic acid (1:9)	Esterification	120 °C; 3 h; S/L 1:25 (Optimal)	Microfluidization	Nanofibril bundles: W: 20–80 nm L: > 4 µm	Before Mf: ↑ from 49 to 60	Before Mf: ↓ from 1400 to 1376 After Mf: ↓ to 904	DES pretreated fibers with higher initial and maximum degradation temperatures compared to original fibers (e.g., T_{max} from 331 to 352 °C); Carboxylic acid content of 0.26 mmol/g	(Q. Liu et al., 2019)
Microcrystalline cellulose	ChCl-formic acid (1:2)	Esterification	90 °C, 2 h (Optimal)	Ball Milling	CNCs Aver. D: 8 nm CNFs Aver. D: 11 nm	69–72	-	The recovery rate of ChCl-FA reached 92% after three cycles of reuse; The recycled ChCl-FA (after the third cycle) showed a performance similar to that of the fresh DES	(M. Wu et al., 2021)
Bleached softwood kraft pulp	ChCl-anhydrous citric acid (aCA) (1:1)	Esterification	90 °C, 2 h (Optimal)	High-pressure homogenization	Aver. D: 21 nm	↑ from 69 to 81	-	CNF with a mass yield of 84%, 0.09 mmol/g of carboxylic groups, high thermal stability (T_{on} = 313 °C, T_{max} = 364 °C) and excellent dispersibility in water	(W. Liu et al., 2021)
Sugarcane bagasse	Microwave assisted: ChCl-lactic acid-$AlCl_3.6H_2O$ (1:1:0.2) ChCl-oxalic acid-$AlCl_3.6H_2O$ (1:1:0.2)	Esterification	100 °C, 20 min (Optimal)	Sweeping frequency ultrasound (30 min) + High-intensity ultrasonication	W: 15–17 nm, L: 400–600 nm, H: 6–7 nm	58–61	-	CNFs with 0.74–0.84 mmol/g of carboxylic acid groups and improved thermal stability	(Ji et al., 2021)
Elephant grass (*Pennisetum purpureum*) stalks	Three step pretreatment: 1- ChCl-glycerol (1:2) + coffee-derived solid acid (SC-SO_3H) catalyst 2-Bleaching (7% $NaClO_2$) 3- ChCl-oxalic acid (1:1)	-	1-140 °C, 3 h 2-90 °C, 4 h 3-80 °C, 3 h	Ultrasonication	D: 2–6 nm L: 800–1000 nm	Before Us: ↑ from 47 to 73–74	-	Oxalic acid dihydrate could be easily recovered by recrystallization; SC-SO_3H catalyst could also be recovered and reused	(X.-Q. Wu et al., 2021)
Commercial softwood dissolving pulp	Urea-LiCl (5:1) + Succinic anhydride	Esterification (Succinylation)	70–80 °C, 2 h (Optimal)	Microfluidization	Individual nanofibrils: CNF70: H: 0.5–4 nm CNF80: H: 1.5–4.5 nm	Before Mf: ↑ from 65 to 68–69 After Mf: ↓ to 57–58	Before Mf: ↓ from 1816 to 1646–1651	DES pretreated cellulose with 0.57–0.69 mmol/g of carboxyl groups; Highly viscous CNFs with typical shear-thinning properties; The thermal stability of the succinylated CNFs decreased compared to the original dissolving pulp	(Selkälä et al., 2016)
Dialdehyde cellulose obtained from bleached kraft birch pulp	Aminoguanidine hydrochloride-Glycerol (1:2)	Cationization	70 °C, 10 min	Microfluidization	Individual nanofibrils: W: ~ 5 nm	Before Mf: ↑ from 57 to 63	-	Cationic charge density of ~0.92 mmol/g; The DES was reused five times without decreasing the reaction efficiency	(Li et al., 2018)
Bleached birch pulp (*Betula pendula*)	Betaine hydrochloride-glycerol (1:2) (2:3)	Cationization	150 °C, 1 h (Optimal)	Microfluidization	D: 17–20 nm L: > 500 nm	↓ from 75 to 68–74	Before Mf: ↓ from 3500 to 690–780	Cationic charge of 0.05–0.06 mmol/g; CNFs with thermal stability comparable to that of the original birch cellulose (T_{max} only decreased from 346 °C to 339–341 °C); CNF mass yields of 70–73%	(Hong et al., 2020a)
Softwood dissolving cellulose pulp	Sulfamic acid-urea (1:2)	Sulfation	150 °C, 30 min	Microfluidization	W: ~ 4 nm, with a minor presence of elemental fibril aggregates D: 7–17 nm	-	Before Mf: ↓ from 1822 to 310	Sulfate group content of 2.40 mmol/g; CNFs with a transparency over 95% at 390–700 nm, viscosity over 2500 mPa s at a shear rate below 1 s^{-1} and shear thinning behavior	(Sirviö et al., 2019)
Bleached kraft pulp board	Sulfamic acid-glycerol (1:3)	Sulfation	100 °C, 1 and 1.5 h	Grinding (G)	D: 10–25 nm	↓ from 64.0 to 53.3–61.7	Before G: ↓ from 1012 to 638–412	Sulfate groups of 0.18–0.70 mmol/g; DES pretreatment reduced up to 35% the energy consumption of the grinder	(Li et al., 2021)

The dimensions of the CNFs are sometimes related to a specific pretreatment condition or to different pretreatment conditions

used the K_2CO_3-glycerol DES to pretreat wood sawdust prior to fibrillation by twin-screw extrusion and found that this pretreatment enabled a decrease of the energy consumption of the extruder by about 24%. The ChCl-LA system was also used and compared with ChCl-urea and ChCl-glycerol DESs for the pretreatment of Mongolian oak to subsequently obtain LCNFs by high-pressure homogenization (Kwon et al., 2021). Although the ChCl-LA pretreatment resulted in higher lignin and hemicellulose removals than the other two DESs, less efficient defibrillation was observed in the LCNFs prepared from this DES, according to the authors. Very recently, C. Liu et al. (2022) deployed a very fast (30 s at 110 ºC) microwave-assisted NADES pretreatment (betaine hydrochloride-glycerol) followed by microfluidization to prepare LCNFs from energy cane bagasse. Under an optimal betaine hydrochloride-glycerol molar ratio (1:2), a LCNF with lignin content of 15%, ca. 8 nm in diameter and several micrometers in length was obtained. The highly entangled network structure of the obtained LCNF and the binding effect of lignin provided to the LCNF superior rheological properties. The esterification reaction between cellulose and betaine hydrochloride was also confirmed by NMR. At the end of the pretreatment, the NADES could be recovered with recovery percentages higher than 90%, and further reused.

Succinylation of lignocellulosic materials has also been a viable route to prepare LCNFs. For example, Sirviö and Visanko (2017) used a DES based on triethylmethylammonium chloride (TEMACl) and imidazole combined with succinic anhydride to pretreat unbleached spruce groundwood pulp (GWP) with a high lignin content (27%), and compared the reaction efficiency with that for bleached cellulose pulps, pretreated under similar conditions. After the succinylation reaction, the pretreated unbleached GWP exhibited high carboxylic acid contents (1.9–3.3 mmol/g), which were clearly superior to those obtained for bleached pulps. Further microfluidization enabled the production of highly anionic wood nanofibers. Years later, the same research group also employed this pretreatment system for the mechanochemical succinylation of spruce sawdust. Here, the sawdust was simultaneously mixed with the DES plus succinic anhydride, and milled using a planetary ball mill, for 15 min, followed by a thermal post-treatment at 100 ºC for 15, 30, or 60 min. Similarly to Sirviö and Visanko (2017), a significant amount of carboxylic acid groups (up to 3.5 mmol/g) were found on the milled succinylated sawdust samples. The authors concluded that to achieve an effective reaction with succinic anhydride, the presence of a DES is required, since its absence did not result in an increase in the carboxylic acid content compared to the original sawdust. The further microfluidization provided wood nanofibers exhibiting a heterogeneous size distribution (Sirviö et al., 2021). It has been reported that the large size variation on LCNFs could result from the binding effect of lignin that holds the microfibrils together, reducing the fibrillation efficiency (Solala et al., 2020). The succinylation reaction mechanism of lignocelluloses in the presence of imidazole is shown in Fig. 11.

In another investigation, Sirviö (2018) also used the TEMACl-Imidazole DES as a reaction medium, but this time, for the cationization of softwood dissolving cellulose pulp and unbleached spruce GWP in order to obtain cationic cellulose nanofibers (CCNFs) and cationic wood nanofibers (CWNFs), respectively. In addition to DES, betaine hydrochloride was used as cationization reagent and *p*-toluenesulfonyl (tosyl) chloride as a coupling agent. After the cationization reaction (at 70 ºC for 4 h), the cationized unbleached GWP showed a slightly lower cationic group content compared to the cationized dissolving pulp (0.70 mmol/g vs 0.92 mmol/g, respectively). Despite that, both cationized pulps were fibrillated by microfluidization, yielding long nanofibers with diameters of less than 10 nm, as well as some large nanofiber aggregates, especially for CWNFs, with diameters around 200 nm. A possible reaction mechanism for the cationization of lignocellulose using this pretreatment was proposed (Fig. 12).

Cationic lignocellulose nanofibers (CLCNFs) from sugarcane bagasse (24% of lignin) were also produced by Yao et al. (2022), through the use of a DES composed of tetraalkylammonium hydroxide and 1,

3-dimethylurea (TEAOH and 1,3-DMU) together with glycidyltrimethylammonium chloride (GTAC). CLCNFs with 1.0–1.8 mmol/g of quaternary ammonium groups and high fibrillation degrees (76–93%) were obtained after high-pressure homogenization. Compared to a reference LCNF (prepared without cationic modification), CLCNFs showed better individualized structures with a homogeneous size distribution and higher transmittances in the UV–visible range. Representative TEM images and visual appearances of the LCNF and CLCNF are shown in Fig. 13.

The sulfation of lignocelluloses via sulfamic acid-urea pretreatment for further production of LCNFs has also been performed in several works (Li et al., 2019; Sirviö and Visanko, 2019, 2020; Zhu et al., 2022). Using this DES system, Sirviö and Visanko, 2019 were able to introduce a high content of sulfate groups (3.1 mmol/g) onto unbleached spruce GWP and sawdust, a very close value to that obtained using a bleached dissolving pulp (3.0 mmol/g). It was therefore concluded that the presence of lignin and hemicelluloses did not impair the reactivity of both GWP and sawdust with the DES. According to the authors, this reaction occurs on the aliphatic OH-groups of lignocellulose, which are converted into sulfate esters, while the aromatic moieties remain unreactive, due to the selectivity of sulfamic acid. After microfluidization, individual anionic wood nanofibers with diameters around 3 nm were obtained. Some large nanofiber aggregates were also observed, probably because the presence of lignin hindered the complete nanofibrillation of the fibers. The same DES pretreatment and subsequent microfluidization was used to prepare LCNFs, by the same authors, aiming to investigate the LCNF efficiency as adsorbents for heavy metals (namely, lead and copper) (Sirviö and Visanko, 2020). The same approach was used by Zhu et al., 2022 to produce highly sulfated LCNFs (up to 3.5 mmol/g) that were further processed into aerogels showing satisfactory thermal insulating performance and fire retardancy properties. In turn, Li et al., 2019 used this DES pretreatment with simultaneous milling followed by post-heating (105 ºC for 0.5 h) aiming to produce anionic sawdust nanofibers after microfluidization. This strategy allowed them to pretreat spruce timber sawdust using considerably higher consistencies (20–60 wt%) than those that are typically used (1–5 wt%). The increase in the consistency led to a decrease trend in the sulfate groups of the obtained anionic nanofibers; however, the amount of sulfate groups remained high, ranging from 3.1 to ~1.2 mmol/g (from 20 to 60 wt% of consistency).

From these studies, some conclusions can be drawn about the role of lignin. Different authors observed that oppositely to bleached CNFs, some large nanofiber aggregates can be present in the LCNFs, indicating that the presence of lignin in the lignocellulosic feedstocks hinders their complete nanofibrillation (Sirviö, 2018; Sirviö et al., 2021). In addition to cellulose nanofibers, the LCNFs can also have some coarse and irregular particles that may originate from lignin (Sirviö, 2018). Nevertheless, it appears that lignin does not affect to a great extent the diameters of cellulose nanofibrils and does not impair the introduction of functional groups by DESs into the cellulose structure (Sirviö and Visanko, 2019; Q. Zhang et al., 2021). In fact, some authors have even assumed that the chemical modifications may also occur in the OH-groups of lignin (Sirviö and Visanko, 2020). Compared to CNFs, LCNFs have improved interfacial compatibility with other polymers due to the presence of both hydrophilic and hydrophobic groups in lignin, and UV-blocking performance (Sirviö, 2018; Q. Zhang et al., 2021).

Table 2 provides an overview of the DES pretreatment conditions used in literature to prepare LCNFs, as well as the main properties of the resultant LCNFs.

7. Applications of CNFs and LCNFs prepared from DES pretreatments

Several applications have been studied for the (ligno)nanocelluloses ((L)CNFs) produced from DES pretreatments. This type of (L)CNFs have been used as adsorbents, for the removal of lead and copper (Sirviö and
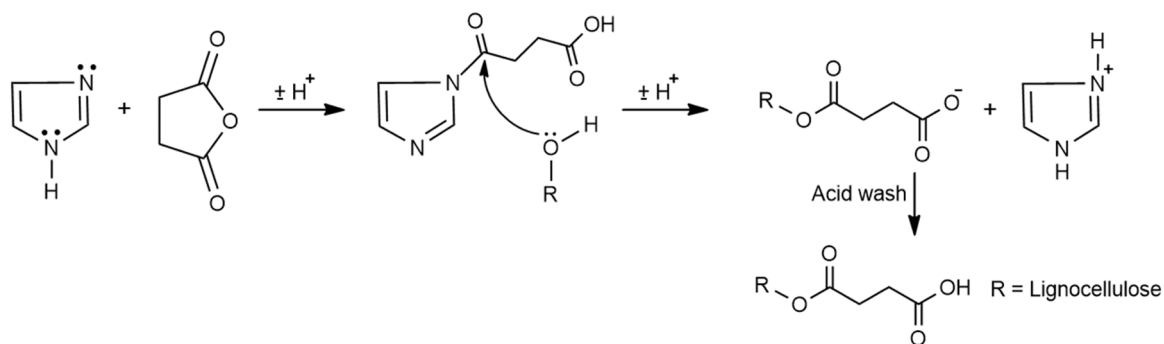
Fig. 11. Reaction mechanism of OH-groups of lignocelluloses with succinic anhydride in the presence of imidazole (Sirviö and Visanko, 2017).
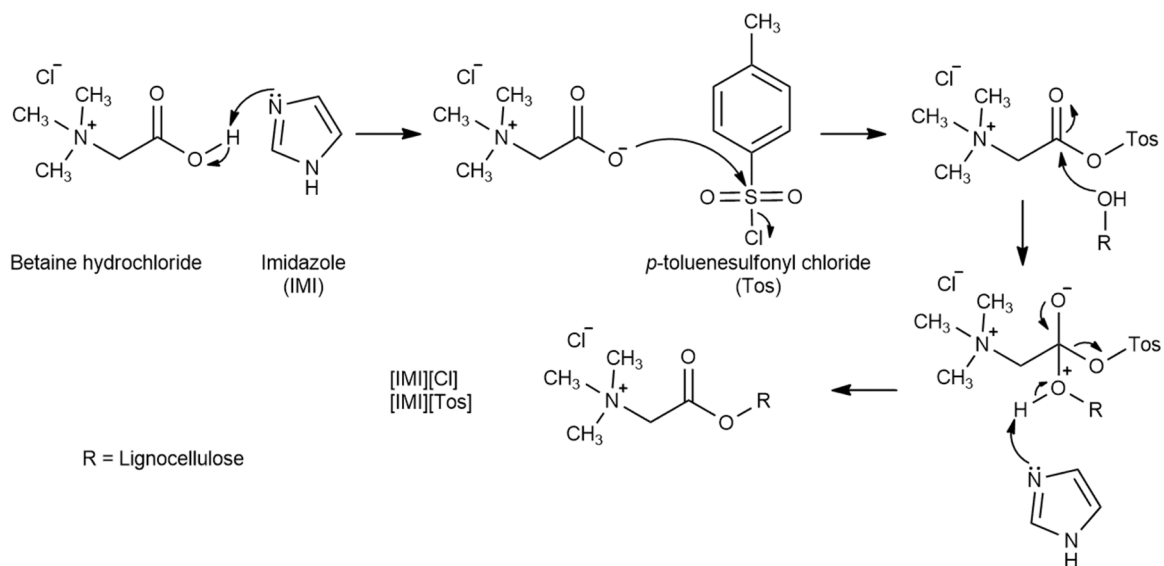

Fig. 12. Possible reaction mechanism for the cationization of lignocellulose by tosylation using imidazole-based DES and betaine hydrochloride (Sirviö, 2018).
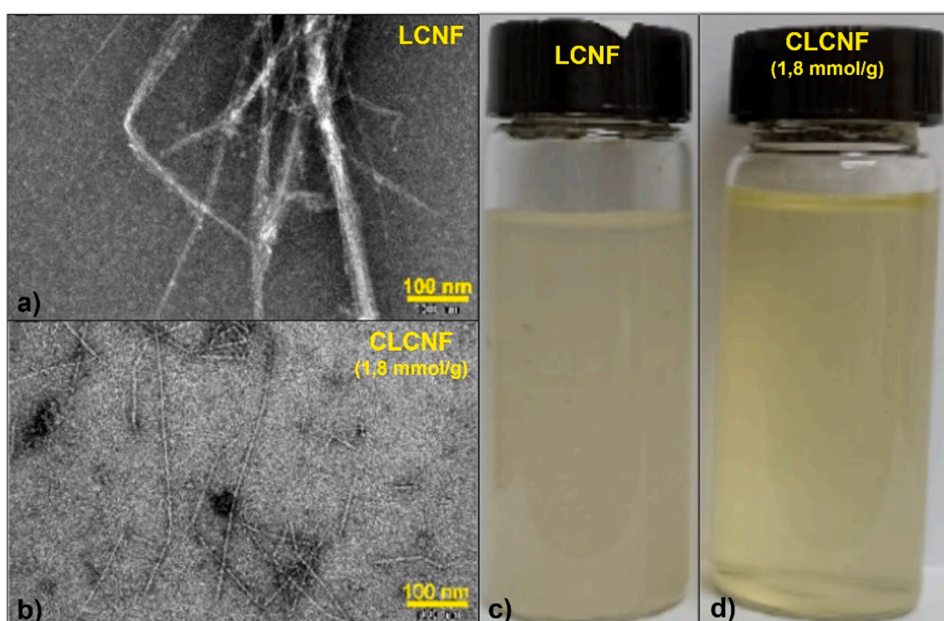

Fig. 13. TEM images of LCNF (a) and CLCNF (b) and their correspondent visual appearances (c and d, respectively). Adapted from Yao et al. (2022).

Table 2
Pretreatment conditions and LCNF properties obtained by different DES systems.

Raw material (lignin content)	DES pretreatment			Mechanical treatment	LCNF properties			Ref.
	DES system (Molar ratio)	Functionalization	Conditions		Dimensions	Crystallinity (%)	Additional outcomes	
luffa (17.8%)	ChCl-oxalic acid (1:1)	Lignin possibly mitigated the esterification	90 ºC, 150 min (Optimal)	Ultrasonication	D: 11–134 nm, Aver. D: 28 nm	72	Total nanocellulose mass yield of 59%; LCNF degradation with T_{max} = 343 ºC	(Hong et al., 2020b)
Poplar wood chips (0.8–17.5%)	ChCl-lactic acid (1:9)	Esterification	100 ºC, 3 h	Colloid milling	D: 20–100 nm, L: few microns	69–73	Lignin had no obvious effect on the dispersion of lignocelluloses using ChCl-LA DES; Similar diameters of LCNFs were obtained regardless of the initial lignin content; The LCNFs exhibited mass yields of ~ 80%	(Q. Zhang et al., 2021)
Energy cane bagasse (32.3%)	Microwave assisted ChCl-lactic acid (1:10)	Esterification	110 ºC, 30 min (Optimal)	Ultrasonication (Us)	-	Before Us: ↑ from 44 to 71	LCNF exhibiting good suspending stability (one month before precipitation), highly entangled structure, with shear-thinning and solid-like elastic behaviors (at 0.5 wt%); Lignin can act as a cross-linking (binder) agent; Recoverable yield of NADES ~ 90%	(C. Liu et al., 2020)
Wheat straw (22.1%) Corn stalk (24.4%) Rapeseed stem (18.5%)	- ChCl-lactic acid (1:2; 1:5) - ChCl-levulinic acid (1:2); - ChCl-malic acid (1:1); - ChCl-glutaric acid (1:1); - K_2CO_3-glycerol (1:5)	-	80 or 100 ºC, 8–24 h	Microfluidization	Individual nanofibrils: Aver. D: 4–6 nm	38–54	ChCl-LA and K_2CO_3-glycerol DESs resulted in the highest delignification yields and LCNF viscosities (1360–555 Pa s)	(Suopajärvi et al., 2020)
Mongolian oak (~22.5%)	- ChCl-lactic acid - ChCl-urea - ChCl-glycerol (1:2 for all DESs)	-	100 and 140 ºC, 6 h	High-pressure homogenization	D < 10 nm	59–69	TEM analysis revealed less effective defibrillation for the ChCl-LA pretreated samples	(Kwon et al., 2021)
Energy cane bagasse (32.3%)	Microwave assisted betaine hydrochloride-glycerol (1:2)	Esterification	110 ºC, 30 s	Microfluidization	Aver. D: ~ 8 nm; L: several microns	↑ from 44 to 56	Recovery percentages of NADES higher than 90%; LCNF with 15.2% of lignin and superior rheological properties was obtained; However, the thermal stability of the LCNF decreased after NADES pretreatment (T_{on} decreased from 307 ºC to 285 ºC and T_{max} decreased from 396 ºC to 340 ºC)	(C. Liu et al., 2022)
Spruce groundwood pulp (27.4%)	Triethylmethylammonium chloride-Imidazole (3:7) + Succinic anhydride	Succinylation	70 ºC, 2 h	Microfluidization (Mf)	Individual nanofibrils: D: ~5 nm Nanofibril bundles: D: ~20–500 nm (1.9 mmol/g carboxyl)	Before Mf: ↓ from 47 to 37–38	Highly anionic wood nanofibers with a carboxylic acid content of 1.9–3.3 mmol/g; The succinylated samples were obtained with high yields (ranged from 92 to 95%)	(Sirviö and Visanko, 2017)
Spruce sawdust (29.4%)	Triethylmethylammonium chloride-Imidazole (3:7) + Succinic anhydride	Succinylation	Ball milling (15 min) + thermal post-treatment at 100 ºC, 15,30, 60 min	Microfluidization	Individual nanofibrils: W: few nanometers Nanofibrils aggregates: W: several hundred nanometers	-	Milled sawdust with up to 3.5 mmol/g of carboxylic acid groups was obtained using the 60 min post-heating at 100 °C	(Sirviö et al., 2021)

Table 2 (*continued*)

Raw material (lignin content)	DES pretreatment			Mechanical treatment	LCNF properties			Ref.
	DES system (Molar ratio)	Functionalization	Conditions		Dimensions	Crystallinity (%)	Additional outcomes	
Spruce groundwood pulp (27%)	Triethylmethylammonium chloride-Imidazole (1:2) + betaine hydrochloride + *p*-Toluenesulfonyl chloride	Cationization	70 °C, 4 h	Microfluidization	Individual nanofibrils: D: ~ 4 nm Nanofiber aggregates: D: up to ~ 200 nm	Before Mf: ↓ from 52 to 46	Cationic wood nanofibers (CWNF) with a cationic group content of 0.70 mmol/g, which was slightly lower than that of the reference cationized dissolving pulp (0.92 mmol/g); Typical shear thinning behavior of CWNF solution (0.3%); Significantly lower viscosity than that of the reference cationized pulp	(Sirviö, 2018)
Sugarcane bagasse (24%)	Tetraalkylammonium hydroxide - 1,3-dimethylurea (1:2) + Glycidyltrimethylammonium chloride	Cationization	RT (24 °C), 8 h	High-pressure homogenization	D: 5–8 nm	↓ from 51 to 27–33	Cationic lignocellulose nanofibers (CLCNFs) with 1–1.8 mmol/g of cationic groups and fibrillation degrees of 76–93% were obtained; CLCNFs showed lower thermal stability than the initial sugarcane bagasse	(Yao et al., 2022)
Spruce groundwood pulp (GWP, 27.4%) and sawdust (28.6%)	Sulfamic acid-urea (1:2)	Sulfation	150 °C, 30 min	Microfluidization	Individual nanofibrils D: ~ 3 nm from both sources + Large nanofiber aggregates	-	The sulfate groups content was 3.1 mmol/g for both DES-treated GWP and sawdust; Similar value was obtained using a reference bleached pulp (3.0 mmol/g); The mass yields of sulfated GWP and sawdust were very high (92–94%) compared to the bleached pulp (74%)	(Sirviö and Visanko, 2019)
Softwood chemithermomechanical pulp	Sulfamic acid- urea (1:2)	Sulfation	130 °C, 3, 5 or 7 h	Microfluidization	Aver. H: 1.7–3.4 nm L: 2–4 μm	↓ from 65 to 29–42	LCNFs with sulfate content of 1.9–3.5 mmol/g and excellent colloidal stability; LCNF gels with a solid-like behavior	(Zhu et al., 2022)
Spruce timber sawdust (28.6%)	Sulfamic acid-urea (1:2)	Sulfation	Ball milling (30 min) + thermal post-treatment at 105 °C, 30 min	Microfluidization	W: 2–5 nm	↓ from 62 to 27–48	DES anionization of the sawdust achieved at high consistencies (20–60 wt %); Anionic sawdust nanofibers with a sulfate group content up to 3.1 mmol/g	(Li et al., 2019)

The dimensions of the LCNFs are sometimes related to a specific pretreatment condition or to different pretreatment conditions

Visanko, 2020) and polygalacturonic acid (Yao et al., 2022) from water, as stabilizers of oil-water Pickering emulsions (Sirviö et al., 2021; M. Wu et al., 2021, Ojala et al., 2018) and magnetic particles in magneto-rheological fluids (C. Liu et al., 2022), as a crosslinker to reinforce sodium alginate (SA)/chitosan (CS) hydrogels (Deng et al., 2021), as strength reinforcement material in board sheets (Laitinen et al., 2020; Suopajärvi et al., 2017), to produce aerogels (Zhu et al., 2022), films (Li et al., 2017) and composite materials (Sirviö and Visanko, 2019).

Deng et al. (2021), for instance, pretreated waste cotton with ChCl-oxalic acid (1:2) followed by ball milling to obtain a CNF, which was subsequently applied in the preparation of SA/CS/CNF hydrogels. The CNF acted as a crosslinker agent, strengthening the three-dimensional entangled network of the hydrogel, which was demonstrated by the observed increases in the storage modulus and loss modulus of the SA/CS/CNF hydrogels. Additionally, the incorporation of CNF reduced the swelling performance of the hydrogels. When used as a carrier for drug (indomethacin) release, the SA/CS/CNF (with 1 wt% of CNF) hydrogel led to a reduction of about 50% in the drug release rate in simulated gastric juice compared to the pure SA/CS hydrogel.

Another interesting application was investigated by Zhu et al. (2022), who used sulfated LCNFs, previously obtained by sulfamic acid-urea DES pretreatment combined with microfluidization, to prepare aerogels via ice templating and freeze-drying. The produced aerogels exhibited a highly porous structure, low apparent density, good mechanical properties and relatively good thermal insulating performance with thermal conductivities of 31–32 mW/m.K. Moreover, the sulfate groups introduced on the LCNFs during DES pretreatment conferred flame retardancy and self-extinguishing behavior to the aerogels.

The stabilization of oil-water Pickering emulsions using DES-(L)CNFs has also been studied. As an example, Sirviö et al. (2021) used three succinylated LCNF samples with carboxyl acid contents between 0.44 and 3.47 mol/g to stabilize a water-soybean oil emulsion. The addition of LCNFs led to a significant reduction of the particle size and span value of the emulsion. When the LCNF with higher carboxylic acid content (3.47 mmol/g) was used, the particle size was decreased almost 5 times compared to the emulsion without LCNF (initial particle size of 11.3 μm).

Of all these applications, the preparation of films and composite films from DES-(L)CNFs have been those that stand out the most, so this review will provide a necessary compilation and detailed discussion of these two applications.

7.1. (L)CNF films

The (ligno)nanocellulose-based films are typically prepared by solvent casting or vacuum filtration of the diluted dispersions of (L)CNFs for the solvent removal. In solvent casting, as the solvent evaporates, the nanofibers approach each other, increasing their interactions by hydrogen bonding and finally aggregating to obtain films. However, this method is very time-consuming and the wrinkling of the films can be very difficult to avoid. Alternatively, the vacuum filtration leads to a faster solvent removal and the fibrils concentrate on the filter forming a densely packed network. After that, the wet film is peeled from the filter and is often placed under pressure and heat to accelerate the drying and to mitigate the wrinkling (Alves et al., 2019; W. Liu et al., 2022). A schematic representation of these two film preparation methods is shown in Fig. 14.

Li et al. (2017), for instance, used the solving casting method to prepare films from CNFs produced using two different DESs, based on ammonium thiocyanate-urea and guanidine hydrochloride-urea. Translucent films with good thermal stability and mechanical properties were obtained. More specifically, the tensile strength (T.S.), Young's modulus (Y.M.) and elongation at break (E.B.) of the films ranged from 135 to 189 MPa, 6.4 to 7.7 GPa and 5.3 to 9.4%, respectively. According to the authors, the T.S. values were comparable with those of periodate-based nanocellulose films and higher than those of several enzymatically pretreated nanocelluloses, while Y.M. values were similar to those of TEMPO-CNF films. The films pretreated with ammonium thiocyanate-urea revealed to be more uniform and showed superior strength properties than guanidine hydrochloride-urea films. Opaque CNF films with high strength properties were also obtained by Sirviö et al. (2020), after the mechanical disintegration of a bleached hardwood kraft pulp pretreated with ChCl-IMI and ChCl-urea. The prepared films possessed T.S. values above 200 MPa (up to 235 MPa for ChCl-IMI films) and were considered by the authors to be among the highest reported for cellulose nanomaterials after an extensive comparation with the literature data. ChCl-IMI DES pretreatment led to better mechanical properties than ChCl-urea, being the toughness of the film the property that differed the most (11.9 vs 8.9 MJ/m^3, respectively). In contrast, the oxygen barrier properties of the films prepared from the ChCl-urea pretreatment were superior to those obtained from ChCl-IMI. At a RH of 50%, a very low oxygen permeability value (25 cm^3 μm [m^2 d atm]$^{-1}$) was obtained for ChCl-urea films, while for ChCl-IMI films the lowest OP value was only 100 cm^3 μm [m^2 d atm]$^{-1}$. When the RH was increased to 80%, the relative difference between the OP values was not so pronounced; however, the ChCl-urea DES still led to the lowest OP (393 vs 486 cm^3 μm [m^2 d atm]$^{-1}$). It was suggested that the difference between the OP values was due to some molecular properties, namely of the two HBDs (urea and imidazole). Sirviö and his coworkers also recycled the ChCl-IMI DES system and observed that the mechanical properties (specific tensile strength and modulus) of the resultant films were similar to those of the films produced from pristine ChCl-IMI. A similar approach was used by Jonasson et al. (2020) to prepare films from DES-pretreated aspen wood. Here, contrary to what happened in Sirviö et al. (2020) work, the ChCl-urea films had higher strength and only slightly lower stiffness than those obtained from ChCl-IMI (142 vs 119 MPa and 12.1 vs 12.9 GPa, respectively). Strong self-standing films with a T.S. of 163–213 MPa and Y.M. of 9.0–11.0 GPa were also prepared from the pretreatment of moso bamboo with ChCl-lactic acid (Q. Liu et al., 2019). The excellent aspect ratio and high DP of the produced CNF were pointed out as the main reasons for the high strength properties achieved. W. Liu et al. (2021) also fabricated films by vacuum filtration method from CNFs obtained by the pretreatment of bleached softwood kraft pulp with another acidic DES, based on ChCl-citric acid. With this procedure, they were able to obtain semi-transparent (transmittance up to 65% at 550 nm) and flexible films with a maximum T.S. of 175 MPa and toughness of 7.5 MJ/m^3. The CNF sample with the highest crystallinity and uniform diameter distribution was the one that led to the best mechanical properties. Two DES systems, composed of ChCl-oxalic acid and ChCl-urea, were compared for the pretreatment of degummed ramie fibers to produce CNFs for further preparation of CNF films by solvent casting (Yu et al., 2019). It was observed that the ChCl-oxalic acid CNF film exhibited lower T.S, Y.M. and E.B. than that of ChCl-urea CNF film: 52 vs 86 MPa, 2.3 vs 3.0 GPa and 1.8 vs 2.9%, respectively. These differences on mechanical properties were attributed by the authors to the degradation and damage of ramie fibers during the ChCl-oxalic acid pretreatment, which resulted in CNFs with lower DP and degradation temperature. Years later, the same research group also used ChCl-oxalic acid to directly pretreat raw ramie fibers, and this time, after solvent casting, flexible and opaque CNF films with a T.S. of 98 MPa, Y.M. of 2.8 GPa and E.B. of 7.7% were obtained (Yu et al., 2021). After vacuum filtration of CNFs produced from betaine hydrochloride-glycerol DES, Hong et al., 2020a also achieved good mechanical properties in their films (T.S. ranging from ∼ 80 to 100 MPa). Lakovaara et al. (2021) adopted a different approach, in which they modified pre-prepared CNF films using TEMACl-imidazole as reaction medium combined with *n*-octylsuccinic anhydride (OSA) aiming to obtain CNF films with increased hydrophobicity. After the CNF film submersion into the DES/OSA system, at 80 ºC for 1 h, the modified film exhibited improved mechanical properties at 0%, 50% and 100% RH compared to the reference (unmodified) CNF film. The
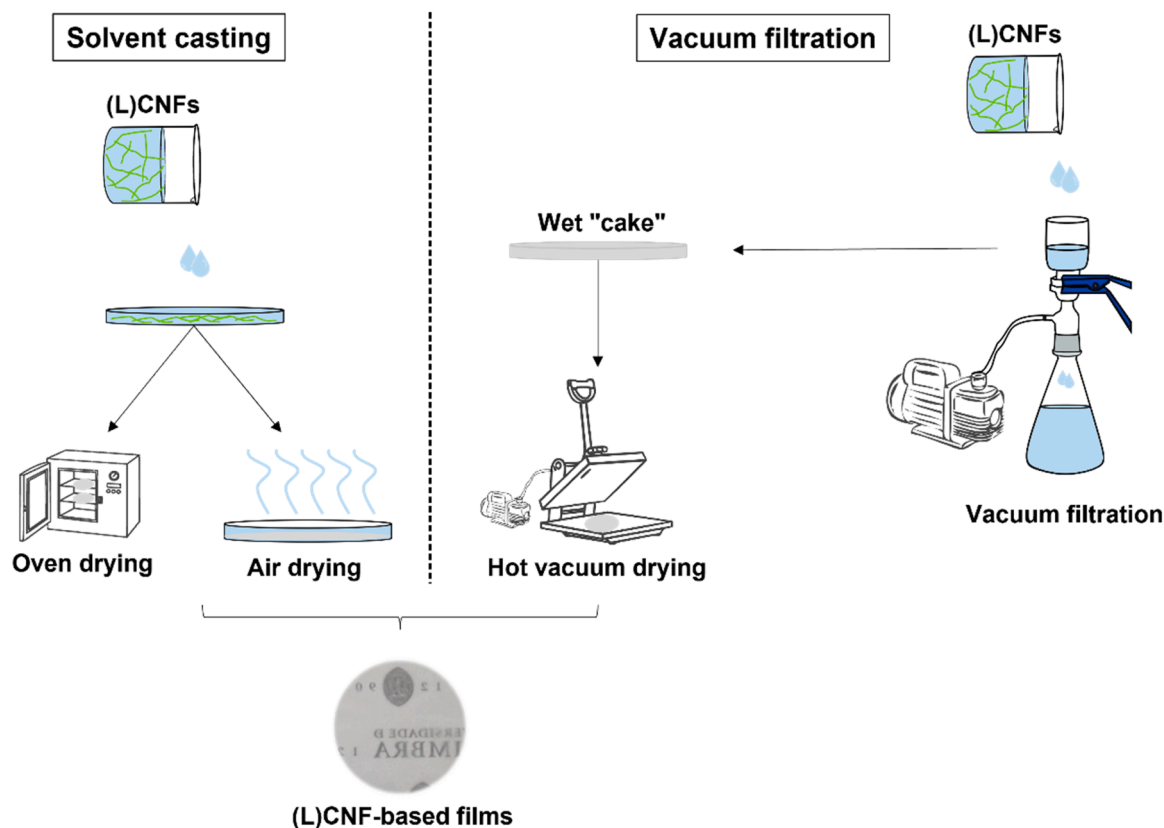
Fig. 14. Schematic representation of the two main procedures used to prepare (L)CNF films.

increase in hydrophobicity of DES/OSA modified CNF film was proven by its higher contact angle compared to the reference one, which in turn led to a lower moisture uptake of the film.

In sum, the mechanical properties of the films obtained from DES-CNFs are comparable or even higher to those of the films obtained with CNFs produced by TEMPO and periodate oxidation, enzymatic and mechanical pretreatments, as shown by Sirviö et al. (2020). In terms of gas barrier properties, there is not much information available; however, it was demonstrated that films produced from ChCl-urea had very low permeability to oxygen (50% RH). Thus, the OP values for films produced with other DES systems are necessary to fully understand the potential of DES-CNF films for packaging applications. Studies concerning water vapor permeabilities (WVPs) of these films are also lacking in the literature. Generally, the WVP of unmodified nanocelluloses is poor due to their hydrophilic character, but still, it will be important to compare the WVP of the DES-CNF films with other CNF films.

Films produced from LCNFs pretreated with different DES systems have also been reported. For instance, Sirviö and Visanko (2017) were able to obtain interesting mechanical properties for films produced from the succinylation of groundwood pulps (24.7% of lignin) using TEMACl-imidazole (DES) combined with succinic anhydride. After vacuum filtration and drying of three LCNFs produced with different carboxylic acid contents, the T.S. values of the films varied from 72 to 113 MPa and the Y.M. from 4.1 to 6.2 GPa. By TEM analysis, the authors observed that the LCNF with superior carboxylic acid content had lower aspect ratio hindering the entanglement with other nanofibers, which likely contributed to the lower Y.M. and T.S. of the film obtained with this particular CNF. In return, the presence of shorter fibers in the LCNF led to a more transparent film since the absorption and reflection of the light is less intense in this case. In another study, the same research group obtained LCNF films from the mechanochemical and thermal succinylation of spruce sawdust and concluded again that an increase in the carboxylic content of LCNFs had a negative impact on the mechanical properties of the films. The LCNF film with the lowest carboxylic content led to better mechanical properties, although, overall, all produced films exhibited relatively low mechanical properties (see Table 3) (Sirviö et al., 2021). LCNF films with strong flame resistance and good UV-blocking performance were obtained by Li et al. (2019). In this work, LCNFs were produced based on the sulfation of wood sawdust in sulfamic acid-urea DES under simultaneous milling. The films prepared from these LCNFs showed a blocking performance for UV light (200–400 nm region) over 90%, and optical transmittances (at 600 nm) ranging from 41 to 68%. In addition, the presence of lignin and the introduced sulfate groups gave to the LCNF films great flame-resistant ability, having been obtained limiting oxygen index (LOI) values 46–108% higher than that of a non-derivatizing nanocellulose film used as reference (Li et al., 2017). These LCNF films also exhibited good T.S. (up to 65 MPa) and Y.M. (up to 5 GPa). A comparison of the mechanical properties between films produced from the pretreatment of wheat straw, corn stalk, and rapeseed stem with four acidic DESs and one alkaline DES (K_2CO_3-glycerol) was carried out by Suopajärvi et al. (2020). Overall, flexible and opaque films were successfully fabricated using the vacuum filtration method from all DES-treated LCNFs. However, the alkaline DES treatment led to LCNF films with better T.S. and Y. M. (101–170 MPa and 5.2–8.6 GPa) compared with films from the ChCl-lactic acid DES (67–132 MPa and 3.9–6.9 GPa), that exhibited the best mechanical properties among the films from acidic DES-CNF. Flexible and foldable films with a T.S. of 134 MPa and E.B. of 10.6% were also obtained by Hong et al. (2020b), when these authors used another acidic DES (ChCl-oxalic acid) for the pretreatment of luffa sponge combined with ultrasonication.

Table 3
Preparation method, mechanical and other relevant properties of CNF and LCNF films obtained from the pretreatment with different deep eutectic solvents.

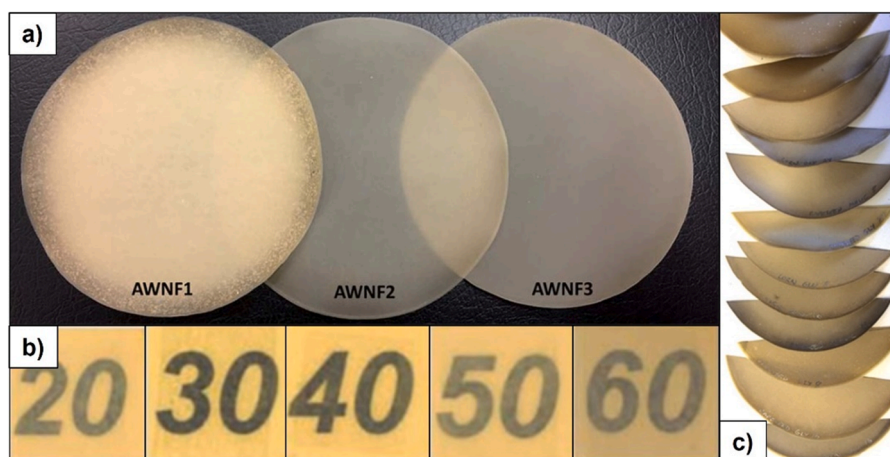| (L)CNF production method (DES + mechanical treatment)		Film formation method	Grammage (g/m²)	Thickness (µm)	Mechanical (L)CNF film properties			Additional film properties	Ref.
					Tensile strength (MPa)	Young's modulus (GPa)	Elongation at break (%)		
Ammonium thiocyanate-urea (1:2) + Mf; Guanidine hydrochloride-urea (1:2) + Mf	CNF	Solvent casting + air drying (2 weeks)	57	-	135–189	6.4–7.7	5.3–9.4	Translucent films with good thermal stability	(Li et al., 2017)
ChCl-oxalic acid (1:1) + BM ChCl-urea (1:2) + BM	CNF	Solvent casting + oven drying (60 °C, overnight)	129	140 160	52 86	2.3 3.0	1.8 2.9	ChCl-oxalic acid led to a sharper ↓ in the DP and T_{max} of the CNFs, which in turn resulted in worse mechanical properties of the films	(Yu et al., 2019)
ChCl-lactic acid (1:9) + Mf	CNF	Vacuum filtration + vacuum drying (93 °C, 9 min, 70 mbar)	40	22	163–213	9.0–11.0	2.0–4.7	The high aspect ratio and DP of the CNFs contributed to the excellent mechanical properties achieved	(Q. Liu et al., 2019)
ChCl-urea (1:2) + Mf ChCl-imidazole (3:7) + Mf	CNF	Vacuum filtration + air drying (few hours) + hot-pressing (120 °C, 15 min, 200 kPa)	-	-	142±35 119±19	12.1±0.3 12.9±0.4	2.4±0.8 2.1±0.5	DES-CNF films with ↑ thermal stability and stiffness than the carboxymethylated and TEMPO oxidised CNF films but with ↓ T.S. and E.B.	(Jonasson et al., 2020)
ChCl-imidazole (3:7) + Mf ChCl-urea + Mf	CNF	Vacuum filtration (800 mbar) + vacuum drying (93 °C, 10 min, 930 mbar)	60	-	235 219	9.9 10.2	7.7 6.1	CNF films with good oxygen barrier properties, even at 80% RH. The recycling and reuse of ChCl-imidazole did not affect the mechanical properties of the DES-based CNF films	(Sirviö et al., 2020)
Betaine hydrochloride-glycerol (1:2) + Mf Betaine hydrochloride-glycerol (2:3) + Mf	CNF	Vacuum filtration + vacuum drying (93 °C, 10 min, 800 mbar)	~ 80	-	86–93 93–99	4.3–5.5 4.4–5.3	3.1–3.6 3.1–4.4	Self-standing CNF films with good mechanical performance	(Hong et al., 2020a)
ChCl-oxalic acid (1:1) + BM	CNF	Solvent casting + vacuum drying (40 °C)	127	137	98±2	2.8±0.0	7.7±1.1	Flexible and opaque films with a brownish-yellow color	(Yu et al., 2021)
1- ChCl-glycerol (1:2) + coffee-derived solid acid (SC-SO₃H) catalyst 2-Bleaching (7% NaClO₂) 3- ChCl-Oxalic acid (1:1) + Us	CNF	Vacuum filtration + pressing (room temperature, 12 h)	-	43±2	78–80	-	9.3–13.6	Colorless and transparent films were obtained	(X.-Q. Wu et al., 2021)
ChCl-citric acid monohydrate (1:1) + HPH ChCl-anhydrous citric acid (1:1) + HPH	CNF	Vacuum filtration + vacuum drying (60 °C, 4 h, 250 N)	-	-	74–124 111–175	2.9–4.3 3.4–4.8	-	Semi-transparent and flexible cellulose nanopapers were obtained	(W. Liu et al., 2021)
Triethylmethylammonium chloride-Imidazole (3:7) + Succinic anhydride + Mf	LCNF	Vacuum filtration + vacuum drying (93 °C, 9 min, 70 mbar)	80	53–64	72–113	4.1–6.2	3.3–5.7	Films composed of shorter nanofiber bundles had lower T.S. but higher transparency	(Sirviö and Visanko, 2017)
Sulfamic acid-urea (1:2) + Mf	LCNF	Vacuum filtration + vacuum drying (93 °C, 10 min)	80	-	Up to 65	Up to 5	~ 1.8	Films with strong flame resistance, good UV-blocking performance (over 90%) and transmittances of 41–68% (at 600 nm)	(Li et al., 2019)
ChCl-oxalic acid (1:1) + Us	LCNF	Vacuum filtration + vacuum drying (93 °C, 10 min, 800 mbar)	~ 80	61±1	134±5	3.7±0.7	10.6±0.3	Flexible and foldable films	(Hong et al., 2020b)
ChCl-lactic acid (1:2) + Mf ChCl-lactic acid (1:5) + Mf ChCl-levulinic acid (1:2) + Mf ChCl-malic acid (1:1) + Mf ChCl-glutaric acid (1:1) + Mf K₂CO₃-glycerol (1:5) + Mf	LCNF	Vacuum filtration + vacuum drying (94 °C, 10 min, 900 mbar)		60–76 56–75 61–89 61–91 60–93 53–89	67–114 72–132 24–77 35–67 46–82 101–170	3.9–5.9 4.4–6.9 2.4–5.6 3.1–6.4 3.8–6.4 5.2–8.6	1.4–5.3 1.4–5.8 1.1–4.0 1.2–5.6 1.6–4.8 3.7–6.0	Flexible and opaque nanopapers were prepared. K₂CO₃-glycerol DES pretreatment resulted in films with better mechanical properties for all tested biomasses (wheat, corn and rapeseed) compared to the acidic DES treatments	(Suopajärvi et al., 2020)
Triethylmethylammonium chloride-Imidazole (3:7) + Succinic anhydride + Mf	LCNF	Vacuum filtration + vacuum drying (93 °C, 9 min, 900 mbar)	-	-	21–50	1.7–4.4	1.2–3.2	Films with relatively weak mechanical properties were obtained	(Sirviö et al., 2021)
ChCl-lactic acid (1:2) + HPH ChCl-urea (1:2) + HPH ChCl-glycerol (1:2) + HPH	LCNF	Vacuum filtration + hot pressing (105 °C, 1 min, 15 MPa)	-	-	Up to ~ 41 Up to ~ 73 Up to ~ 73	Up to ~ 1.4 Up to ~ 1.5 Up to ~ 1.6	-	-	(Kwon et al., 2021)

Fig. 15. Visual appearances of DES-LCNF films prepared by a) Sirviö and Visanko (2017) b) Li et al. (2019) and c) Suopajärvi et al. (2020).

The visual appearances of the LCNF films obtained from some of the studies discussed above are shown in Fig. 15.

As can be seen in Table 3, the mechanical properties of the DES-LCNF films do not seem to reach values as high as those exhibited by the films prepared from DES-CNFs. This behavior was also reported for other LCNF films produced with other pretreatments, and may be related to the fact that lignin hinders the establishment of hydrogen bonds between fibrils and to the amorphous character of lignin (Jiang et al., 2019; Trovagunta et al., 2021). Contrarily to this, some other studies have found that lignin present in LCNFs can keep or even improve the mechanical properties of the films compared to pure CNF films due to the binder effect of lignin (X. Liu et al., 2019b; Y. Zhang et al., 2020). Although lignin also causes the reduction of the transparency of the films, due to the chromophores present in its structure, as can be seen in Fig. 15 a) and b), DES-LCNF films with good transparency were already obtained. Similar to DES-CNF films, there is still a lack of information about the barrier properties of DES-LCNF films. Despite that, it was found that when the LCNFs are hot-pressed in the presence of water, lignin in LCNF films is plasticized, providing to the films smoother surfaces with fewer and smaller pores, which in turn will contribute to improve their oxygen barrier performance and to prevent water penetration (Rojo et al., 2015). Additionally, the more hydrophobic character of lignin than cellulose may also allow preventing the formation of hydrogen bonds between the OH-groups of cellulose and water molecules, and thus, be beneficial for the barrier properties of the films (Chen et al., 2018). It is also important to emphasize that the production of LCNFs and their corresponding films is more economically favorable than in the case of CNFs, which is an important advantage for their eventual industrialization.

7.2. Nanocomposite films

Nanocomposite films composed of DES-(L)CNFs and different types of polymers have also been prepared. For example, Li et al. (2021) used a CNF obtained from sulfamic acid-glycerol DES pretreatment to fabricate polyvinyl alcohol (PVA)/CNF nanocomposite films by solvent casting method. Compared to the neat PVA films, the composite films showed improved mechanical properties: T.S. increased from 11 MPa to a maximum of 44 MPa and the Y.M. increased from 221 up to 1529 MPa. Oppositely, the E.B. was reduced when the CNF was added, which was ascribed to the intra and intermolecular H-bonds formed between PVA and CNF. PVA/LCNF films were also fabricated by Sirviö and Visanko (2019). In this work, the LCNFs were produced from the treatment of unbleached spruce GWP and sawdust with sulfamic acid-urea. The resultant composite films (10 wt% of LCNF) exhibited strong UV-blocking properties with a minor impact on the transparency, which

make them eventually suitable for optical applications. The LCNFs also improved the mechanical properties of PVA, but to a lesser extent than those obtained when a CNF from a bleached cellulose pulp was used in the composites. LCNFs produced using microwave assisted DES (ChCl-lactic acid) pretreatment in combination with ultrasonication were also successfully used for the enhancement of the mechanical and UV-resistant properties of polyanionic cellulose (PAC). PAC/LCNF composite films with a T.S. of 56 MPa and 23.6% of E.B. were obtained (C. Liu et al., 2020).

Other composite materials consisting of DES-(L)CNFs + polylactic acid (PLA) have also been fabricated (Q. Zhang et al., 2021; S. Liu et al., 2021). For instance, uniform LCNF/PLA composites were obtained by Q. Zhang et al. (2021) when they combined esterified LCNFs with different lignin contents, prepared from ChCl-lactic acid pretreatment, with PLA using a direct blending method. The presence of lignin had a binding effect and improved the interfacial compatibility between LCNFs and PLA, which in turn led to a significant increase of the flexural strength of the PLA. Using 20 wt% of LCNF in the composite, the flexural strength was ca. 120% higher than that of the pure PLA, whereas the T.S. and E.B. remained nearly unchanged.

8. Deep eutectic solvents for the production of (ligno)cellulose nanocrystals

DESs have also been employed for the hydrolysis and dissolution of the amorphous domains of cellulose fibers to yield CNCs. Sirviö et al. (2016) utilized four different DES systems based on ChCl and organic acids (anhydrous oxalic acid and dihydrate, p-toluenesulfonic acid and levulinic acid) for the pretreatment of dissolving cellulose pulp (60–120 ºC, 2–6 h) followed by microfluidization aiming to individualize CNCs. Among of all DESs tested, the ChCl-oxalic acid dihydrate was the only DES system that allowed them to successfully obtain CNCs (TEM image in Fig. 16a). Under the conditions tested for this DES (100–120 ºC and 2–6 h), the produced CNCs showed CrIs of 66–71%, 0.20–0.27 mmol/g of carboxylic acid content, widths of 10–16 nm and lengths of 337–390 nm. CNCs also exhibited transmittances (at 800 nm) ranging from 45 to 75% and good thermal stability. An ultrafast method was developed by Y. Liu et al. (2017) to fabricate CNCs. Here, cotton fibers were pretreated using ChCl-oxalic acid (1:1) under microwave radiation (800 W) at 70–100 ºC for 3 or 5 min, and mechanically disintegrated by ultrasonication for 30 min. After DES pretreatment, the authors stated that 94% of the DES could be recycled by distillation, and further reused maintaining its effectiveness. The microwave assisted DES pretreatment under 800 W power, at 80 ºC for 3 min was considered the optimal one, which led to a high yield of CNCs (74.2%). The obtained CNCs showed diameters ranging from 3 to 25 nm, lengths of 100–350 nm, high
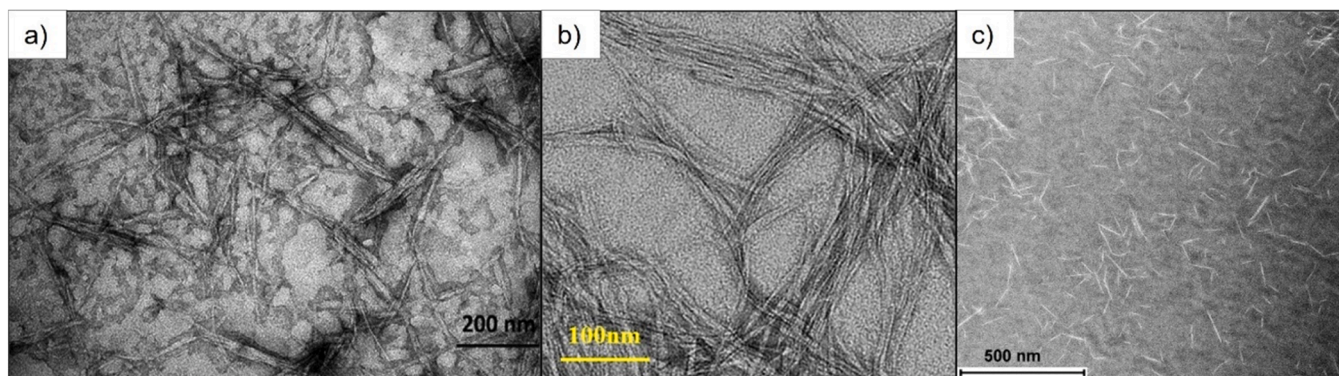
Fig. 16. TEM images of the produced CNCs by **a)** Sirviö et al. (2016); **b)** Lu et al. (2021b); **c)** Selkälä et al. (2020).

crystallinity (82%) and thermal stability (T_{max} = 354 ºC). According to the authors, the properties of the produced CNCs were comparable to those of CNCs obtained by conventional methods but the DES was considered to be more eco-friendly and efficient. Ling et al. (2019) studied the effect of the pretreatment conditions on the properties of CNCs obtained from cotton fibers. The pretreatment was performed using ChCl-oxalic acid with different molar ratios of the DES components (1:1, 1:2, and 1:3) for two temperatures (80 ºC and 100 ºC) followed by ultrasonication. It was found that higher oxalic acid ratios led to higher carboxylic group contents in the CNC that were introduced by the esterification of the OH-groups at the C6 position of cellulose, promoting the breakage of hydrogen bonds and thus yielding CNCs with better dispersion and larger aspect ratio. In combination with ChCl-oxalic acid DES, Yang et al. (2019) used $FeCl_3 \cdot 6 H_2O$ as catalyst to improve the hydrolysis activity in order to prepare CNCs from bleached eucalyptus kraft pulp. Under optimal reaction conditions (ChCl:oxalic acid:$FeCl_3 \cdot 6 H_2O$ in a molar ratio of 1:4.43:0.1 at 80 °C for 6 h), the yield of CNCs was determined to be over 90% based on the cellulose content in BEKP. The resultant whisker-like CNCs showed a higher thermal stability than the CNCs obtained by conventional sulfuric acid hydrolysis, as well as a high crystallinity (> 80%) and excellent dispersibility in water. Moreover, the DES:$FeCl_3 \cdot 6 H_2O$ system could be recovered by a simple separation process and directly reused, at least three times, to produce CNCs. Lu et al. (2021a) also utilized a catalyst (ammonium persulfate) combined with ChCl-oxalic acid to manufacture CNCs. In this study, cellulose II nanocrystals with a yield of 82%, CrI of 77% and an average diameter of 9 nm were obtained after the treatment. Wang et al. (2020) also used the ChCl-oxalic acid DES system to pretreat cotton fibers combined with high-pressure homogenization, producing short rod-shaped CNCs with diameters of 50–100 nm, lengths of 500–800 nm, a high crystallinity (77.6%) and thermal stability (T_{max} = 343 ºC). After the pretreatment, the used DES was distilled in a rotary evaporator and a high recyclability (above 85%) was achieved for the DES. Again, the recycled DES could be used at least three times without losing its pretreatment efficiency. The authors also claimed that the DES hydrolysis mechanism is somewhat similar to the acid hydrolysis. When the DES is heated, the ChCl is dissociated into $[Ch]^+$ and $[Cl]^-$ ions being diffused into the cellulose molecular chain space. Next, the $[Cl]^-$ ions will interact with the hydrogen of the OH-groups, while the $[Ch]^+$ cations will attack the oxygen of the OH-groups. $[Cl]^-$ anions will also interact with the carbon atoms of the β-1,4- glycosidic bonds while $[Ch]^+$ will interact with the oxygen atoms. These interactions cause the breakdown of the hydrogen bonding network and β-1,4- glycosidic bonds mainly in the amorphous regions of cellulose fibers, thus allowing the CNCs to be isolated. Using oxalic acid as hydrogen bond donor will also led to the esterification of the OH-groups providing good dispersion stability to the CNCs. In another study, Douard et al. (2021) used the design of experiment method to optimize the CNC extraction with ChCl-oxalic acid (1:1) from cotton fibers, varying three parameters:

cotton fibers concentration (1–2%), temperature (60–95 ºC) and treatment time (2–16 h). The method followed by the authors included the design and experiments, the study of the response modelled through regression and the optimization of parameters. Two mathematical models were then developed to describe the evolution of the yield and crystallinity of the CNCs. It was concluded that the crystallinity model was able to predict the experimental crystallinity values of the obtained CNCs, while the yield model was less accurate, only providing a tendency. Another important outcome was given by Lim et al. (2021), when they produced nanocrystals from a bleached rice straw pulp by treatment with ChCl-oxalic acid (1:1) and compared the DES-CNC properties to those of sulfuric acid (SA)-CNC prepared by the conventional sulfuric acid hydrolysis. It was observed that both treatments led to the introduction of negatively charged groups on the surface of CNCs, i.e., carboxyl groups in DES-CNC and sulphate groups in SA-CNC. However, the latter had a smaller particle size than the DES-CNC (diameter: 5 vs 8 nm; length: 222 vs 302 nm), indicating that sulfuric acid hydrolysis was more effective than the DES treatment. Despite that, the thermal stability of the DES-CNC was superior to that of SA-CNC (T_{max} of 334 and 308 ºC, respectively).

In addition to ChCl-oxalic acid, other DESs have been employed to obtain CNCs. For example, Fan et al. (2020) tested the ChCl-lactic acid (1:2) system for the extraction of CNCs from grape pomace. After 6 h of treatment at 80 ºC, rod-like CNCs with a crystallinity of 95.2%, 0.63 mmol/g of carboxylic groups and a diameter of 22±4 nm and length of 241±45 nm were obtained. Lu et al. (2021b), on the other hand, utilized ChCl-formic acid (1:2) + *p*-toluenesulfonic acid (PTSA) combined with microwave radiation (500 W) to fabricate a CNC from a dissolving pulp. The CNC was obtained with a high yield (87.6%), showing the typical rod-like morphology of CNCs with diameters of 13–18 nm and lengths of 120–150 nm (Fig. 16b). The CNC showed a good water dispersibility because of the negatively charged carboxyl groups introduced on their surface (0.93 mmol/g). After four cycles of reusing the recycled DES system and PTSA, a yield of CNC production of 56% was still obtained. Alternatively to acidic DESs, Smirnov et al. (2020) employed ChCl-urea for the treatment of microcrystalline cellulose (at 110 ºC for 2 and 4 days) having obtained CNCs without a significant chemical surface modification and with average particle dimensions of 20 × 100 × 700 nm. Both the DP and crystallinity barely changed during the DES treatment. The H-bond interactions between the cellulose OH-groups, the carbonyl group (C = O) of urea and the chloride ions were demonstrated to be the key factors for the disruption of the microcrystalline cellulose particles. Rod-like cationic CNCs have also been prepared by sequential sodium periodate oxidation and cationization using a DES based on aminoguanidine hydrochloride and glycerol (Selkälä et al., 2020; Wang et al., 2022). Applying this procedure, Selkälä et al., 2020 fabricated a CNC with a cationic charge density of ~ 2.7 meq/g, widths ranging from 5 to 17 nm and lengths from 30 to 170 nm (Fig. 16c).

Unbleached cellulose materials have also been used for the production of lignocellulose nanocrystals. Jiang et al. (2020a) successfully extracted LCNCs from a softwood thermomechanical pulp (30.8% of lignin) using a binary (ChCl-oxalic acid, 1:1) and a ternary DES (ChCl-oxalic acid-*p*-toluenesulfonic acid, 2:1:1) followed by mechanical blending. Under the same reaction conditions (80 ℃, 3 h), the ternary DES enabled the fabrication of LCNCs with a higher yield (66% vs 39%), carboxylic groups (0.43 mmol/g vs 0.29 mmol/g) and thermal stability (T_{max} = 358 ℃ vs T_{max} = 344 ℃) compared to the LCNCs produced with the binary DES. The produced LCNCs exhibited the typical rod-like appearance of nanocrystals, and spherical aggregates resultant from the presence of lignin were also observed. According to the authors, different simultaneous mechanisms can explain the production of LCNCs using the ternary DES:

✓ The acidic DES can selectively break the ether linkages of lignin, without further condensation reactions.
✓ The Cl⁻ anions can interact with the OH-groups of lignocellulose causing the disruption of the H-bonds established in the lignin-carbohydrate complex.
✓ The sulfonic acid group of *p*-toluenesulfonic acid can catalyze the lignin solubilization, whereas the toluene moiety (lipophilic part) can prevent the reaggregation of the separated lignin through π-π stacking or hydrophobic interactions (Chen et al., 2017).
✓ The penetration of H⁺ into the amorphous domains of cellulose chains enables the hydrolysis of cellulose, while the Cl⁻ anions can cleave the H-bonds between the adjacent CNCs.
✓ The carboxylic groups introduced by the esterification reaction with oxalic acid facilitate the separation of the CNCs due to repulsive electrostatic forces.

More recently, Shu et al. (2022) also used a ternary DES, composed of ChCl (HBA), lactic acid and *p*-toluenesulfonic acid (HBDs), followed by microfluidization, to produce LCNCs from poplar. Under optimized conditions (ChCl:lactic acid:*p*-toluenesulfonic acid molar ratio of 2:10:1, 100 ℃), ribbon-like LCNCs with a yield of 64.6%, high lignin content (27.6%), high thermal stability (T_{max} = 370 ℃) and strong gel-like behavior were obtained. A different approach was explored by Jiang et al. (2021) who used solely oxalic acid dihydrate combined with microfluidization to produce LCNCs from a softwood thermomechanical pulp. Compared to the authors previous studies (Jiang et al., 2020a, 2020b), here, higher LCNC yields (over 70%) were obtained in a shorter reaction time (30 min). The use of only one chemical made it easier the recycling of the oxalic acid, and its performance after four reuse cycles was similar to that of pristine oxalic acid.

Table 4 compiles the DES pretreatment conditions used to produce (L)CNCs, as well as their corresponding properties, from several published studies.

9. Applications of (L)CNCs prepared from DES pretreatments

One of the applications that has been proposed for DES-CNCs is the strength reinforcement in nanocomposite films. For example, plasticized chitosan-based films were reinforced by 2 wt% of a CNC obtained from ChCl-urea (1:2) treatment, which led to an increase in the T.S, Y.M. and E.B. from 11 to 20 MPa, 26 to 37 MPa, and 63 to 79%, respectively (Smirnov et al., 2020). This reinforcing capacity was also observed by Lu et al. (2021b), when they used a CNC, produced from ChCl-formic acid DES combined with *p*-toluenesulfonic acid, to fabricate CNC/gelatin nanocomposite films. Compared to the neat gelatin film, the addition of 1 wt% of CNC into the gelatin matrix caused an increase of 188% and 131% in the T.S. (26 to 75 MPa) and Y.M. (983 to 2273 MPa), respectively. In another study, a CNC extracted from ChCl-oxalic acid was shown to be a suitable reinforcing agent to produce starch-based bioplastic films: a T.S. of 22 MPa, a much higher value than that reported for pure starch films (4–8 MPa), was achieved (De et al., 2021).

An alternative application has been the use of DES-CNCs as stabilizers of oil-water Pickering emulsions. In this regard, a CNC obtained from ChCl-oxalic acid was used for the stabilization of a marine diesel oil-water Pickering emulsion (Laitinen et al., 2017). The use of DES-CNC resulted in a significant oil-droplet size reduction (from ~ 52 μm to less than 10 μm) compared to the reference oil-water emulsion without any added dispersant. The DES-CNC also allowed to prevent the oil droplet coalescence over 6 weeks forming a stable creaming layer, and, compared with two commercial CNCs, the DES-CNC had a similar performance. On the other hand, Ojala et al. (2018) compared the performance of an unmodified CNF (obtained from ChCl-urea), a succinylated CNF (obtained from urea-LiCl + succinic anhydride) and a carboxylated CNC (obtained from ChCl-oxalic acid) for the stabilization of oil-water emulsions. Although CNC allowed the oil-droplet reduction, it was not as efficient as succinylated CNF to slow down the creaming and prevent the coalescence of the emulsions, but better compared to the unmodified CNF. It was concluded that the web-like morphology of the CNFs was able to prevent the droplets from being packed as tightly as those stabilized with CNC, forming a thicker emulsion layer, while the rigid structure of CNC did not benefit its stabilization performance. In another study, a cationic CNC prepared by sodium periodate oxidation followed by treatment with aminoguanidine hydrochloride-glycerol, was also used to stabilize a Pickering emulsion (Wang et al., 2022). When the cationic CNC content increased from 0.01 to 0.5 wt% the size of the emulsion droplets decreased and the emulsion stability was improved. An unmodified CNC and an anionic CNC (obtained by TEMPO oxidation) were also used as emulsifiers, and it was observed that these two CNCs led to a non-uniform and polydisperse particle size distribution; additionally, the emulsion droplets were larger compared to those of the cationic CNC. The authors stated that the enhancement of the emulsion stabilization using the cationic CNC was due to the electrostatic attraction established between the negative charges at the oil-water interface and the positively charged CNC. In addition, the emulsion droplets were prevented from coalescing due to their surface positive charges, which generated strong repulsive electrostatic forces between the droplets.

Self-healing nanocomposite hydrogels have also been prepared using DES-CNCs (Fan et al., 2020; R. Wu et al., 2020). According to the authors, the incorporation of CNCs considerably increases the number of H-bonds and the cross-linking degree in the hydrogel, allowing better mechanical strength and improved self-healing performance (Fan et al., 2020).

10. Conclusions, challenges, and future perspectives

This review aimed to provide an overview on the use of deep eutectic solvents for the production of cellulose nanofibrils and cellulose nanocrystals, and also to discuss their applications.

It is clear that there are several DES systems options that can be used to obtain cellulose micro/nanofibrils with different types of surface chemical functionalization, including esterification, succinylation, cationization and sulfation. These distinct modifications confer to the materials distinct properties, and enable a broader spectrum of applications of (L)CNFs. Based on the high content of charged functional groups obtained for some of the DES-CNF materials, it seems that cellulosic materials with a high degree of fibrillation have been produced. This has been achieved for a wide range of raw materials using appropriate choices of DESs and mechanical treatments. However, in this matter, it should be recommended that this property should be more systematically evaluated in (L)CNFs produced using DES: only one report was found mentioning 76–93% of fibrillation degree for cationic DES-based LCNFs having 1–0–1.8 mmol/g cationic content, which is in a similar range of values obtained for TEMPO-oxidized and phosphorylated CNFs. The measure of the content of nanosized material (in wt%) will allow to compare better the performance of the several DES systems to that of the conventional chemical pretreatments in the effective

Table 4

Pretreatment conditions and (L)CNC properties obtained by different DES systems.

Raw material	DES pretreatment		Mechanical treatment	(L)CNC properties				Ref.
	DES system (Molar ratio)	Conditions			Dimensions	Crystallinity (%)	Additional outcomes	
Softwood dissolving pulp	ChCl-oxalic acid (1:1)	100–120 °C, 2–6 h	Microfluidization	CNC	W: 10–16 nm L: 337–390 nm	66–71	Carboxylic acid content of 0.20–0.27 mmol/g; CNC suspensions (0.1%) with transmittances ranging from 45 to 75% at 800 nm	(Sirviö et al., 2016)
Softwood dissolving pulp	ChCl-oxalic acid (1:1)	100 °C, 6 h	Microfluidization	CNC	W: 3–8 nm L: 50–350 nm	68	CNC with a carboxylic acid content of 0.23 mmol/g	(Laitinen et al., 2017)
Cotton fibers	Microwave assisted (800 W) ChCl-oxalic acid (1:1)	80 °C, 3 min (Optimal)	Ultrasonication	CNC	D: 3–25 nm L: 100–350 nm	↑ from 65 to 82	CNC with high purity and yield (74.2%); The DP ↓ from 1600 to 149; The CNC had a higher T_{max} (354 °C) compared to cotton fibers (335 °C); The DES was recycled and remained effective	(Y. Liu et al., 2017)
Softwood dissolving pulp	ChCl-oxalic acid (1:1)	100 °C, 6 h	Microfluidization	CNC	W: 3–5 nm L: 50–350 nm	-	CNC with 0.17 mmol/g of carboxyl groups and a mass yield of 75%	(Ojala et al., 2018)
Cotton fibers	ChCl-oxalic acid (1:1; 1:2; 1:3)	80 and 100 °C; 1 h	Ultrasonication	CNC	H: 5–10 nm L: 122–206 nm	↓ 93.4 to 67.3–75.3	The breakdown of hydrogen bonding was more extensive using the DES with higher acid content (ChCl:oxalic acid = 1:3)	(Ling et al., 2019)
Cotton fibers	ChCl-oxalic acid (1:1)	90 °C, 6 h	High-pressure homogenization	CNC	D: 50–100 nm L: 500–800 nm	↑ from 63.5 to 77.6	CNC suspension stable even after one month; High recyclability rate (> 85%) of the DES was achieved	(Wang et al., 2020)
Cotton fibers	ChCl-oxalic acid (1:1)	95 °C, 6 h	None (centrifugation + dialysis)	CNC	Aver. H: 11 nm L: 257 nm	81	CNC yield of 43.6±1.9%; Two mathematical models were developed to predict the CNC yield and crystallinity based on different treatment conditions	(Douard et al., 2021)
Bleached rice straw pulp	ChCl-oxalic acid (1:1)	80 °C, 4 h	None (centrifugation)	CNC	Aver. D: 8 nm L: 302 nm	76.7	Rod-like CNCs with a yield of 55.1%, a polydispersity index of 0.56, T_{onset} = 288 °C and T_{max} = 334 °C	(Lim et al., 2021)
Bleached eucalyptus kraft pulp	ChCl-oxalic acid + FeCl₃0.6 H₂O (1:4.43:0.1)	80 °C, 6 h (Optimal)	None (centrifugation + dialysis)	CNC	W: 5–20 nm L: 50–300 nm	↑ from 75.7 to 81.9	CNCs were prepared at a high yield (73%), showing higher thermal stability than the conventional sulfuric acid CNCs	(Yang et al., 2019)
Bleached eucalyptus kraft pulp	ChCl-oxalic acid (1:1) + Ammonium persulfate	80 °C, 120 min	None (precipitation + centrifugation)	CNC	Aver. D: 9 nm L: 100–200 nm	↑ from 65.8 to 76.6	Cellulose type-II CNC with a yield of 82.3% and good thermal stability	(Lu et al., 2021a)
Grape pomace	ChCl-lactic acid (1:2)	80 °C, 6 h	None (centrifugation)	CNC	Aver. D: 22 nm L: 242 nm	↑ from 89.6 to 95.2	CNC with 0.63 mmol/g of carboxylic acid groups	(Fan et al., 2020)
Dissolving pulp	Microwave assisted (500 W) ChCl-formic acid (1:2) + p-toluenesulfonic acid	90 °C, 45 min	None (centrifugation)	CNC	D: 13–18 nm L: 120–150 nm	↑ from 65 to 81	CNC with 0.93 mmol/g of carboxyl groups and a yield of 87.6%	(Lu et al., 2021b)
Microcrystalline cellulose	ChCl-urea (1:2)	110 °C, 2 h, 2 and 4 days	None (Centrifugation + redispersion)	CNC	Aver. size of 20×100×700 nm	79–85	The DP (330) of initial cellulose did not change during the DES treatment; Stable CNC dispersions in water for at least 1 month	(Smirnov et al., 2020)
Softwood dissolving pulp	Periodate oxidation + Aminoguanidine hydrochloride-glycerol	75 °C, 3 h (periodate oxidation) + 80 °C, 10 min (DES)	Microfluidization	CNC	W: 5–17 nm L: 30–170 nm	-	CNC with a cationic charge density of 2.4–3 meq/g in the pH range of 3–9	(Selkälä et al., 2020)
Bleached sulfate eucalyptus pulp	Periodate oxidation + Aminoguanidine hydrochloride-glycerol (1:2)	70 °C, 20 min	Ultrasonication	CNC	D: 5–50 nm L: 100–300 nm	↑ from 43.9 to 50.0	CNC with lower thermal stability compared to initial pulp, T_{max} = 212 °C vs T_{max} = 355 °C, respectively	(Wang et al., 2022)
Softwood thermomechanical pulp (30.5% of lignin)	ChCl-oxalic acid (1:1)	90 °C, 6 h (Optimal)	Mechanical blending	LCNC	Width ~ 7 nm Thickness of 4 nm	60	Ribbon-like LCNC with a 57% yield, 0.30 mmol/g carboxylic acid groups and 32.6% of lignin; Spherical lignin nanoparticles of 20–50 nm in diameter were observed in the LCNCs	(Jiang et al., 2020b)
Softwood thermomechanical pulp (30.8% of lignin)	ChCl-oxalic acid-p-toluenesulfonic acid (2:1:1)	80 °C, 3 h (Optimal)	Mechanical blending	LCNC	Width ~ 6 nm Thickness of 3.3 nm	57.4	LCNC with a yield of 66%, lignin content of 47.6%, 0.43 mmol/g of carboxylic acid groups and a T_{max} of 358 °C; LCNC suspension (0.05%) with a transmittance (at 650 nm) of 43.0%	(Jiang et al., 2020a)
Poplar (30.1% of lignin)	ChCl-lactic acid-p-toluenesulfonic acid (2:10:1)	100 °C, 3 h (Optimal)	Microfluidization	LCNC	W: 16–34 nm Aver. H: 1.2 nm L: ~ 200 nm	↓ from 53.7 to 44.6	LCNC with a yield of 64.7% and 27.7% of lignin content and high thermal stability (T_{max} = 370 °C); LCNC suspensions showed high viscosity and strong gel-like behavior	(Shu et al., 2022)
Softwood thermomechanical pulp (~30% of lignin)	Oxalic acid dihydrate	110 °C, 30 min	Microfluidization	LCNC	Aver. W: 7 nm Aver. H: 4 nm L: 200–300 nm	↑ from 55 to 72	LCNC with a yield over 70%, lignin content of 42.3%, satisfactory thermal stability (T_{max} = 340 °C) and 0.58 mmol/g of carboxylic groups	(Jiang et al., 2021)

The dimensions of the (L)CNCs are sometimes related to a specific pretreatment condition or to different pretreatment conditions.

production of cellulose nanofibrils.

Films produced from the DES-(L)CNFs were also discussed. Overall, films with very good mechanical properties could be obtained by using DES-(L)CNFs, being in some cases comparable to the best-performing (L) CNF films obtained by conventional methods (e.g., TEMPO oxidation). However, there is a lack of information about the gas barrier properties of the films which is crucial to evaluate the film's potential to be used as alternatives to fossil-based plastics. The combination of DES-(L)CNFs with different polymers (e.g., PLA and PVA) has also been studied aiming the enhancement of their mechanical properties.

Regarding the production of (L)CNCs, the use of DESs allows for similar morphology, dimensions and crystallinity of the nanocrystals compared to the typical concentrated sulfuric acid hydrolysis. However, the DESs allow to obtain CNCs at significantly higher yields (44–88%) and with better thermostability, compared to the conventional methods of CNC production (mass yields limited to a maximum of ~50%). DESs-CNCs have a huge potential to be applied in several fields, being already used to enhance the mechanical properties of nanocomposite films, stabilize oil-water Pickering emulsions and as cross-linkers in nano-composite hydrogels.

DESs can be produced from compounds present in living cells (e.g., amino acids, organic acids, carbohydrates), the so-called natural deep eutectic solvents, which may be viewed as an advantage over other systems used to produce nanocelluloses. Additionally, they can be easily prepared by simply mixing (and heating) two or more components without needing purification steps, which is an advantage over the ionic liquids, for instance, which involve more complex and high-cost synthesis steps. They are also considered to be biocompatible and biodegradable, and their physiochemical properties (viscosity, density, vapor pressure, freezing point, polarity, etc.) are tunable by varying the HBAs and HBDs, their molar ratios and temperature.

One of the most important and distinctive aspects that was shown throughout this review, was the fact that the use of DESs for the production of nanocelluloses does not generate hazardous wastes, and they can be easily recycled by distillation using a rotatory evaporator. According to different authors, high recyclability rates ($>$ 85%) are indeed obtained with this simple recovery process, and the recovered DESs can be reused several times without losing efficiency compared to the fresh DESs. This is of utmost importance for the eventual scale-up of the nanocellulose production using DESs since it will mitigate the problem of the DES disposal and reduce the manufacturing costs. However, due to the lack of systematic studies, further investigations into the recycling and reuse of DESs are needed. Additionally, for a possible industrialization of these methods to produce nanocelluloses, a detailed economic analysis is needed, addressing, for example, the cost of reagents required to obtain the DESs, the costs of energy involved in the production, both for the pretreatment of lignocellulosic materials and subsequent mechanical treatment (especially in the case of (L)CNFs), and the costs associated with recycling the DESs. Nowadays, this information is practically non-existent and the limited data available is quite superficial, only addressing the savings in the energy involved in the mechanical treatment.

Declaration of Competing Interest

The authors declare the following financial interests/personal relationships which may be considered as potential competing interests: Ricardo Oliveira de Almeida reports financial support was provided by Foundation for Science and Technology. Ricardo Oliveira de Almeida reports a relationship with Foundation for Science and Technology that includes: funding grants. There is no conflict of interests.

Data Availability

Data will be made available on request.

Acknowledgments

References

Abbott, A.P., Capper, G., Davies, D.L., Rasheed, R.K., Tambyrajah, V., 2003. Novel solvent properties of choline chloride/urea mixtures. Chem. Commun. 1, 70–71. https://doi.org/10.1039/B210714G.

Abbott, A.P., Boothby, D., Capper, G., Davies, D.L., Rasheed, R.K., 2004. Deep eutectic solvents formed between choline chloride and carboxylic acids: versatile alternatives to ionic liquids. J. Am. Chem. Soc. 126, 9142–9147. https://doi.org/10.1021/ja048266j.

Abitbol, T., Rivkin, A., Cao, Y., Nevo, Y., Abraham, E., Ben-Shalom, T., Lapidot, S., Shoseyov, O., 2016. Nanocellulose, a tiny fiber with huge applications. Curr. Opin. Biotechnol. 39, 76–88. https://doi.org/10.1016/j.copbio.2016.01.002.

Abushammala, H., Krossing, I., Laborie, M.-P., 2015. Ionic liquid-mediated technology to produce cellulose nanocrystals directly from wood. Carbohydr. Polym. 134, 609–616. https://doi.org/10.1016/j.carbpol.2015.07.079.

Ai, Y., Zhang, L., Cui, M., Huang, R., Qi, W., He, Z., Klemeš, J.J., Su, R., 2022. Toward cleaner production of nanocellulose: a review and evaluation. Green. Chem. 24, 6406–6434. https://doi.org/10.1039/D2GC01669A.

Almeida, R.O., Ramos, A., Alves, L., Posti, E., Ferreira, P.J.T., Carvalho, M.G.V.S., Rasteiro, M.G., Gamelas, J.A.F., 2021. Production of nanocellulose gels and films from invasive tree species. Int. J. Biol. Macromol. 188, 1003–1011. https://doi.org/10.1016/j.ijbiomac.2021.08.015.

Alves, L., Ferraz, E., Gamelas, J.A.F., 2019. Composites of nanofibrillated cellulose with clay minerals: a review. Adv. Colloid Interface Sci. 272, 101994 https://doi.org/10.1016/j.cis.2019.101994.

Amiralian, N., Annamalai, P.K., Memmott, P., Martin, D.J., 2015. Isolation of cellulose nanofibrils from Triodia pungens via different mechanical methods. Cellulose 22, 2483–2498. https://doi.org/10.1007/s10570-015-0688-x.

Aoki, D., Nishio, Y., 2010. Phosphorylated cellulose propionate derivatives as thermoplastic flame resistant/retardant materials: influence of regioselective phosphorylation on their thermal degradation behaviour. Cellulose 17, 963–976. https://doi.org/10.1007/s10570-010-9440-8.

Arantes, V., Dias, I.K.R., Berto, G.L., Pereira, B., Marotti, B.S., Nogueira, C.F.O., 2020. The current status of the enzyme-mediated isolation and functionalization of nanocelluloses: production, properties, techno-economics, and opportunities. Cellulose 27, 10571–10630. https://doi.org/10.1007/s10570-020-03332-1.

Aulin, C., Johansson, E., Wågberg, L., Lindström, T., 2010. Self-organized films from cellulose i nanofibrils using the layer-by-layer technique. Biomacromolecules 11, 872–882. https://doi.org/10.1021/bm100075e.

Berglund, L., Anugwom, I., Hedenström, M., Aitomäki, Y., Mikkola, J.-P., Oksman, K., 2017. Switchable ionic liquids enable efficient nanofibrillation of wood pulp. Cellulose 24, 3265–3279. https://doi.org/10.1007/s10570-017-1354-2.

Bhagwat, P., Amobonye, A., Singh, S., Pillai, S., 2021. Deep eutectic solvents in the pretreatment of feedstock for efficient fractionation of polysaccharides: current status and future prospects. Biomass Convers. Biorefinery 12, 171–195. https://doi.org/10.1007/s13399-021-01745-x.

Bondeson, D., Mathew, A., Oksman, K., 2006. Optimization of the isolation of nanocrystals from microcrystalline cellulose by acid hydrolysis. Cellulose 13, 171–180. https://doi.org/10.1007/s10570-006-9061-4.

Brinchi, L., Cotana, F., Fortunati, E., Kenny, J.M., 2013. Production of nanocrystalline cellulose from lignocellulosic biomass: technology and applications. Carbohydr. Polym. 94, 154–169. https://doi.org/10.1016/j.carbpol.2013.01.033.

Cao, X., Ding, B., Yu, J., Al-Deyab, S.S., 2012. Cellulose nanowhiskers extracted from TEMPO-oxidized jute fibers. Carbohydr. Polym. 90, 1075–1080. https://doi.org/10.1016/j.carbpol.2012.06.046.

Chang, X.X., Mubarak, N.M., Mazari, S.A., Jatoi, A.S., Ahmad, A., Khalid, M., Walvekar, R., Abdullah, E.C., Karri, R.R., Siddiqui, M.T.H., Nizamuddin, S., 2021. A review on the properties and applications of chitosan, cellulose and deep eutectic solvent in green chemistry. J. Ind. Eng. Chem. 104, 362–380. https://doi.org/10.1016/j.jiec.2021.08.033.

Chen, L., Zhu, J.Y., Baez, C., Kitin, P., Elder, T., 2016. Highly thermal-stable and functional cellulose nanocrystals and nanofibrils produced using fully recyclable organic acids. Green. Chem. 18, 3835–3843. https://doi.org/10.1039/C6GC00687F.

Chen, L., Dou, J., Ma, Q., Li, N., Wu, R., Bian, H., Yelle, D.J., Vuorinen, T., Fu, S., Pan, X., Zhu, J. (J.Y.)., 2017. Rapid and near-complete dissolution of wood lignin at ≤80°C by a recyclable acid hydrotrope. Sci. Adv. 3, e1701735 https://doi.org/10.1126/sciadv.1701735.

Chen, Y., Fan, D., Han, Y., Lyu, S., Lu, Y., Li, G., Jiang, F., Wang, S., 2018. Effect of high residual lignin on the properties of cellulose nanofibrils/films. Cellulose 25, 6421–6431. https://doi.org/10.1007/s10570-018-2006-x.

Chen, Y., Yu, D., Liu, Z., Xue, Z., Mu, T., 2022. Thermal, chemical, electrochemical, radiolytic and biological stability of ionic liquids and deep eutectic solvents. N. J. Chem. 46, 17640–17668. https://doi.org/10.1039/D2NJ03148E.

Choi, Y.H., van Spronsen, J., Dai, Y., Verberne, M., Hollmann, F., Arends, I.W.C.E., Witkamp, G.-J., Verpoorte, R., 2011. Are natural deep eutectic solvents the missing link in understanding cellular metabolism and physiology. Plant Physiol. 156, 1701–1705. https://doi.org/10.1104/pp.111.178426.

Coutinho, J.A.P., Pinho, S.P., 2017. Special issue on deep eutectic solvents: a foreword. Fluid Phase Equilib. 448, 1. https://doi.org/10.1016/j.fluid.2017.06.011.

Cui, S., Zhang, S., Ge, S., Xiong, L., Sun, Q., 2016. Green preparation and characterization of size-controlled nanocrystalline cellulose via ultrasonic-assisted enzymatic hydrolysis. Ind. Crops Prod. 83, 346–352. https://doi.org/10.1016/j.indcrop.2016.01.019.

Cunha, S.C., Fernandes, J.O., 2018. Extraction techniques with deep eutectic solvents. TrAC Trends Anal. Chem. 105, 225–239. https://doi.org/10.1016/j.trac.2018.05.001.

De, D., Naga Sai, M.S., Aniya, V., Satyavathi, B., 2021. Strategic biorefinery platform for green valorization of agro-industrial residues: a sustainable approach towards biodegradable plastics. J. Clean. Prod. 290, 125184 https://doi.org/10.1016/j.jclepro.2020.125184.

Deng, W., Tang, Y., Mao, J., Zhou, Y., Chen, T., Zhu, X., 2021. Cellulose nanofibril as a crosslinker to reinforce the sodium alginate/chitosan hydrogels. Int. J. Biol. Macromol. 189, 890–899. https://doi.org/10.1016/j.ijbiomac.2021.08.172.

Dhali, K., Ghasemlou, M., Daver, F., Cass, P., Adhikari, B., 2021. A review of nanocellulose as a new material towards environmental sustainability. Sci. Total Environ. 775, 145871 https://doi.org/10.1016/j.scitotenv.2021.145871.

Douard, L., Bras, J., Encinas, T., Belgacem, M.N., 2021. Natural acidic deep eutectic solvent to obtain cellulose nanocrystals using the design of experience approach. Carbohydr. Polym. 252, 117136 https://doi.org/10.1016/j.carbpol.2020.117136.

Dufresne, A., 2012. Nanocellulose: From nature to high performance tailored materials. De Gruyter. https://doi.org/10.1515/9783110254600.

El Achkar, T., Fourmentin, S., Greige-Gerges, H., 2019. Deep eutectic solvents: an overview on their interactions with water and biochemical compounds. J. Mol. Liq. 288, 111028 https://doi.org/10.1016/j.molliq.2019.111028.

El Achkar, T., Greige-Gerges, H., Fourmentin, S., 2021. Basics and properties of deep eutectic solvents: a review. Environ. Chem. Lett. 19, 3397–3408. https://doi.org/10.1007/s10311-021-01225-8.

Espinosa, E., Rol, F., Bras, J., Rodríguez, A., 2019. Production of lignocellulose nanofibers from wheat straw by different fibrillation methods. Comparison of its viability in cardboard recycling process. J. Clean. Prod. 239, 118083 https://doi.org/10.1016/j.jclepro.2019.118083.

Fan, Q., Jiang, C., Wang, W., Bai, L., Chen, H., Yang, H., Wei, D., Yang, L., 2020. Eco-friendly extraction of cellulose nanocrystals from grape pomace and construction of self-healing nanocomposite hydrogels. Cellulose 27, 2541–2553. https://doi.org/10.1007/s10570-020-02977-2.

Fang, Z., Hou, G., Chen, C., Hu, L., 2019. Nanocellulose-based films and their emerging applications. Curr. Opin. Solid State Mater. Sci. 23, 100764 https://doi.org/10.1016/j.cossms.2019.07.003.

Francisco, M., van den Bruinhorst, A., Kroon, M.C., 2013. Low-transition-temperature mixtures (LTTMs): a new generation of designer solvents. Angew. Chem. Int. Ed. 52, 3074–3085. https://doi.org/10.1002/anie.201207548.

Frone, A.N., Panaitescu, D.M., Donescu, D., Spataru, C.I., Radovici, C., Trusca, R., Somoghi, R., 2011. Preparation and characterization of pva composites with cellulose nanofibers obtained by ultrasonication. BioResources 6, 487–512.

García, G., Aparicio, S., Ullah, R., Atilhan, M., 2015. Deep eutectic solvents: physicochemical properties and gas separation applications. Energy Fuels 29, 2616–2644. https://doi.org/10.1021/ef5028873.

Ghanadpour, M., Carosio, F., Larsson, P.T., Wågberg, L., 2015. Phosphorylated cellulose nanofibrils: a renewable nanomaterial for the preparation of intrinsically flame-retardant materials. Biomacromolecules 16, 3399–3410. https://doi.org/10.1021/acs.biomac.5b01117.

González-Rivera, J., Husanu, E., Mero, A., Ferrari, C., Duce, C., Tinè, M.R., D'Andrea, F., Pomelli, C.S., Guazzelli, L., 2020. Insights into microwave heating response and thermal decomposition behavior of deep eutectic solvents. J. Mol. Liq. 300, 112357 https://doi.org/10.1016/j.molliq.2019.112357.

Gopi, S., Balakrishnan, P., Chandradhara, D., Poovathankandy, D., Thomas, S., 2019. General scenarios of cellulose and its use in the biomedical field. Mater. Today Chem. 13, 59–78. https://doi.org/10.1016/j.mtchem.2019.04.012.

Granja, P.L., Pouységu, L., Pétraud, M., De Jéso, B., Baquey, C., Barbosa, M.A., 2001. Cellulose phosphates as biomaterials. I. Synthesis and characterization of highly phosphorylated cellulose gels: Cellulose Phosphates as Biomaterials. I. J. Appl. Polym. Sci. 82, 3341–3353. https://doi.org/10.1002/app.2193.

Habibi, Y., 2014. Key advances in the chemical modification of nanocelluloses. Chem. Soc. Rev. 43, 1519–1542. https://doi.org/10.1039/C3CS60204D.

Habibi, Y., Lucia, L.A., Rojas, O.J., 2010. Cellulose nanocrystals: chemistry, self-assembly, and applications. Chem. Rev. 110, 3479–3500. https://doi.org/10.1021/cr900339w.

Hammond, O.S., Bowron, D.T., Edler, K.J., 2017. The effect of water upon deep eutectic solvent nanostructure: an unusual transition from ionic mixture to aqueous solution. Angew. Chem. Int. Ed. 56, 9782–9785. https://doi.org/10.1002/anie.201702486.

Hansen, B.B., Spittle, S., Chen, B., Poe, D., Zhang, Y., Klein, J.M., Horton, A., Adhikari, L., Zelovich, T., Doherty, B.W., Gurkan, B., Maginn, E.J., Ragauskas, A., Dadmun, M., Zawodzinski, T.A., Baker, G.A., Tuckerman, M.E., Savinell, R.F., Sangoro, J.R., 2021. Deep eutectic solvents: a review of fundamentals and applications. Chem. Rev. 121, 1232–1285. https://doi.org/10.1021/acs.chemrev.0c00385.

Heinze, T., 2015. Cellulose: structure and properties. Adv. Polym. Sci. 271, 1–52. https://doi.org/10.1007/12_2015_319.

Ho, T.T.T., Zimmermann, T., Hauert, R., Caseri, W., 2011. Preparation and characterization of cationic nanofibrillated cellulose from etherification and high-shear disintegration processes. Cellulose 18, 1391–1406. https://doi.org/10.1007/s10570-011-9591-2.

Ho, T.T.T., Abe, K., Zimmermann, T., Yano, H., 2015. Nanofibrillation of pulp fibers by twin-screw extrusion. Cellulose 22, 421–433. https://doi.org/10.1007/s10570-014-0518-6.

Hong, S., Yuan, Y., Li, P., Zhang, K., Lian, H., Liimatainen, H., 2020a. Enhancement of the nanofibrillation of birch cellulose pretreated with natural deep eutectic solvent. Ind. Crops Prod. 154, 112677 https://doi.org/10.1016/j.indcrop.2020.112677.

Hong, S., Song, Y., Yuan, Y., Lian, H., Liimatainen, H., 2020b. Production and characterization of lignin containing nanocellulose from luffa through an acidic deep eutectic solvent treatment and systematic fractionation. Ind. Crops Prod. 143, 111913 https://doi.org/10.1016/j.indcrop.2019.111913.

Ijardar, S.P., Singh, V., Gardas, R.L., 2022. Revisiting the physicochemical properties and applications of deep eutectic solvents. Molecules 27, 1368. https://doi.org/10.3390/molecules27041368.

Im, W., Oh, K., Rajabi Abhari, A., Youn, H.J., Lee, H.L., 2019. Recycling of isopropanol for cost-effective, environmentally friendly production of carboxymethylated cellulose nanofibrils. Carbohydr. Polym. 208, 365–371. https://doi.org/10.1016/j.carbpol.2018.12.093.

Inagaki, N., Nakamura, S., Asai, H., Katsuura, K., 1976. Phosphorylation of cellulose with phosphorous acid and thermal degradation of the product. J. Appl. Polym. Sci. 20, 2829–2836. https://doi.org/10.1002/app.1976.070201017.

Isci, A., Kaltschmitt, M., 2022. Recovery and recycling of deep eutectic solvents in biomass conversions: a review. Biomass-. Convers. Biorefinery 12, 197–226. https://doi.org/10.1007/s13399-021-01860-9.

Iskak, N.A.M., Julkapli, N.M., Hamid, S.B.A., 2017. Understanding the effect of synthesis parameters on the catalytic ionic liquid hydrolysis process of cellulose nanocrystals. Cellulose 24, 2469–2481. https://doi.org/10.1007/s10570-017-1273-2.

Isogai, A., Hänninen, T., Fujisawa, S., Saito, T., 2018. Review: Catalytic oxidation of cellulose with nitroxyl radicals under aqueous conditions. Prog. Polym. Sci. 86, 122–148. https://doi.org/10.1016/j.progpolymsci.2018.07.007.

Ji, Q., Yu, X., Yagoub, A.E.-G.A., Chen, L., Zhou, C., 2021. Efficient cleavage of strong hydrogen bonds in sugarcane bagasse by ternary acidic deep eutectic solvent and ultrasonication to facile fabrication of cellulose nanofibers. Cellulose 28, 6159–6182. https://doi.org/10.1007/s10570-021-03876-w.

Jiang, J., Carrillo-Enríquez, N.C., Oguzlu, H., Han, X., Bi, R., Song, M., Saddler, J.N., Sun, R.-C., Jiang, F., 2020a. High production yield and more thermally stable lignin-containing cellulose nanocrystals isolated using a ternary acidic deep eutectic solvent. ACS Sustain. Chem. Eng. 8, 7182–7191. https://doi.org/10.1021/acssuschemeng.0c01724.

Jiang, J., Carrillo-Enríquez, N.C., Oguzlu, H., Han, X., Bi, R., Saddler, J.N., Sun, R.-C., Jiang, F., 2020b. Acidic deep eutectic solvent assisted isolation of lignin containing nanocellulose from thermomechanical pulp. Carbohydr. Polym. 247, 116727 https://doi.org/10.1016/j.carbpol.2020.116727.

Jiang, J., Zhu, Y., Zargar, S., Wu, J., Oguzlu, H., Baldelli, A., Yu, Z., Saddler, J., Sun, R., Tu, Q., Jiang, F., 2021. Rapid, high-yield production of lignin-containing cellulose nanocrystals using recyclable oxalic acid dihydrate. Ind. Crops Prod. 173, 114148 https://doi.org/10.1016/j.indcrop.2021.114148.

Jiang, Y., Liu, X., Yang, Q., Song, X., Qin, C., Wang, S., Li, K., 2019. Effects of residual lignin on composition, structure and properties of mechanically defibrillated cellulose fibrils and films. Cellulose 26, 1577–1593. https://doi.org/10.1007/s10570-018-02229-4.

Jonasson, S., Bünder, A., Niittylä, T., Oksman, K., 2020. Isolation and characterization of cellulose nanofibers from aspen wood using derivatizing and non-derivatizing pretreatments. Cellulose 27, 185–203. https://doi.org/10.1007/s10570-019-02754-w.

Kalhor, P., Ghandi, K., 2019. Deep eutectic solvents for pretreatment, extraction, and catalysis of biomass and food waste. Molecules 24, 4012. https://doi.org/10.3390/molecules24224012.

Kargarzadeh, H., Mariano, M., Gopakumar, D., Ahmad, I., Thomas, S., Dufresne, A., Huang, J., Lin, N., 2018. Advances in cellulose nanomaterials. Cellulose 25, 2151–2189. https://doi.org/10.1007/s10570-018-1723-5.

Klemm, D., Heublein, B., Fink, H.-P., Bohn, A., 2005. Cellulose: fascinating biopolymer and sustainable raw material. Angew. Chem. Int. Ed. 44, 3358–3393. https://doi.org/10.1002/anie.200460587.

Kumar, R., Rai, B., Gahlyan, S., Kumar, G., 2021. A comprehensive review on production, surface modification and characterization of nanocellulose derived from biomass and its commercial applications. Express Polym. Lett. 15, 104–120. https://doi.org/10.3144/expresspolymlett.2021.11.

Kwon, G.-J., Bandi, R., Yang, B.-S., Park, C.-W., Han, S.-Y., Park, J.-S., Lee, E.-A., Kim, N.-H., Lee, S.-H., 2021. Choline chloride based deep eutectic solvents for the lignocellulose nanofibril production from Mongolian oak (Quercus mongolica. Cellulose 28, 9169–9185. https://doi.org/10.1007/s10570-021-04102-3.

Laitinen, O., Ojala, J., Sirviö, J.A., Liimatainen, H., 2017. Sustainable stabilization of oil in water emulsions by cellulose nanocrystals synthesized from deep eutectic solvents. Cellulose 24, 1679–1689. https://doi.org/10.1007/s10570-017-1226-9.

Laitinen, O., Suopajärvi, T., Liimatainen, H., 2020. Enhancing packaging board properties using micro- and nanofibers prepared from recycled board. Cellulose 27, 7215–7225. https://doi.org/10.1007/s10570-020-03264-w.

Lakovaara, M., Sirviö, J.A., Ismail, M.Y., Liimatainen, H., Sliz, R., 2021. Hydrophobic modification of nanocellulose and all-cellulose composite films using deep eutectic solvent as a reaction medium. Cellulose 28, 5433–5447. https://doi.org/10.1007/s10570-021-03863-1.

Lavoine, N., Desloges, I., Dufresne, A., Bras, J., 2012. Microfibrillated cellulose – its barrier properties and applications in cellulosic materials: a review. Carbohydr. Polym. 90, 735–764. https://doi.org/10.1016/j.carbpol.2012.05.026.

Lazko, J., Sénéchal, T., Landercy, N., Dangreau, L., Raquez, J.-M., Dubois, P., 2014. Well defined thermostable cellulose nanocrystals via two-step ionic liquid swelling-

hydrolysis extraction. Cellulose 21, 4195–4207. https://doi.org/10.1007/s10570-014-0417-x.

Lee, S.-Y., Chun, S.-J., Kang, I.-A., Park, J.-Y., 2009. Preparation of cellulose nanofibrils by high-pressure homogenizer and cellulose-based composite films. J. Ind. Eng. Chem. 15, 50–55. https://doi.org/10.1016/j.jiec.2008.07.008.

Li, P., Sirviö, J.A., Haapala, A., Liimatainen, H., 2017. Cellulose nanofibrils from nonderivatizing urea-based deep eutectic solvent pretreatments. ACS Appl. Mater. Interfaces 9, 2846–2855. https://doi.org/10.1021/acsami.6b13625.

Li, P., Sirviö, J.A., Asante, B., Liimatainen, H., 2018. Recyclable deep eutectic solvent for the production of cationic nanocelluloses. Carbohydr. Polym. 199, 219–227. https://doi.org/10.1016/j.carbpol.2018.07.024.

Li, P., Sirviö, J.A., Hong, S., Ämmälä, A., Liimatainen, H., 2019. Preparation of flame-retardant lignin-containing wood nanofibers using a high-consistency mechano-chemical pretreatment. Chem. Eng. J. 375, 122050 https://doi.org/10.1016/j.cej.2019.122050.

Li, P., Wang, Y., Hou, Q., Liu, H., Lei, H., Jian, B., Li, X., 2020. Preparation of cellulose nanofibrils from okara by high pressure homogenization method using deep eutectic solvents. Cellulose 27, 2511–2520. https://doi.org/10.1007/s10570-019-02929-5.

Li, W., Xue, Y., He, M., Yan, J., Lucia, L.A., Chen, J., Yu, J., Yang, G., 2021. Facile preparation and characteristic analysis of sulfated cellulose nanofibril via the pretreatment of sulfamic acid-glycerol based deep eutectic solvents. Nanomaterials 11, 2778. https://doi.org/10.3390/nano11112778.

Liimatainen, H., Visanko, M., Sirviö, J.A., Hormi, O.E.O., Niinimaki, J., 2012. Enhancement of the nanofibrillation of wood cellulose through sequential periodate–chlorite oxidation. Biomacromolecules 13, 1592–1597. https://doi.org/10.1021/bm300319m.

Liimatainen, H., Visanko, M., Sirviö, J., Hormi, O., Niinimäki, J., 2013. Sulfonated cellulose nanofibrils obtained from wood pulp through regioselective oxidative bisulfite pre-treatment. Cellulose 20, 741–749. https://doi.org/10.1007/s10570-013-9865-y.

Liimatainen, H., Suopajärvi, T., Sirviö, J., Hormi, O., Niinimäki, J., 2014. Fabrication of cationic cellulosic nanofibrils through aqueous quaternization pretreatment and their use in colloid aggregation. Carbohydr. Polym. 103, 187–192. https://doi.org/10.1016/j.carbpol.2013.12.042.

Lim, W.-L., Gunny, A.A.N., Kasim, F.H., Gopinath, S.C.B., Kamaludin, N.H.I., Arbain, D., 2021. Cellulose nanocrystals from bleached rice straw pulp: acidic deep eutectic solvent versus sulphuric acid hydrolyses. Cellulose 28, 6183–6199. https://doi.org/10.1007/s10570-021-03914-7.

Ling, Z., Edwards, J.V., Guo, Z., Prevost, N.T., Nam, S., Wu, Q., French, A.D., Xu, F., 2019. Structural variations of cotton cellulose nanocrystals from deep eutectic solvent treatment: Micro and nano scale. Cellulose 26, 861–876. https://doi.org/10.1007/s10570-018-2092-9.

Liu, C., Li, B., Du, H., Lv, D., Zhang, Y., Yu, G., Mu, X., Peng, H., 2016. Properties of nanocellulose isolated from corncob residue using sulfuric acid, formic acid, oxidative and mechanical methods. Carbohydr. Polym. 151, 716–724. https://doi.org/10.1016/j.carbpol.2016.06.025.

Liu, C., Li, M.-C., Chen, W., Huang, R., Hong, S., Wu, Q., Mei, C., 2020. Production of lignin-containing cellulose nanofibers using deep eutectic solvents for UV-absorbing polymer reinforcement. Carbohydr. Polym. 246, 116548 https://doi.org/10.1016/j.carbpol.2020.116548.

Liu, C., Li, Z., Li, M.-C., Chen, W., Xu, W., Hong, S., Wu, Q., Mei, C., 2022. Lignin-containing cellulose nanofibers made with microwave-aid green solvent treatment for magnetic fluid stabilization. Carbohydr. Polym. 291, 119573 https://doi.org/10.1016/j.carbpol.2022.119573.

Liu, K., Du, H., Zheng, T., Liu, W., Zhang, M., Liu, H., Zhang, X., Si, C., 2021. Lignin-containing cellulose nanomaterials: preparation and applications. Green. Chem. 23, 9723–9746. https://doi.org/10.1039/D1GC02841C.

Liu, Q., Yuan, T., Fu, Q., Bai, Y., Peng, F., Yao, C., 2019. Choline chloride-lactic acid deep eutectic solvent for delignification and nanocellulose production of moso bamboo. Cellulose 26, 9447–9462. https://doi.org/10.1007/s10570-019-02726-0.

Liu, S., Zhang, Q., Gou, S., Zhang, L., Wang, Z., 2021. Esterification of cellulose using carboxylic acid-based deep eutectic solvents to produce high-yield cellulose nanofibers. Carbohydr. Polym. 251, 117018 https://doi.org/10.1016/j.carbpol.2020.117018.

Liu, W., Du, H., Liu, K., Liu, H., Xie, H., Si, C., Pang, B., Zhang, X., 2021. Sustainable preparation of cellulose nanofibrils via choline chloride-citric acid deep eutectic solvent pretreatment combined with high-pressure homogenization. Carbohydr. Polym. 267, 118220 https://doi.org/10.1016/j.carbpol.2021.118220.

Liu, W., Liu, K., Du, H., Zheng, T., Zhang, N., Xu, T., Pang, B., Zhang, X., Si, C., Zhang, K., 2022. Cellulose nanopaper: fabrication, functionalization, and applications. Nano-Micro Lett. 14, 104. https://doi.org/10.1007/s40820-022-00849-x.

Liu, X., Jiang, Y., Song, X., Qin, C., Wang, S., Li, K., 2019a. A bio-mechanical process for cellulose nanofiber production – towards a greener and energy conservation solution. Carbohydr. Polym. 208, 191–199. https://doi.org/10.1016/j.carbpol.2018.12.071.

Liu, X., Li, Y., Ewulonu, C.M., Ralph, J., Xu, F., Zhang, Q., Wu, M., Huang, Y., 2019b. Mild alkaline pretreatment for isolation of native-like lignin and lignin-containing cellulose nanofibers (LCNF) from crop waste. ACS Sustain. Chem. Eng. 7, 14135–14142. https://doi.org/10.1021/acssuschemeng.9b02800.

Liu, Y., Wang, H., Yu, G., Yu, Q., Li, B., Mu, X., 2014. A novel approach for the preparation of nanocrystalline cellulose by using phosphotungstic acid. Carbohydr. Polym. 110, 415–422. https://doi.org/10.1016/j.carbpol.2014.04.040.

Liu, Y., Guo, B., Xia, Q., Meng, J., Chen, W., Liu, S., Wang, Q., Liu, Y., Li, J., Yu, H., 2017. Efficient cleavage of strong hydrogen bonds in cotton by deep eutectic solvents and facile fabrication of cellulose nanocrystals in high yields. ACS Sustain. Chem. Eng. 5, 7623–7631. https://doi.org/10.1021/acssuschemeng.7b00954.

Loow, Y.-L., New, E.K., Yang, G.H., Ang, L.Y., Foo, L.Y.W., Wu, T.Y., 2017. Potential use of deep eutectic solvents to facilitate lignocellulosic biomass utilization and conversion. Cellulose 24, 3591–3618. https://doi.org/10.1007/s10570-017-1358-y.

Lu, Q.-L., Wu, J., Li, Y., Huang, B., 2021a. Isolation of thermostable cellulose II nanocrystals and their molecular bridging for electroresponsive and pH-sensitive bio-nanocomposite. Ind. Crops Prod. 173, 114127 https://doi.org/10.1016/j.indcrop.2021.114127.

Lu, Q.-L., Wu, J., Li, Y., Li, L., Huang, B., 2021b. One-pot green extraction of high charge density cellulose nanocrystals with high yield for bionanocomposites. J. Mater. Sci. 56, 12212–12223. https://doi.org/10.1007/s10853-021-06085-9.

Ma, Y., Xia, Q., Liu, Y., Chen, W., Liu, S., Wang, Q., Liu, Y., Li, J., Yu, H., 2019. Production of nanocellulose using hydrated deep eutectic solvent combined with ultrasonic treatment. ACS Omega 4, 8539–8547. https://doi.org/10.1021/acsomega.9b00519.

Man, Z., Muhammad, N., Sarwono, A., Bustam, M.A., Vignesh Kumar, M., Rafiq, S., 2011. Preparation of cellulose nanocrystals using an ionic liquid. J. Polym. Environ. 19, 726–731. https://doi.org/10.1007/s10924-011-0323-3.

Marchel, M., Cieśliński, H., Boczkaj, G., 2022. Deep eutectic solvents microbial toxicity: current state of art and critical evaluation of testing methods. J. Hazard. Mater. 425, 127963 https://doi.org/10.1016/j.jhazmat.2021.127963.

Martínez, G.M., Townley, G.G., Martínez-Espinosa, R.M., 2022. Controversy on the toxic nature of deep eutectic solvents and their potential contribution to environmental pollution. Heliyon 8, e12567. https://doi.org/10.1016/j.heliyon.2022.e12567.

Martins, M.A.R., Pinho, S.P., Coutinho, J.A.P., 2019. Insights into the nature of eutectic and deep eutectic mixtures. J. Solut. Chem. 48, 962–982. https://doi.org/10.1007/s10953-018-0793-1.

Mateo, S., Peinado, S., Morillas-Gutiérrez, F., La Rubia, M.D., Moya, A.J., 2021. Nanocellulose from agricultural wastes: products and applications—a review. Processes 9, 1594. https://doi.org/10.3390/pr9091594.

Meng, X., Ballerat-Busserolles, K., Husson, P., Andanson, J.-M., 2016. Impact of water on the melting temperature of urea + choline chloride deep eutectic solvent. N. J. Chem. 40, 4492–4499. https://doi.org/10.1039/C5NJ02677F.

Missoum, K., Belgacem, M., Bras, J., 2013. Nanofibrillated cellulose surface modification: a review. Materials 6, 1745–1766. https://doi.org/10.3390/ma6051745.

Mokhena, T.C., John, M.J., 2020. Cellulose nanomaterials: new generation materials for solving global issues. Cellulose 27, 1149–1194. https://doi.org/10.1007/s10570-019-02889-w.

Moon, R.J., Martini, A., Nairn, J., Simonsen, J., Youngblood, J., 2011. Cellulose nanomaterials review: structure, properties and nanocomposites. Chem. Soc. Rev. 40, 3941–3994. https://doi.org/10.1039/C0CS00108B.

Nechyporchuk, O., Belgacem, M.N., Bras, J., 2016. Production of cellulose nanofibrils: a review of recent advances. Ind. Crops Prod. 93, 2–25. https://doi.org/10.1016/j.indcrop.2016.02.016.

Noguchi, Y., Homma, I., Matsubara, Y., 2017. Complete nanofibrillation of cellulose prepared by phosphorylation. Cellulose 24, 1295–1305. https://doi.org/10.1007/s10570-017-1191-3.

Noremylia, M.B., Hassan, M.Z., Ismail, Z., 2022. Recent advancement in isolation, processing, characterization and applications of emerging nanocellulose: a review. Int. J. Biol. Macromol. 206, 954–976. https://doi.org/10.1016/j.ijbiomac.2022.03.064.

Nuessle, A.C., Ford, F.M., Hall, W.P., Lippert, A.L., 1956. Some aspects of the cellulose-phosphate-urea reaction. Text. Res. J. 26, 32–39. https://doi.org/10.1177/004051755602600105.

Ojala, J., Visanko, M., Laitinen, O., Österberg, M., Sirviö, J., Liimatainen, H., 2018. Emulsion stabilization with functionalized cellulose nanoparticles fabricated using deep eutectic solvents. Molecules 23, 2765. https://doi.org/10.3390/molecules23112765.

Olszewska, A., Eronen, P., Johansson, L.-S., Malho, J.-M., Ankerfors, M., Lindström, T., Ruokolainen, J., Laine, J., Österberg, M., 2011. The behaviour of cationic NanoFibrillar Cellulose in aqueous media. Cellulose 18, 1213–1226. https://doi.org/10.1007/s10570-011-9577-0.

Omar, K.A., Sadeghi, R., 2022. Physicochemical properties of deep eutectic solvents: a review. J. Mol. Liq. 360, 119524 https://doi.org/10.1016/j.molliq.2022.119524.

Pääkkö, M., Ankerfors, M., Kosonen, H., Nykänen, A., Ahola, S., Österberg, M., Ruokolainen, J., Laine, J., Larsson, P.T., Ikkala, O., Lindström, T., 2007. Enzymatic hydrolysis combined with mechanical shearing and high-pressure homogenization for nanoscale cellulose fibrils and strong gels. Biomacromolecules 8, 1934–1941. https://doi.org/10.1021/bm061215p.

Pang, Z., Wang, P., Dong, C., 2018. Ultrasonic pretreatment of cellulose in ionic liquid for efficient preparation of cellulose nanocrystals. Cellulose 25, 7053–7064. https://doi.org/10.1007/s10570-018-2070-2.

Pedrosa, J.F.S., Rasteiro, M.G., Neto, C.P., Ferreira, P.J.T., 2022. Effect of cationization pretreatment on the properties of cationic Eucalyptus micro/nanofibrillated cellulose. Int. J. Biol. Macromol. 201, 468–479. https://doi.org/10.1016/j.ijbiomac.2022.01.068.

Pere, J., Tammelin, T., Niemi, P., Lille, M., Virtanen, T., Penttilä, P.A., Ahvenainen, P., Grönqvist, S., 2020. Production of high solid nanocellulose by enzyme-aided fibrillation coupled with mild mechanical treatment. ACS Sustain. Chem. Eng. 8, 18853–18863. https://doi.org/10.1021/acssuschemeng.0c05202.

Pereira, B., Arantes, V., 2020. Production of cellulose nanocrystals integrated into a biochemical sugar platform process via enzymatic hydrolysis at high solid loading. Ind. Crops Prod. 152, 112377 https://doi.org/10.1016/j.indcrop.2020.112377.

Petroudy, S.R.D., Chabot, B., Loranger, E., Naebe, M., Shojaeiarani, J., Gharehkhani, S., Ahvazi, B., Hu, J., Thomas, S., 2021. Recent advances in cellulose nanofibers

preparation through energy-efficient approaches: a review. Energies 14, 6792. https://doi.org/10.3390/en14206792.

Phanthong, P., Karnjanakom, S., Reubroycharoen, P., Hao, X., Abudula, A., Guan, G., 2017. A facile one-step way for extraction of nanocellulose with high yield by ball milling with ionic liquid. Cellulose 24, 2083–2093. https://doi.org/10.1007/s10570-017-1238-5.

Phanthong, P., Reubroycharoen, P., Hao, X., Xu, G., Abudula, A., Guan, G., 2018. Nanocellulose: extraction and application. Carbon Resour. Convers. 1, 32–43. https://doi.org/10.1016/j.crcon.2018.05.004.

Pirich, C.L., Picheth, G.F., Fontes, A.M., Delgado-Aguilar, M., Ramos, L.P., 2020. Disruptive enzyme-based strategies to isolate nanocelluloses: a review. Cellulose 27, 5457–5475. https://doi.org/10.1007/s10570-020-03185-8.

Pradhan, D., Jaiswal, A.K., Jaiswal, S., 2022. Emerging technologies for the production of nanocellulose from lignocellulosic biomass. Carbohydr. Polym. 285, 119258 https://doi.org/10.1016/j.carbpol.2022.119258.

Rambabu, N., Panthapulakkal, S., Sain, M., Dalai, A.K., 2016. Production of nanocellulose fibers from pinecone biomass: evaluation and optimization of chemical and mechanical treatment conditions on mechanical properties of nanocellulose films. Ind. Crops Prod. 83, 746–754. https://doi.org/10.1016/j.indcrop.2015.11.083.

Raza, M., Abu-Jdayil, B., 2022. Cellulose nanocrystals from lignocellulosic feedstock: a review of production technology and surface chemistry modification. Cellulose 29, 685–722. https://doi.org/10.1007/s10570-021-04371-y.

Reid, J.D., Mazzeno, L.W., 1949. Preparation and properties of cellulose phosphates. Ind. Eng. Chem. 41, 2828–2831. https://doi.org/10.1021/ie50480a039.

Ribeiro, R.S.A., Pohlmann, B.C., Calado, V., Bojorge, N., Pereira Jr, N., 2019. Production of nanocellulose by enzymatic hydrolysis: trends and challenges. Eng. Life Sci. 19, 279–291. https://doi.org/10.1002/elsc.201800158.

Rodriguez, R.N., van den Bruinhorst, A., Kollau, L.J.B.M., Kroon, M.C., Binnemans, K., 2019. Degradation of deep-eutectic solvents based on choline chloride and carboxylic acids. ACS Sustain. Chem. Eng. 7, 11521–11528. https://doi.org/10.1021/acssuschemeng.9b01378.

Rojo, E., Peresin, M.S., Sampson, W.W., Hoeger, I.C., Vartiainen, J., Laine, J., Rojas, O.J., 2015. Comprehensive elucidation of the effect of residual lignin on the physical, barrier, mechanical and surface properties of nanocellulose films. Green. Chem. 17, 1853–1866. https://doi.org/10.1039/C4GC02398F.

Rol, F., Belgacem, M.N., Gandini, A., Bras, J., 2019. Recent advances in surface-modified cellulose nanofibrils. Prog. Polym. Sci. 88, 241–264. https://doi.org/10.1016/j.progpolymsci.2018.09.002.

Saito, T., Kimura, S., Nishiyama, Y., Isogai, A., 2007. Cellulose nanofibers prepared by tempo-mediated oxidation of native cellulose. Biomacromolecules 8, 2485–2491. https://doi.org/10.1021/bm0703970.

Saito, T., Hirota, M., Tamura, N., Kimura, S., Fukuzumi, H., Heux, L., Isogai, A., 2009. Individualization of nano-sized plant cellulose fibrils by direct surface carboxylation using TEMPO catalyst under neutral conditions. Biomacromolecules 10, 1992–1996. https://doi.org/10.1021/bm900414t.

Sanchez-Salvador, J.L., Campano, C., Negro, C., Monte, M.C., Blanco, A., 2021. Increasing the possibilities of TEMPO-mediated oxidation in the production of cellulose nanofibers by reducing the reaction time and reusing the reaction medium. Adv. Sustain. Syst. 5, 2000277. https://doi.org/10.1002/adsu.202000277.

Satlewal, A., Agrawal, R., Bhagia, S., Sangoro, J., Ragauskas, A.J., 2018. Natural deep eutectic solvents for lignocellulosic biomass pretreatment: recent developments, challenges and novel opportunities. Biotechnol. Adv. 36, 2032–2050. https://doi.org/10.1016/j.biotechadv.2018.08.009.

Selkälä, T., Sirviö, J.A., Lorite, G.S., Liimatainen, H., 2016. Anionically stabilized cellulose nanofibrils through succinylation pretreatment in urea-lithium chloride deep eutectic solvent. ChemSusChem 9, 3074–3083. https://doi.org/10.1002/cssc.201600903.

Selkälä, T., Suopajärvi, T., Sirviö, J.A., Luukkonen, T., Kinnunen, P., de Carvalho, A.L.C.B., Liimatainen, H., 2020. Surface modification of cured inorganic foams with cationic cellulose nanocrystals and their use as reactive filter media for anionic dye removal. ACS Appl. Mater. Interfaces 12, 27745–27757. https://doi.org/10.1021/acsami.0c05927.

Shu, F., Guo, Y., Huang, L., Zhou, M., Zhang, G., Yu, H., Zhang, J., Yang, F., 2022. Production of lignin-containing nanocellulose from poplar using ternary deep eutectic solvents pretreatment. Ind. Crops Prod. 177, 114404 https://doi.org/10.1016/j.indcrop.2021.114404.

Siro, I., Plackett, D., 2010. Microfibrillated cellulose and new nanocomposite materials: a review. Cellulose 17, 459–494. ⟨https://doi.org/10.1007/s10570-010-9405-y⟩.

Sirviö, J.A., 2018. Cationization of lignocellulosic fibers with betaine in deep eutectic solvent: facile route to charge stabilized cellulose and wood nanofibers. Carbohydr. Polym. 198, 34–40. https://doi.org/10.1016/j.carbpol.2018.06.051.

Sirviö, J.A., Visanko, M., 2017. Anionic wood nanofibers produced from unbleached mechanical pulp by highly efficient chemical modification. J. Mater. Chem. A 5, 21828–21835. https://doi.org/10.1039/C7TA05668K.

Sirviö, J.A., Visanko, M., 2019. Highly transparent nanocomposites based on poly(vinyl alcohol) and sulfated UV-absorbing wood nanofibers. Biomacromolecules 20, 2413–2420. https://doi.org/10.1021/acs.biomac.9b00427.

Sirviö, J.A., Visanko, M., 2020. Lignin-rich sulfated wood nanofibers as high-performing adsorbents for the removal of lead and copper from water. J. Hazard. Mater. 383, 121174 https://doi.org/10.1016/j.jhazmat.2019.121174.

Sirviö, J.A., Visanko, M., Liimatainen, H., 2015. Deep eutectic solvent system based on choline chloride-urea as a pre-treatment for nanofibrillation of wood cellulose. Green Chem. 17, 3401–3406. https://doi.org/10.1039/C5GC00398A.

Sirviö, J.A., Visanko, M., Liimatainen, H., 2016. Acidic deep eutectic solvents as hydrolytic media for cellulose nanocrystal production. Biomacromolecules 17, 3025–3032. https://doi.org/10.1021/acs.biomac.6b00910.

Sirviö, J.A., Ukkola, J., Liimatainen, H., 2019. Direct sulfation of cellulose fibers using a reactive deep eutectic solvent to produce highly charged cellulose nanofibers. Cellulose 26, 2303–2316. https://doi.org/10.1007/s10570-019-02257-8.

Sirviö, J.A., Hyypiö, K., Asaadi, S., Junka, K., Liimatainen, H., 2020. High-strength cellulose nanofibers produced via swelling pretreatment based on a choline chloride–imidazole deep eutectic solvent. Green. Chem. 22, 1763–1775. https://doi.org/10.1039/C9GC04119B.

Sirviö, J.A., Isokoski, E., Kantola, A.M., Komulainen, S., Ämmälä, A., 2021. Mechanochemical and thermal succinylation of softwood sawdust in presence of deep eutectic solvent to produce lignin-containing wood nanofibers. Cellulose 28, 6881–6898. https://doi.org/10.1007/s10570-021-03973-w.

Sjöström, E., 1993. Wood chemistry: Fundamentals and applications, second ed. Academic Press, San Diego. https://doi.org/10.1016/C2009-0-03289-9.

Smirnov, M.A., Sokolova, M.P., Tolmachev, D.A., Vorobiov, V.K., Kasatkin, I.A., Smirnov, N.N., Klaving, A.V., Bobrova, N.V., Lukasheva, N.V., Yakimansky, A.V., 2020. Green method for preparation of cellulose nanocrystals using deep eutectic solvent. Cellulose 27, 4305–4317. https://doi.org/10.1007/s10570-020-03100-1.

Smith, E.L., Abbott, A.P., Ryder, K.S., 2014. Deep eutectic solvents (DESs) and their applications. Chem. Rev. 114, 11060–11082. https://doi.org/10.1021/cr300162p.

Solala, I., Iglesias, M.C., Peresin, M.S., 2020. On the potential of lignin-containing cellulose nanofibrils (LCNFs): a review on properties and applications. Cellulose 27, 1853–1877. https://doi.org/10.1007/s10570-019-02899-8.

Suopajärvi, T., Sirviö, J.A., Liimatainen, H., 2017. Nanofibrillation of deep eutectic solvent-treated paper and board cellulose pulps. Carbohydr. Polym. 169, 167–175. https://doi.org/10.1016/j.carbpol.2017.04.009.

Suopajärvi, T., Ricci, P., Karvonen, V., Ottolina, G., Liimatainen, H., 2020. Acidic and alkaline deep eutectic solvents in delignification and nanofibrillation of corn stalk, wheat straw, and rapeseed stem residues. Ind. Crops Prod. 145, 111956 https://doi.org/10.1016/j.indcrop.2019.111956.

Supian, M.A.F., Amin, K.N.M., Jamari, S.S., Mohamad, S., 2020. Production of cellulose nanofiber (CNF) from empty fruit bunch (EFB) via mechanical method. J. Environ. Chem. Eng. 8, 103024 https://doi.org/10.1016/j.jece.2019.103024.

Taheri, H., Samyn, P., 2016. Effect of homogenization (microfluidization) process parameters in mechanical production of micro- and nanofibrillated cellulose on its rheological and morphological properties. Cellulose 23, 1221–1238. https://doi.org/10.1007/s10570-016-0866-5.

Taheri, H., Hietala, M., Suopajärvi, T., Liimatainen, H., Oksman, K., 2021. One-step twin-screw extrusion process to fibrillate deep eutectic solvent-treated wood to be used in wood fiber-polypropylene composites. ACS Sustain. Chem. Eng. 9, 883–893. https://doi.org/10.1021/acssuschemeng.0c07750.

Tan, X.Y., Abd Hamid, S.B., Lai, C.W., 2015. Preparation of high crystallinity cellulose nanocrystals (CNCs) by ionic liquid solvolysis. Biomass-.-. Bioenergy 81, 584–591. https://doi.org/10.1016/j.biombioe.2015.08.016.

Tanaka, R., Saito, T., Isogai, A., 2012. Cellulose nanofibrils prepared from softwood cellulose by TEMPO/NaClO/NaClO2 systems in water at pH 4.8 and 6.8. Int. J. Biol. Macromol. 51, 228–234. https://doi.org/10.1016/j.ijbiomac.2012.05.016.

Teo, H.L., Wahab, R.A., 2020. Towards an eco-friendly deconstruction of agro-industrial biomass and preparation of renewable cellulose nanomaterials: a review. Int. J. Biol. Macromol. 161, 1414–1430. https://doi.org/10.1016/j.ijbiomac.2020.08.076.

Thomas, B., Raj, M.C., B., Athira, K.B.H., Rubiyah, M.H., Joy, J., Moores, A., Drisko, G.L., Sanchez, C., 2018. Nanocellulose, a versatile green platform: from biosources to materials and their applications. Chem. Rev. 118, 11575–11625. https://doi.org/10.1021/acs.chemrev.7b00627.

Tomé, L.I.N., Baião, V., Silva, W., Brett, C.M.A., 2018. Deep eutectic solvents for the production and application of new materials. Appl. Mater. Today 10, 30–50. https://doi.org/10.1016/j.apmt.2017.11.005.

Trovagunta, R., Zou, T., Österberg, M., Kelley, S.S., Lavoine, N., 2021. Design strategies, properties and applications of cellulose nanomaterials-enhanced products with residual, technical or nanoscale lignin—a review. Carbohydr. Polym. 254, 117480 https://doi.org/10.1016/j.carbpol.2020.117480.

Turbak, A.F., Snyder, F.W., & Sandberg, K.R. (1983). Microfibrillated cellulose, a new cellulose product: Properties, uses, and commercial potential. United States of America.

Vanderfleet, O.M., Cranston, E.D., 2021. Production routes to tailor the performance of cellulose nanocrystals. Nat. Rev. Mater. 6, 124–144. https://doi.org/10.1038/s41578-020-00239-y.

Wågberg, L., Decher, G., Norgren, M., Lindström, T., Ankerfors, M., Axnäs, K., 2008. The build-up of polyelectrolyte multilayers of microfibrillated cellulose and cationic polyelectrolytes. Langmuir 24, 784–795. https://doi.org/10.1021/la702481v.

Wang, H., Li, J., Zeng, X., Tang, X., Sun, Y., Lei, T., Lin, L., 2020. Extraction of cellulose nanocrystals using a recyclable deep eutectic solvent. Cellulose 27, 1301–1314. https://doi.org/10.1007/s10570-019-02867-2.

Wang, J., Zhang, K., Zhang, L., Song, Z., Shang, S., Liu, H., Wang, D., 2022. Preparation and stabilization of Pickering emulsions by cationic cellulose nanocrystals synthesized from deep eutectic solvent. Int. J. Biol. Macromol. 209, 1900–1913. https://doi.org/10.1016/j.ijbiomac.2022.04.164.

Wei, Z., Wang, D., Chen, Y., Yu, D., Ding, Q., Li, R., Wu, C., 2022. The H-bond evolution of cellulose nanofibrils treated with choline chloride/oxalic acid. Cellulose 29, 3675–3687. https://doi.org/10.1007/s10570-022-04517-6.

Wu, M., Liao, K., Liu, C., Yu, G., Rahmaninia, M., Li, H., Li, B., 2021. Integrated and sustainable preparation of functional nanocellulose via formic acid/choline chloride solvents pretreatment. Cellulose 28, 9689–9703. https://doi.org/10.1007/s10570-021-04157-2.

Wu, R., Liu, K., Ren, J., Yu, Z., Zhang, Y., Bai, L., Wang, W., Chen, H., Yang, H., 2020. Cellulose nanocrystals extracted from grape pomace with deep eutectic solvents and application for self-healing nanocomposite hydrogels. Macromol. Mater. Eng. 305, 1900673. https://doi.org/10.1002/mame.201900673.

Wu, X.-Q., Liu, P.-D., Liu, Q., Xu, S.-Y., Zhang, Y.-C., Xu, W.-R., Liu, G.-D., 2021. Production of cellulose nanofibrils and films from elephant grass using deep eutectic solvents and a solid acid catalyst. RSC Adv. 11, 14071–14078. https://doi.org/10.1039/D1RA02259H.

Xie, H., Du, H., Yang, X., Si, C., 2018. Recent strategies in preparation of cellulose nanocrystals and cellulose nanofibrils derived from raw cellulose materials. Int. J. Polym. Sci. *2018*. https://doi.org/10.1155/2018/7923068.

Yang, X., Xie, H., Du, H., Zhang, X., Zou, Z., Zou, Y., Liu, W., Lan, H., Zhang, X., Si, C., 2019. Facile extraction of thermally stable and dispersible cellulose nanocrystals with high yield via a green and recyclable $FeCl_3$-catalyzed deep eutectic solvent system. ACS Sustain. Chem. Eng. 7, 7200–7208. https://doi.org/10.1021/acssuschemeng.9b00209.

Yao, L., Zou, X., Zhou, S., Zhu, H., Chen, G., Wang, S., Liu, X., Jiang, Y., 2022. Cationic lignocellulose nanofibers from agricultural waste as high-performing adsorbents for the removal of dissolved and colloidal substances. Polymers 14, 910. https://doi.org/10.3390/polym14050910.

Yi, T., Zhao, H., Mo, Q., Pan, D., Liu, Y., Huang, L., Xu, H., Hu, B., Song, H., 2020. From cellulose to cellulose nanofibrils—a comprehensive review of the preparation and modification of cellulose nanofibrils. Materials 13, 5062. https://doi.org/10.3390/ma13225062.

Yu, W., Wang, C., Yi, Y., Zhou, W., Wang, H., Yang, Y., Tan, Z., 2019. Choline chloride-based deep eutectic solvent systems as a pretreatment for nanofibrillation of ramie fibers. Cellulose 26, 3069–3082. https://doi.org/10.1007/s10570-019-02290-7.

Yu, W., Wang, C., Yi, Y., Wang, H., Yang, Y., Zeng, L., Tan, Z., 2021. Direct pretreatment of raw ramie fibers using an acidic deep eutectic solvent to produce cellulose nanofibrils in high purity. Cellulose 28, 175–188. https://doi.org/10.1007/s10570-020-03538-3.

Zhang, H., Chen, Y., Wang, S., Ma, L., Yu, Y., Dai, H., Zhang, Y., 2020. Extraction and comparison of cellulose nanocrystals from lemon (Citrus limon) seeds using sulfuric acid hydrolysis and oxidation methods. Carbohydr. Polym. 238, 116180 https://doi.org/10.1016/j.carbpol.2020.116180.

Zhang, L., Tsuzuki, T., Wang, X., 2015. Preparation of cellulose nanofiber from softwood pulp by ball milling. Cellulose 22, 1729–1741. https://doi.org/10.1007/s10570-015-0582-6.

Zhang, M., Zhang, X., Liu, Y., Wu, K., Zhu, Y., Lu, H., Liang, B., 2021. Insights into the relationships between physicochemical properties, solvent performance, and applications of deep eutectic solvents. Environ. Sci. Pollut. Res. 28, 35537–35563. https://doi.org/10.1007/s11356-021-14485-2.

Zhang, Q., De Oliveira Vigier, K., Royer, S., Jérôme, F., 2012. Deep eutectic solvents: syntheses, properties and applications. Chem. Soc. Rev. 41, 7108–7146. https://doi.org/10.1039/c2cs35178a.

Zhang, Q., Ma, R., Ma, L., Zhang, L., Fan, Y., Wang, Z., 2021. Contribution of lignin in esterified lignocellulose nanofibers (LCNFs) prepared by deep eutectic solvent treatment to the interface compatibility of LCNF/PLA composites. Ind. Crops Prod. 166, 113460 https://doi.org/10.1016/j.indcrop.2021.113460.

Zhang, S., Li, S.-N., Wu, Q., Li, Q., Huang, J., Li, W., Zhang, W., Wang, S., 2021. Phosphorus containing group and lignin toward intrinsically flame retardant cellulose nanofibril-based film with enhanced mechanical properties. Compos. Part B: Eng. 212, 108699 https://doi.org/10.1016/j.compositesb.2021.108699.

Zhang, Y., Wei, Y., Qian, Y., Zhang, M., Zhu, P., Chen, G., 2020. Lignocellulose enabled highly transparent nanopaper with tunable ultraviolet-blocking performance and superior durability. ACS Sustain. Chem. Eng. 8, 17033–17041. https://doi.org/10.1021/acssuschemeng.0c04145.

Zhekenov, T., Toksanbayev, N., Kazakbayeva, Z., Shah, D., Mjalli, F.S., 2017. Formation of type III Deep Eutectic Solvents and effect of water on their intermolecular interactions. Fluid Phase Equilib. 441, 43–48. https://doi.org/10.1016/j.fluid.2017.01.022.

Zhu, Y., Yu, Z., Zhu, J., Zhang, Y., Ren, X., Jiang, F., 2022. Developing flame-retardant lignocellulosic nanofibrils through reactive deep eutectic solvent treatment for thermal insulation. Chem. Eng. J. 445, 136748 https://doi.org/10.1016/j.cej.2022.136748.